CURRENT AND PROJECTED CLIMATE CHANGE IMPACTS OVER INNER NIGER DELTA WETLAND OF MALI

BY

MOUSSA IBRAHIM MAIGA

B.Sc. (Theoretical Physics), M.Sc. (Atmospheric and Environmental Physics)

(MCS/20/7727)

MAY, 2025

CURRENT AND PROJECTED CLIMATE CHANGE IMPACTS OVER INNER NIGER DELTA WETLAND OF MALI

BY

MOUSSA IBRAHIM MAIGA

B.Sc. (Theoretical Physics), M.Sc. (Atmospheric and Environmental Physics)

(MCS/20/7727)

A Thesis of the Doctoral Research Program of the West African Climate Systems, under the West African Science Service Centre on Climate Change and Adapted Land Use, in the Department of Meteorology and Climate Science submitted to the School of Postgraduate Studies in partial fulfilment of the requirements for the award of the degree of Doctor of Philosophy in Meteorology and Climate Science of the Federal University of Technology, Akure, Nigeria.

MAY, 2025

DECLARATION

I hereby declare that this Thesis was written by me and is a correct record of my own research work. It has not been presented in any previous application for any degree of this or any University.

All citations and sources of information are clearly acknowledged by means of references.

Candidate's Name: Moussa Ibrahim Maiga

Signature: Date: 15/06/2025

CERTIFICATION

We certify that this Dissertation entitled "Current and Projected Climate Change Impacts Over Inner Niger Delta Wetlands of Mali" is the outcome of the research carried out by Moussa Ibrahim Maiga under the WASCAL DRP-WACS in the Department of Meteorology and Climate Science of the Federal University of Technology, Akure.

Prof. Elijah Adesanya Adefisan …………………………………..

(Major Supervisor) Signature Date

Department of Meteorology and Climate Science,
The Federal University of Technology,
Akure, Nigeria.

Dr Souleymane Sanogo **15/06/2025**

(Co-Supervisor) Signature Date

Department of Physics,
Faculty of Science and Technology (FST).
University of Technical and Technological Sciences of Bamako (USTT-B)
Bamako, Mali.

Prof. Ifeoluwa Adebowale Balogun …………………………………..

(Director) Signature Date

Doctoral Research Program – West African Climate Systems
West African Science Service Center on Climate Change and
Adapted Land Use (DRP-WACS, WASCAL),
Federal University of Technology,
Akure, Nigeria.

ABSTRACT

This study aimed to evaluate the ability of selected RCMs and GCMs of CORDEX-CORE in reproducing the spatio-temporal patterns of some climatic variables, analyse the future climate scenarios over West Africa sub-region and assess the projected impact on changes in water density of the Inner Niger Delta (IND) wetland of Mali. A combinational metrics of three RCMs driven by three GCMs was used from 1970 to 2005 for evaluation. Three major climate variables, such as precipitation, air temperature, and evaporation, were evaluated using statistical parameters such as correlation coefficient (R), Mbias and RMSE compared to ERA5 data as observation. Results produced R values of 0.91 for the Sahel, 0.95 for the savannah, and 0.88 for the Guinea Coast for precipitation. Negative Mbias values reveal an underestimation of precipitation by the RCMs compared to ERA5. RMSE values range from 27.34mm to 151.53mm overall. For evaporation, R values are 0.93 for the Sahel, 0.93 for the savannah, and 0.86 for the Guinea Coast, with negative Mbias values except for CCLM5 simulations. RMSE varies from 9.54mm to 61.41mm overall. Air temperature R values are 0.86 for the Sahel, 0.93 for the savannah, and 0.93 for the Guinea Coast, with positive Mbias indicating that RCMs overestimate air temperature.

Annual changes in precipitation, evaporation, air temperature, and runoff for West Africa were assessed under RCP 2.6 and RCP 8.5. RCP 2.6 shows moderate, regionally varied changes. Under RCP 8.5, precipitation and runoff decrease sharply, especially in the Sahel and coastal zones, while evaporation and temperature increase significantly, intensifying water stress across the region.

Seasonal change in the precipitation, evaporation, air temperature and total runoff for the near and far future periods relative to the historical of the IND under RCP 8.5 and RCP 2.6 scenarios were then analysed. Precipitation shows high inter-model variability. Under RCP 8.5, the decrease is marked in MAM and JJA, with an increase in SON. Evaporation follows complex patterns across models. Temperature increases systematically. Runoff varies across seasons and models, which could affect water availability in the Inner Niger Delta (IND).

SWAT hydrological model was used to assess the impacts of climate change on streamflow and runoff at three hydrometric stations of the IND with continuous and reliable data: Mopti, Diré and Tombouctou. The results showed a general increase in streamflow and runoff over the three stations studied. Under RCP2.6, increases were particularly pronounced in the months of September, October, November and December (SOND), reaching up to 90% in some localities. In contrast, under RCP8.5, although increases were still significant, they were more moderate and more concentrated in the wet season (JJA and MAM). These hydrological changes will have major implications for water availability, flood frequency, and water resource management in the Inner Niger Delta, while increased seasonal variability could impact the resilience of ecosystems and socio-economic activities dependent on the Niger River.

DEDICATION

In memory of my late father, Mr Ibrahim Maiga you are not here to witness the completion of the foundations you laid. I know you will be proud and happy wherever you are.

May Allah continue to have mercy on your soul. Amen

To my father and role model, my source of strength and encouragement. Thank you for your endless sacrifices and support for me, and for always believing in me.

ACKNOWLEDGEMENTS

I want to appreciate God for His grace to successfully complete my Ph.D Degree Programme. Many thanks to the Federal Ministry of Education and Research (BMBF), Germany for sponsoring the WASCAL programme at the Federal University of Technology, Akure (FUTA DRP-WACS).

My sincere gratitude goes to my team of supervisors, Prof. Elijah Adesanya Adefisan from the Department of Meteorology and Climate Science, the Federal University of Technology of Akure (FUTA) Nigeria, Dr Souleymane Sanogo from the Department of Physics, Faculty of Science and Technology (FST) Bamako, Mali and Prof. Emmanuel Cheo from the United Nations University (UNU) Bonn, Germany for the tremendous work in supervising and guiding me throughout this research.

I would also like to thank my advisor, Dr. Imoleayo Ezekiel Gbode from the Department of Meteorology and Climate Sciences, the Federal University of Technology, Akure (FUTA), for his valuable collaborations throughout the program.

To my host university, the Federal University of Technology Akure, Nigeria through the Doctoral Research Program West African Climate Systems (DRP-WACS) under the Directorship of Professor I. A. Balogun for the coordination and efforts toward the successful completion of the program I say a big thank you.

I would like to express my gratitude to the Faculty of Science and Technology of Bamako (FST) and United Nations University (UNU) Bonn for providing me with a workspace and their invaluable collaborations throughout the program.

I would also like to thank my colleagues of WASCAL batch five for their moral and technical support throughout these years.

Finally, I would also like to thank my wonderful family for their unwavering support and encouragement throughout my academic journey.

TABLE OF CONTENTS

LIST OF TABLES

Table Number and Title **Page**

LIST OF FIGURES

Figure Number and Title **Page**

LIST OF ACRONYMS

NWP	Numerical Weather Prediction
MCS	Mesoscale Convective System
CMIP	Coupled Model Intercomparison Project
WCRP	The World Climate Research Program
CORDEX	Coordinated Regional Climate Downscaling Experiment
SWAT	The Soil and Water Assessment Tool model
UNDP	United Nations Development Programme
INSTAT	National Institute of Statistics of Mali
IIASA	The International Institute for Applied Systems Analysis
WWF	The World Wide Fund for Nature
WA	West Africa
IND	The Inner Niger Delta
GCM	Global Climate Models
RCM	Regional Climate Models
IPCC	Intergovernmental Panel on Climate Change
SD	Statistical Downscaling
DD	Dynamical Downscaling

R	The correlation coefficient
MB	The Mean Bias
RMSE	The Root Mean Square Error
ITD	Inter Tropical Discontinuity
ITCZ	The Inter-Tropical Convergence Zone
AEJ	The African Easterly Jet
TEJ	Tropical Easterly Jet
AEW	African easterly waves
SST	The Sea Surface Temperature
WAM	West Africa Monsoon
AMMA	African Monsoon Multidisciplinary Analysis
EM-DAT	The Emergency Event Database
SCP	Single-Country Publications
MCP	Multi-Country Publications
GHOZ	The Gas Hydrate Occurrence Zone
FAO	Food and Agriculture Organization of the United Nations
ERA5	Fifth generation ECMWF atmospheric reanalysis of the global data
ECMWF	The European Centre for Medium-Range Weather Forecasts

WRCP	The World Climate Research Program
HRU	Hydrologic Response Units
LULC	Land use and land cover

CHAPTER ONE

INTRODUCTION

1.1 Preamble

West Africa is among the most populous sub-region in Africa, and its climate plays a crucial role in the well-being of its people. Weather and climate conditions in West Africa can have major impacts on agricultural production, water resources sanitation and management and human health and affect other sectors of the economy such as energy production, transport and the Peach (Parker *et al*., 2018). Most of its key economic sectors, such as agriculture, power generation and industry, are highly dependent on the climate, of which seasonal precipitation is a key component (Janicot *et al*., 1996; Sultan *et al*., 2003). Taking into account the variability of the climate and the sometimes, dramatic consequences that this can cause, the evolution of water resources is a matter of concern for many regions of the world. This is true for the African countries of the Sudano-Sahelian zone, which have been subjected to persistent drought for about thirty years (Servat *et al*., 1998; Ardoin *et al*., 2003). Over recent decades, the Sudan-Sahel region has shown considerable year-to-year fluctuations in seasonal rainfall (Rauch *et al*., 2024). Seasonal forecasting appears to be a way to deal with climate variability, however numerical weather forecast information is underutilized in a wide range of economic sectors in decision making (Hamadan, 2002; Morss *et al*., 2008). Numerical Weather Prediction (NWP) on the African continent remains a considerable scientific challenge. The obstacles to be lifted for a realistic forecast are numerous because this requires taking into account the numerous weather conditions and climatic regimes, from the continent ranging from mid-latitude systems at the northern and southern ends of the continent to the climates of equatorial forests and desert areas, all of these systems being exposed to extreme weather conditions, over a large part of temporal and spatial scales (Parker *et al*., 2018).

For NWP, the initialization and modeling of MCS (mesoscale convective system) still remains a major scientific challenge today. Africa's weather systems also play a key role in determining the weather and climate of other regions through complex connections both on intra-seasonal timescales and even at 3-day forecast (Parker *et al*., 2018). Therefore, the development of climate change (CC) projections in this region is of critical importance. These climate change projections make it possible to measure the vulnerability of these regions and thus anticipate the adverse consequences that will result from them by putting in place effective adaptation strategies. Scenes of climate change (CC) have often been made using global climate models (GCMs) in this region (Semyon *et al*., 2001). Several Global Climate Models (GCMs) were used in the Coupled Model Intercomparison Project (CMIP) to understand and project the climates of Africa in general and West Africa sub-region in particular for present, near and far future periods. Climate model data is accessible through the World Climate Research Program (WCRP), which oversees the various phases of CMIP (Meehl *et al*., 2000). This effort has been in place for over 20 years and gradually updated to improve understanding of climate science. For example, when phase 3 of analysed km in the ocean (Meehl *et al.,* 2007) but seven years later, phase 5 of the CMIP (CMIP5) was released with improved resolution of 150 km and 100 km respectively for continent and ocean, (Taylor *et al*., 2012). Given the variability of the climate and sometimes, the dramatic consequences that these can entail, the evolution of water resources is a matter of concern for many regions of the world. This is true for the African countries of the Sudano-Sahelian zone, which have been subjected to persistent drought for about thirty years (Servat *et al*., 1998; Ardoin *et al*., 2003). The economy of Mali is essentially based on agriculture and livestock which depend largely on climatic conditions and in particular on rainfall. The continental intertropical climate is characterized by the alternation of a long dry season and a rainy season ranging from 2 months in the northern part to 5-6 months in the South. Precipitation is irregular in space and time and ranges from less than 100 mm in the north to more than 1,200 mm in the south (DIARRA. 2020).

1.2 Aims and Objectives

1.2.1 Aims

The goal of the study is to evaluate the performances of some selected GCMs of CMIP6 in reproducing the spatio-temporal patterns of climate variables and analyse the future climate scenario in Inner-Niger-delta of Mali and over the entire West African sub-region. The climate change scenarios projections were incorporated into hydrologic models to assess the projected density of the Inner-Niger-delta wetland of Mali.

1.2.2 Specific objectives

Specifical objectives of the research are to:

(i) evaluate the performances of CORDEX models ensemble members and mean on some climatic variables over West Africa;

(ii) analyse the future changes in some climatic variables for near-term period (2021-2060) and long-term period (2061-2100) under RCP 2.6 and RCP8.5 scenarios across West Africa; and

(iii) evaluate and apply the Soil and Water Assessment Tool (SWAT) model to assess the projected CMIP6-based climate change scenarios on some agro-hydrological parameters of the Inner-Niger-delta wetland.

1.3 Justification of the study

Since the end of the 1960s, West Africa (particularly the Sahel) has experienced decades-long episodes of drought with disastrous consequences for the economy and local societies. Many scientists have tried to study the possible causes of this climatic variation. (Hulme *et al*., 2001; Sharon and Nicholson, 2009; and Oettli *et al*., 2011). Mali is a rural country with a large part of the population living in village communities characterized by an organization where the different socio-economic units overlap, with agricultural production (in the broad sense) as their main activity. Nearly 75% of the active population is employed in agriculture and the primary sector represents 33% to 38% of total GDP depending on the year (UNDP 2012). Even in urban areas, a substantial part of the population practices agriculture. Mali is a poor country with, in 2011, a human development index of 0.359 ranked 175th out of 187 countries (UNDP 2012). In 2010, the incidence of monetary poverty was 44% for the whole country and 51% in rural areas. It is in rural areas that extreme poverty (insufficient standard of living to meet basic nutritional needs) is the highest with 27% of the population concerned compared to less than 12% in urban areas (INSTAT, 2011). Mali’s population is projected to increase from 14 million (2011) to 40 million people in 2050 (van Vuuren *et al*., 2007; IIASA, 2011). Food and energy demand as well as improving living standards will increase the pressure on natural resources (CityMayors, 2010). Mali's economy is essentially based on agriculture and livestock which largely depend on climatic conditions and in particular rainfall. Rainfall is controlled by the West African monsoon regime (meteo-Mali report 2016). Observed as well as simulated reservoir management has significant impacts on the Niger’s flow regime. Peak discharges, that are required to inundate large areas within the IND, are reduced during the rainy season, whereas more water is released during the dry season and thus increases the discharges in the low flow period (Zwarts *et al*., 2005).

1.4 Research questions

The catastrophic consequences of the last long period of drought in the Sahel in the 1970s and 1980s led to a strong mobilization of the scientific community in terms of water resources, health and food security for local populations. This poses the problem of the economic dependence of the affected countries, of the development of their agriculture and their breeding (AMMA, 2005). Climate change will have impacts on agriculture in developing countries (IPCC, 2001).

Indeed, GCMs are consistent when it comes to simulating the distribution of changes in temperature or precipitation over a very large spatial scale (tropics, mid-latitudes, etc.). However, at the scale of a particular region, the differences are notable (Bollasina *et al*., 2011; Su *et al*. 2013; Bacmeister *et al*., 2014). The performance of these GCMs is limited by factors which are linked among other things to their coarse resolution which does not allow taking into account the heterogeneities of the surface (variations in vegetation, complex topography, etc.)

The research study answers the following research question:

1- what is the performance of CORDEX models in reproducing the climate of West Africa?
2- What is the impact of climate change on the Inner Niger Delta wetland in long term?
3- How improves adaptation measures of climate change?

1.5 Contributions to knowledge

The following are the contributions of the research to knowledge.

a) It ascertains the reliability of CMIP6 and CORDEX models simulations in capturing key climatic variables across West Africa;

b) enhance understanding of how climate change affects the hydrology and ecosystem dynamics of the Inner Niger Delta wetland and

c) contribute to developing more effective climate adaptation strategies.

1.6 Limitations of the research

A number of limitations are considered in this research:

- The lack of observation data and meteorological infrastructure of the inner Niger delta.

- the RCMs do not simulate the parameters necessary for a complete agrometeorological study.

- the insecurity since 2012 makes the IND an unstable zone.

1.7 Research Outline

This thesis is organized into 5 chapters staring from chapter 1, a brief introduction of the research topic. Chapter 2 is a review of relevant literatures on climate change in West Africa and possible impacts on its ecosystems. Chapter 3 is a description of materials, methods and study area. Chapter 4 presents results and discussion of impact of climate change on the IND wetland. Chapter 5 presents conclusion of impact of climate change on the IND wetland and recommendation for future studies for more scientific added values in the field of impact of climate change on the IND wetland.

CHAPTER TWO

LITERATURE REVIEW

2.1 West Africa atmospheric dynamics

The climate of West Africa (WA) is largely influenced by prevailing wind patterns. The seasonal changes throughout the year are determined by the movement of two major subtropical anticyclones: (1) the Sahara anticyclone, which moves from the southwest to the northeast and produces the dry, hot "harmattan" wind; and (2) the "Saint Helena" anticyclone, which generates the "monsoon" — a cool, moisture-laden sea breeze that travels from the southeast to the northwest over the South Atlantic Ocean (Figure 2.1). The dynamic contact of these two warm dry air masses from the North (harmattan) and wet from the South (monsoon) is the Inter tropical discontinuity (ITD) over the continent of West Africa and the intertropical convergence zone (ITCZ) over Oceans and other parts (Hamilton and Archbold, 1945; Adejokun 1965; and Leroux, 1997). The seasonal pattern of atmospheric circulation is the most consistent factor influencing year-to-year variations in rainfall. A key element in agricultural planning is the timing of the rainy season's onset (Steward, 1994), which is largely determined by the position of the Intertropical Convergence Zone (ITCZ). The ITCZ represents the boundary between the Hadley cell circulations of the Northern and Southern Hemispheres. In West Africa, the ITCZ's movement reflects the transition from the dry northern winter (characterized by Harmattan winds reaching the Guinean coast) to the wet northern summer, when southwesterly monsoon winds bring moisture inland and produce rainfall (Geen *et al.,* 2020).

The West African monsoon onset follows two distinct stages: the pre-onset and the actual onset. The pre-onset typically occurs around mid-May (~14 May), when the ITCZ stabilizes near 5°N.

The actual onset is marked by a rapid northward shift of the ITCZ around late June (~24 June), moving it to approximately 10°N, where it remains throughout August. This northward shift causes the monsoon to have a bimodal rainfall pattern in the Guinea region and a single-peak pattern in the Sahel (Sultan and Janicot, 2003). Often, the beginning of the rainy season is gradual, with early, scattered showers and intermittent dry periods, which can be mistaken for the actual start of the season.

Several researchers (e.g., Hastenrath, 2000; Nesbitt and Zipser, 2003; Stuut *et al.,* 2005) have described the average summer atmospheric circulation over West Africa. Moist southwesterly winds penetrate the continent due to pressure and temperature differences between the cool ocean and the hot desert interior. In the vertical wind profile, two significant jet streams are observed: the African Easterly Jet (AEJ) around 600 hPa and the Tropical Easterly Jet (TEJ) near 150 hPa. These jets significantly influence rainfall patterns—stronger AEJ conditions are typically linked to reduced monsoon activity and dry spells, whereas a more intense TEJ correlates with wetter conditions (Jenkins *et al.,* 2002; Nicholson and Klotter, 2020).

In addition to these mid- and upper-level wind systems, reduced rainfall is also associated with:

(a) strengthening of the Azores anticyclone and weakening of the St. Helena anticyclone, accompanied by warmer sea surface temperatures (SSTs) in the equatorial and southern Atlantic and cooler SSTs in the North Atlantic, which cause the ITCZ to shift southward; and

(b) increased sea-level pressure over the northeastern Atlantic (Jackson *et al*., 2009; Janicot *et al.,* 2009; Nicholson, 2018).

Rainfall patterns in West Africa are defined by a migrating zone of peak precipitation that shifts northward and southward throughout the year. This rainfall zone is situated just south of the surface location of the Intertropical Discontinuity (ITD) and moves in a pattern that closely mirrors the seasonal movement of the Intertropical Convergence Zone (ITCZ). The primary rain belt serves as the center of atmospheric disturbances that are dynamically connected to the mid-level African Easterly Jet (AEJ). The main convective systems in this region are westward-moving mesoscale disturbances known as cloud clusters. Whether these systems develop into long-lasting organized convection depends on various environmental conditions, including vertical wind shear, available buoyant energy, low-level jet activity, and geographic latitude (Laing and Fritsch, 1993). The occurrence and rainfall output of these cloud clusters are further influenced by transient synoptic-scale African Easterly Waves (AEWs) (Houze and Betts, 1981; Thompson *et al.,* 1979).

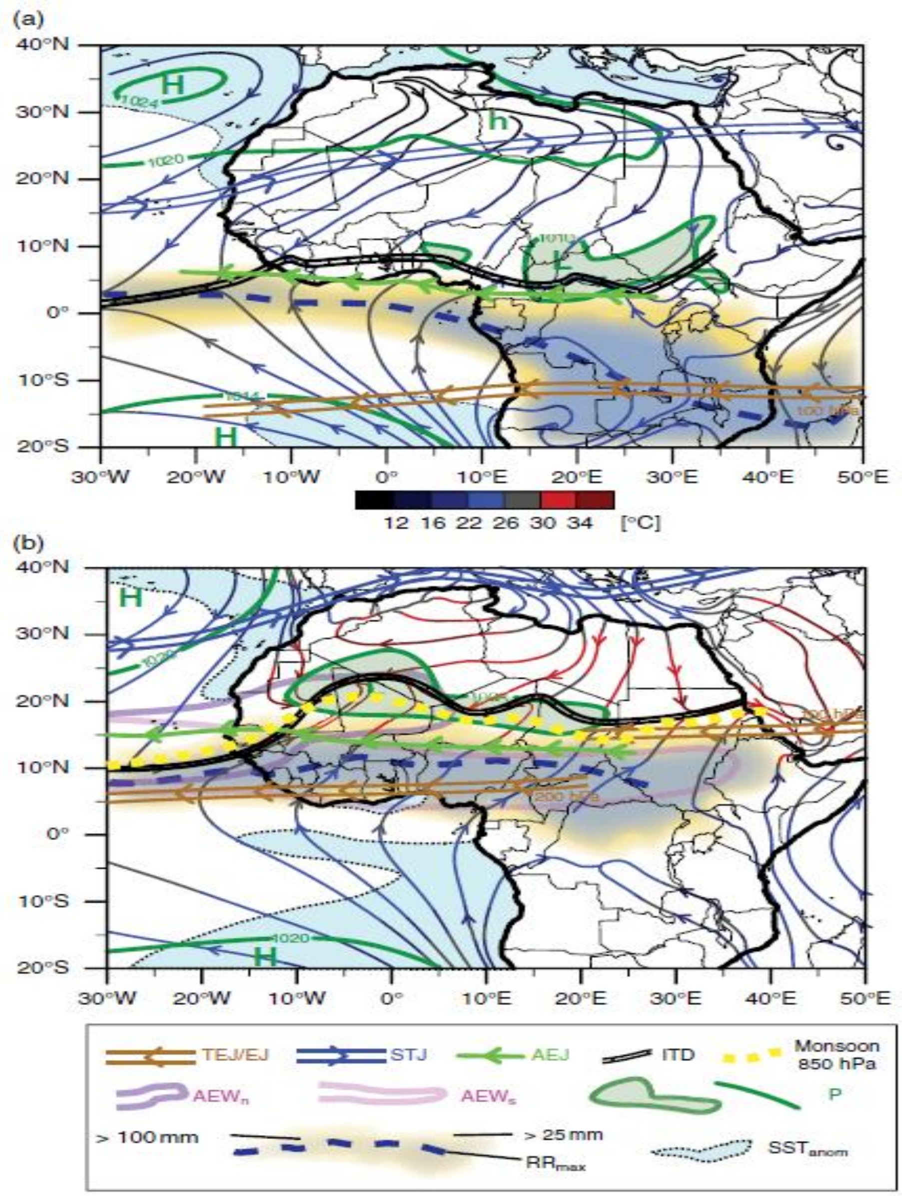

Figure 2.1: Schematic illustration of atmospheric and oceanic features determining the weather and climate of West Africa in (a) January and (b) July (Parker *et al*., 2018).

2.2 The West African Monsoon

In West Africa, as in many tropical regions, rainfall is the most influential weather factor shaping the region's climate. Rainfall across the area is highly variable both spatially and temporally, often leading to favorable or adverse conditions that significantly affect the region's socioeconomic development. Due to its importance, numerous studies have examined various aspects of rainfall patterns in the region (e.g., Druyan, 2011; Daron, 2014; Koudahe *et al*., 2017).

The variability in rainfall over West Africa is primarily controlled by the West African Monsoon (WAM) system, which is strongly influenced by changes in global sea surface temperatures (SSTs) and regional land surface conditions across different timescales (Lu and Delworth, 2005; Dezfuli and Nicholson, 2013; Dieppois *et al*., 2013, 2015). The WAM delivers the bulk of the region's annual rainfall and is driven by the seasonal, radiation-forced shift of the Intertropical Convergence Zone (ITCZ). While it follows a clear annual cycle, the monsoon also exhibits significant variability across multiple timescales.

Intra-seasonal and interannual fluctuations of the WAM have been extensively studied, as they play a critical role in the region's climate dynamics. Superimposed on these longer-term variations are short-term dry spells or drought years, which can have severe environmental and socioeconomic consequences particularly in the Sahel, where agriculture relies heavily on rainfall. As a result, accurately predicting the onset, duration, and distribution of rainfall during the monsoon season is essential for farmers and humanitarian planning.

However, major gaps remain in our understanding of WAM variability, largely due to insufficient observational data. This challenge led to the launch of the African Monsoon Multidisciplinary Analysis (AMMA) project in 2003 to improve scientific knowledge and forecasting capabilities

(Redelsperger *et al.,* 2006). During the rainy season, the WAM dominates the region's climate and contributes more than 75% of the annual rainfall in most areas (Hagos and Cook, 2007). The behavior of the WAM fluctuates at intra-seasonal, inter-seasonal, and interannual scales. The emergence of the changing climate, largely ascribed to human-induced anthropogenic activities, can further amplify these variations thereby causing serious consequences for human health and well-being, agriculture and food security, water resources and hydrological cycles (IPCC, 2007, 2013, 2018). The WAM is prone to large interannual rainfall variability with significant consequences on human and socioeconomic outputs. This is partly due to high dependence on rainfed agriculture, which is already threatened by insufficient rainfall. Therefore, a better knowledge of how climate change will influence the WAM and how such changes will impact socioeconomic outcomes including crop productivity is key to inform policies that may reduce the adverse effects and ensure food security in the region (Sultan and Gaetani, 2016). Thus, the need to improve modeling of the monsoon system and to better quantify the uncertainty in its variability under a warming climate.

2.3 Rainfall Variability and Its Extremes Events Over West Africa

Disasters triggered by extreme weather events are among the most significant contributors to natural catastrophes globally, according to the Emergency Events Database (EM-DAT). Among meteorological variables, precipitation plays a critical role in directly impacting both human life and natural systems. Its extreme variability can lead to severe consequences for society and the environment (Limsakul and Singhruck, 2016). In West Africa, fluctuations in rainfall and river flow intensify water resource management challenges, which in turn influence a wide range of socio-economic problems (Goulden *et al*., 2009).

Droughts and floods alone account for nearly 80% of natural disaster-related deaths and around 70% of economic damages in Sub-Saharan Africa (World Bank, 2010; Vicente-Serrano *et al.,* 2012). Since the 1950s, unprecedented climate changes—largely driven by anthropogenic global warming—have been observed (IPCC, 2014). Variability in rainfall often results in extreme weather events such as heavy downpours, leading to floods, or prolonged dry periods, resulting in drought. In recent years, flooding events have become more intense and frequent, making them a pressing global issue. The social and economic consequences of these events are extensively covered in Intergovernmental Panel on Climate Change (IPCC) assessments (e.g., IPCC, 2013).

Globally, floods affect an estimated 350 million people, and forecasts suggest that flood-related destruction may double by 2050. As one of the most devastating environmental hazards, floods have gained significant attention, especially in the context of ongoing ecological and climatic changes. Rapid population growth and increased urban development have further heightened flood risks. As urbanization continues, the potential impact of flooding is expected to rise accordingly (Walker and Burningham, 2011).

Floods not only cause substantial economic losses but also damage ecosystems and cultural heritage (Jonkman and Vrijling, 2008). Additionally, they pose a threat to human life and contribute to a variety of health issues (Hajat *et al.,* 2005). Gaining a solid understanding of the patterns and future trends of extreme rainfall and flooding is crucial for crafting effective adaptation strategies to mitigate their effects on people and ecosystems. This is especially vital as global warming is anticipated to intensify extreme rainfall events, due to increased atmospheric moisture content. According to the thermodynamic Clausius–Clapeyron principle, the water-holding capacity of the atmosphere rises by about 6–7% for every degree Celsius of temperature increase (Allen and Ingram, 2002; Ingram, 2016).

Flooding, though a natural phenomenon, can lead to widespread destruction, disrupt daily life, and heighten various vulnerabilities—physical, social, economic, and environmental. It is generally defined as the rise of water levels in coastal zones, rivers, reservoirs, and canals beyond their normal limits (Clement, 2013).

Numerous hydrological studies have studied the consequences of the delta on the Niger flood (e g. Nashwan *et al*., 2019; Brunet-Moret *et al*., 1986 and Adnan *et al*., 2019). Thus, due to the flooding, the temporary storage of large quantities of water causes the damping of the flood wave at the exit of the delta. In addition, these floods induce significant water losses by evaporation (the losses by infiltration being negligible), hence the expression of evaporative machine which is perfectly suited to the interior delta of the Niger. These two characteristics of the overall hydrological functioning of the delta are of course closely linked; they are a function of the spatio-temporal extension of the flooding, and therefore of the hydroclimatic conditions (Orange *et al*., 2000). The water loss of the "delta" hydrosystem therefore increases with the annual inflow. It represents 30 to 45% of total water inputs depending on the hydraulicity of the year (Picouet, 1999) and is mainly due to evaporation from the surface of free water (Mahé *et al*., 2000). Water resources have always been an issue for human civilizations.

2.4 Review of downscaling approaches

The formation of precipitation encompasses numerous physical processes, ranging from microscopic droplet interactions within clouds and atmospheric convection to large-scale synoptic weather systems. Accurately representing these complex dynamics is essential to effectively model the high spatial and temporal variability and intermittency of precipitation (IPCC, 2021). Global Climate Models (GCMs) serve as important tools for understanding the Earth's climate—past, present, and potential future scenarios. These models have diverse applications across Earth sciences, engineering, and risk management. Despite their usefulness, GCMs typically function at coarse spatial resolutions, often averaging conditions over areas exceeding one hundred square kilometers. While such scale is suitable for global assessments, it offers limited precision for local or regional predictions (Groenke *et al.,* 2020). Downscaling is an essential method for translating global climate model (GCM) outputs into data at finer spatial resolution, thereby enabling a better understanding of climate impacts at local scales. The variety of downscaling techniques mirrors the differing objectives and available resources for each climate assessment (Trzaska *et al.,* 2014). There is no universally optimal downscaling method; the choice depends on factors such as the required spatial and temporal resolution and the specific climate impacts being studied (Trzaska *et al.,* 2014). Downscaling approaches generally fall into two main categories: statistical downscaling (SD) and dynamical downscaling (DD), the latter often referred to as regional climate models (RCMs). Both approaches can produce station-level data suitable for watershed modeling. However, each method has its own strengths and limitations, particularly regarding ease of application and ability to capture changes in temporal patterns (Flato *et al.,* 2014). The effectiveness of a method is influenced by how accurately it can: (1) resolve fine-scale features like topography and land use; (2) simulate relevant processes and interactions such as weather systems; and (3) apply physical parameterizations at the targeted spatial and temporal resolutions (Rauscher *et al.,* 2010).

2.5 Trends and Prospects from Climatic Research of Inner-Niger-Delta Wetland

The full development of this subsection is published by Maiga *et al.,* (2025).

Summary

The fate of wetlands in arid regions has become a matter of concern in the context of global

warming. The Inner Niger Delta (IND) has received increasing attention from researchers and others to explore whether this largest wetland in Africa will shrivel due to climate change and increasing water use. An essential study goal is to understand what has been done so far in the Research of Inner-Niger-Delta Wetland in order to address its future challenges. The present study provides a comprehensive analysis of climate related research on the IND wetland through bibliometric means to diagnosis the evolution, lag and hotspot of relevant features in the literature. Key aspects of analysis included: (i) trends of IND wetland related research; (ii) nature of collaboration networks; (iii) co-occurrence of keywords; and (iv) emerging themes related to IND wetland over the last three decades, between the years 1991-2022. The results indicate that the IND wetland gained momentum in 2000, peaking in 2013 and then in 2018. IND wetland research has, on average, reached 2.5 publication in 2000 and exceeded 5 papers by 2017. The leading countries that have produced high numbers of published documents were in the order, France, Nigeria, USA, Germany and Mali. Therefore, more efficient scientific collaboration among regional African institutions is recommended to face local perspectives. The identified emerging topics are Niger delta, climate change, floods and rivers. The variables considered in analyses are river discharge, evapotranspiration, water level and rain. Variables relevant to global temperature warming are missing which implies that researches on Inner Niger Delta wetland are less focusing on climate change and variability analyses.

CHAPTER THREE

RESEARCH METHODOLOGY

3.1 Study area

The Inner Niger Delta (IND) in Mali, is the biggest floodplains in Africa covering four million hectares and supporting over one million herders, fishermen and farmers (De Noray, 2003; Zwarts *et al*., 2005). IND wetland represents a vast natural resource that continues to attract many people to live in and around the delta (Liersch *et al*., 2012; Zwarts *et al*., 2005). Wetlands are a valuable natural resource of considerable scientific interest because they are associated with biological diversity, important ecosystem functions and processes, and useful, economically viable products (Mitsch and Gosselink, 1993). Floodplains play a vital role in preserving biodiversity and providing environmental services to human populations (Di Baldassarre, 2012). Since the beginning of the drought in the early 1970s, the IND wetland has been faced with a problem of sustainability of renewable natural resources. The management of these fragile resources, by a population with diverse practices (agriculture, livestock, fishing) in order to ensure their sustainability, involves multiple decision-making criteria and constraints (Kuper *et al*., 2003). Wetlands provide a wide range of ecosystem services that contribute to human well-being, such as fish and fibre, water supply, maintenance of water quality, climate regulation, flood regulation, coastal protection, and recreation and tourism opportunities (Millennium Ecosystem Assessment, 2005). Wetlands are also critical for the conservation of biological diversity. There is increasing recognition of the value of these functions and other ecosystem services provided by wetlands. In particular, wetlands are vitally important for providing the regulating and supporting ecosystem services that underpin water resources management, and can thus be considered as essential components of overall water infrastructure (Emerton and Bos, 2004). Liersch *et al*., (2012) investigated the impacts of climate change and upstream water management on food production in the IND under two population growth scenarios. In their work, the focus was on the assessment of external impacts on the carrying capacity of the IND with regard to the number of people that can be supported by the ecosystem service related to rice production.

During and after the rainy season in Mali (June–October), large areas of the IND are flooded. Naturally, these floodplains provide vital habitats supporting livelihoods in fishing, farming, and stock farming (Zwarts *et al*., 2006). Being already subject to large interannual variations of rainfall, particularly in the Niger and Bani headwaters, these habitats are additionally threatened by a variety of anthropogenic pressures and unsustainable uses (WWF, 2008). All activities in the area of IND wetland are highly depending on flooding patterns and duration, water depths, and the management practices. Hence, all factors that influence the inflow into the wetland. The spatio-temporal inundation patterns within the IND wetland have an impact on food production and food security in the wetland area. Mali's population is projected to increase from 14 million (2011) to 40 million people in 2050 (van Vuuren *et al*., 2007). Food and energy demand as well as improving living standards will increase the pressure on natural resources. Thus, studying the sustainability and the vulnerability of the IND wetland is as important to insure the demand of the growing population. The present study seeks to provides a comprehensive review on trends and prospects of climate-based research on the IND wetland during the last three decades.

3.1.1 Relief

The Inner Niger Delta, located in central Mali, is a vast alluvial plain marked by a generally flat topography, shaped by the fluctuations of the Niger River and its tributaries. This region, characterized by low altitudes below 300 meters, is dominated by sedimentary deposits accumulated over millennia. During the rainy season, the Niger River overflows, transforming the plain into a vast expanse of shallow water, dotted with temporary lakes such as Lake Débo and river channels. These characteristics create a dynamic environment, with landscapes that evolve in rhythm with the hydrological cycles (Gallais, 1967).

The Inner Niger Delta can be divided into homogeneous land areas based on a combination of hydrographic, ecological, demographic and socio-economic factors. There are several divisions, of which we mention here that of Quensiere (1994, after Gallais 1967). Quensiere (1994) divides the Delta into four hydrographic zones.

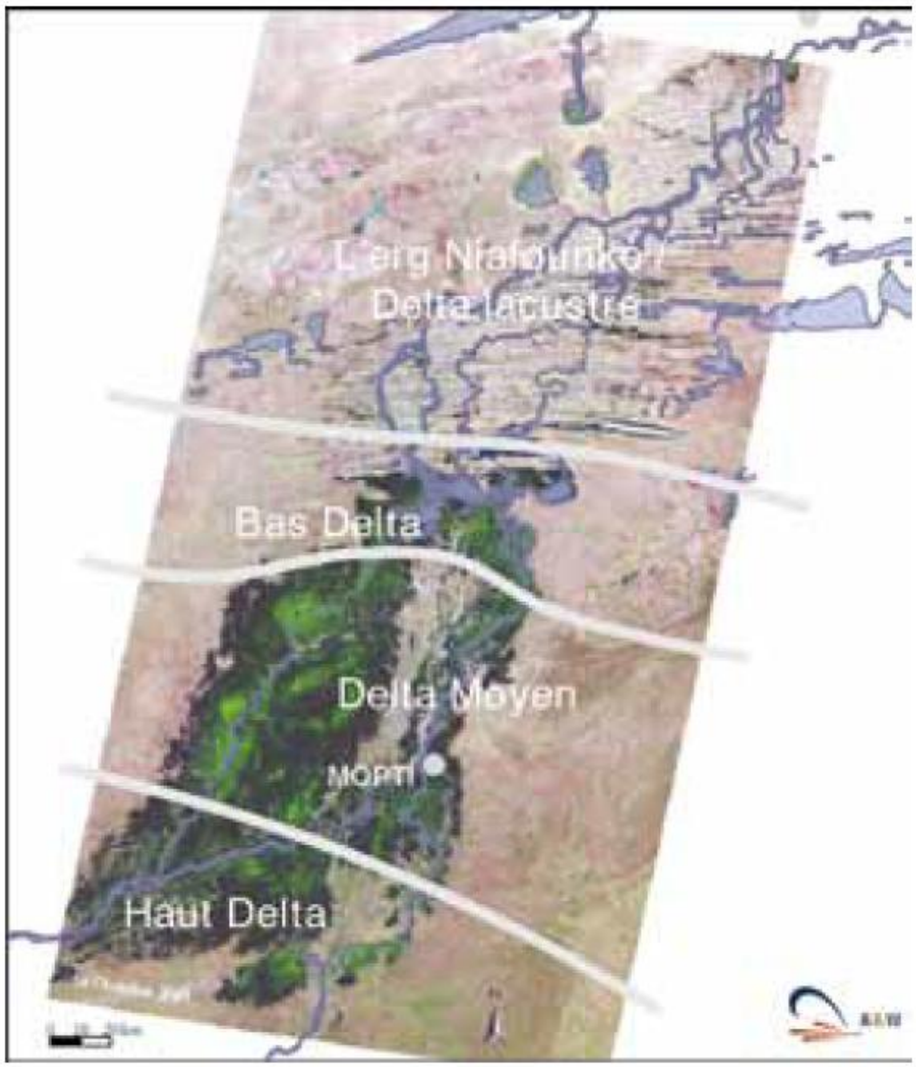

Figure 3.1: Division of the Delta into four zones, according to Quensière (1994, after Gallais 1967)

3.1.2 Climate of IND

Mali is a landlocked country in West Africa covering an area of approximately 1.24 million km^2, 51 percent of which is desert land. Cultivated areas (arable land and land under permanent crops) occupy 43.7 million ha, or 35 percent of the total area. with a Sudano-Sahelian climate characterized by very high average temperatures and the alternation of a wet rainy season (June to September) and a dry season lasting between five and nine months (October–November to May–June). Average precipitation (280 mm/year) decreases from south to north (Bathily 1991).

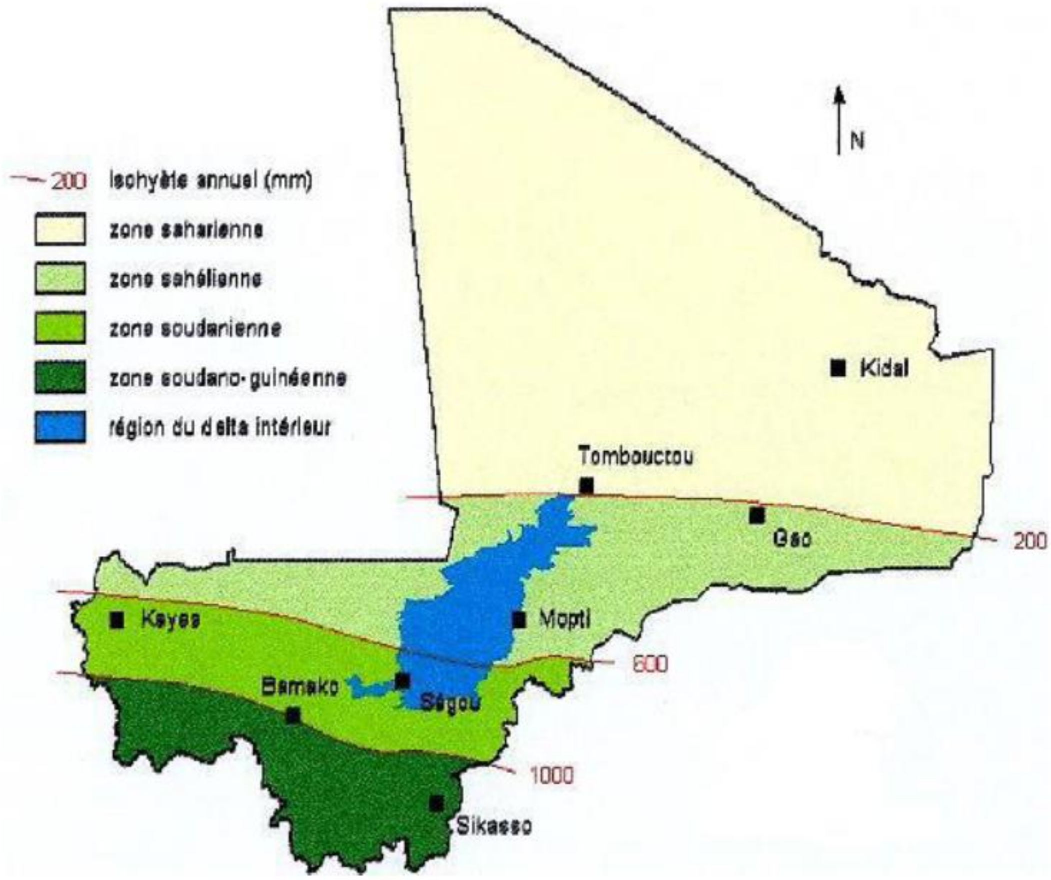

Figure 3.2: Main agro-climate zones of Mali and annually flooded area of the Inner Niger Delta (from FAO)

The country is divided into four major agroclimatic zones:

(i) the Sudano-Guinean or sub-humid zone, covering 6 percent of the country's total area in the south, is characterized by wooded savannah and forests; rainfall exceeds 1,200 mm;

(ii) the Sudanian zone, covering 17 percent of the national territory in the center, is characterized by more or less dense and varied plant cover (Sudanian savannah); rainfall varies from 600 to 1,200 mm;

(iii) the Sahelian zone, covering 26 percent of the territory in the north, has rainfall of 200 to 600 mm; this zone occupies most of the inner Niger Delta (which constitutes a separate agro-ecological zone) with many areas flooded for part of the year and areas of rain-fed agriculture; and

(iv) the Saharan zone, covering 51 percent of the country's total area, extends across the northernmost region, where rainfall is less than 200 mm.

3.1.3 Hydrography

The hydrographic network of the Inner Niger Delta (IND) is a complex system primarily shaped by the Niger River and its tributary, the Bani River. This wetland region is characterized by a vast array of canals, lakes, and swamps, which play a crucial role in the hydrology and ecology of the area.

Table 3.1: The IND Wetland areas from different publications

Publication	Total wetland area (km^2)
(Olivry, 1995)	50 000
(Kuper *et al*., 2003)	36000
(Schuol *et al*., 2008)	80000
(Mahé *et al*., 2009)	73000
(Seiler *et al*., 2009)	40000
(Rebelo *et al*., 2012)	41195
(Ogilvie *et al*., 2015)	20000
(Dembele and Ye, 2017)	11558

3.2 Data sources

3.2.1 Observational data

3.2.1.1 ERA5 data

ERA5 is the fifth-generation atmospheric reanalysis dataset produced by the European Centre for Medium-Range Weather Forecasts (ECMWF) using advanced modeling and data assimilation methods (Hersbach *et al.,* 2020). The ERA5 dataset provides a large number of atmospheric, land, and oceanic climate variables, including more than 200 parameters and variables, spanning from 1940 to the present date in near-real-time. The data covers the Earth on a horizontal resolution of 30km X 30km (0.25^{O} X 0.25^{O}) and resolve the atmosphere using 137 levels from the surface up to a height of 80 km. At the same time, ERA5 also provides a single level dataset, such as precipitation, top of atmosphere radiation, and vertical integrals over the entire depth of the atmosphere (https://www.ecmwf.int/en/forecasts/dataset/ecmwf-reanalysis-v5).

3.2.1.2 In-situ data

The station data used in these studies refer to the meteorological variables recorded at the stations in the wetland and surrounding. Daily precipitation from 1970 to 2005 for the stations of Mopti, Dire, Tombouctou. Daily water level and stream flow from 1990 to 2010 for the stations of Mopti, Dire, Tombouctou.

Table 3.2: The in-situ data and duration collected over the IND

Climatic Variable	Mopti	Dire	Tombouctou
Precipitation	1970 to 2019	1970 to 2019	1970 to 2019
Precipitation	1970 to 2019	1970 to 2019	1970 to 2019
stream flow	1990 to 2010	1990 to 2010	1990 to 2010
water level	1990 to 2010	1990 to 2010	1990 to 2010

3.2.2 Regional climate models and their deriving datasets

3.2.2.1 CORDEX-Africa simulations

The World Climate Research Program (WRCP) sponsors the Coordinated Regional Climate Downscaling Experiment (Giorgi *et al*., 2009; Jones *et al*., 2011; Nikulin *et al*., 2018; https://www.cordex.org/) to harmonize international efforts in downscaling GCMs to the regional level at a horizontal resolution of 0.44°×0.44° and later improved to 0.22°×0.22° in 2019. Datasets are obtained from the three regional climate models (RCMs), CCLM5-0-15 (Sørland *et al*., 2021), RegCM4-7 (Giorgi *et al.,* 2021) and REMO (Remedio *et al*., 2019) from CORDEX-CORE (AFR-22) each was forced by three different global climate models (GCMs), namely MPI-M-MPI-ESM-LR (Giorgetta *et al*., 2013; Stevens *et al*., 2013), NCC-NorESM1-M (Bentsen *et al*., 2013; Iversen *et al.,* 2013), MOHC-HadGEM2-ES and ERA-Interim (Dee *et al*., 2011), and the European Centre for Medium-Range Weather Forecasts Reanalysis (ECMWF-ERAINT) (Dee *et al*., 2011). Available CORDEX-CORE (AFR 22) RCM historical dynamically downscaled simulations data are for the period 1950–2005, 1970–2005 and 1970–2005 for, respectively, CCLM5-0-15, RegCM4-7 and REMO2015 (https://cordex.org/experiment-guidelines/cordex-core/). Due to inadequate quality ground observation data, climate change vulnerability, and the low adaptive capacity of Africa, CORDEX has been treating the continent of Africa as a priority, and an essential domain among other regions covering the larger populated landed areas. The performance of CORDEX RCMs over West Africa has been examined in the past by many studies (Diallo *et al*., 2012; Sylla *et al*., 2013; Klutse *et al*., 2016) as it has been done over other parts of Africa (Maure *et al*., 2018; Ayugi *et al*., 2020). Most of these studies make use of either the output of the first phase of the CORDEX RCMs when ERA-Interim reanalysis was used as driven run (Dee *et al*., 2011; Akinsanola *et al*., 2017) or the second phase when CORDEX RCMs dynamically downscaled CMIP5 GCMs to a lower resolution of 0.44°×0.44° (Taylor *et al*., 2012).

Table 3.3: Some characteristics of the RCMs used

	RCM1: CCLM	RCM2: RegCM	RCM3: REMO
Model version	CCLM5-0-15 (Sørland *et al.,* 2021)	RegCM4-7 (Giorgi *et al*., 2021)	REMO2015 (Remedio *et al*., 2019)
Institution	CLMcom-KIT	ICTP	GERICS
Grid resolution	0.22° × 0.22°	0.22° × 0.22°	0.22° × 0.22°
Vertical levels	51	23	27
Map projection	Rotated pole 0.22◦	Oblique Mercator	Rotated pole 0.22◦
Planetary boundary layer	Turbulent kinetic energy-based surface transfer and PBL parameterization (Raschendorfer, 2001)	Holtslag PBL (Holtslag *et al*. 1990)	Turbulent kinetic energy-based surface transfer and PBL parameterization (Louis, 1979)
Cumulus	Tiedtke parameterization for convection (Tiedtke, 1989)	Tiedtke parameterization for convection (Tiedtke, 1989)	Tiedtke (1989) with modifications from Nordeng (1994) and Pfeifer (2006)
Cloud microphysics scheme	Parameterization of precipitation based on four-category scheme that includes cloud water, rain water, snow, and ice microphysics (Doms *et al*., 2013)	From the European Centre for Medium Weather Forecast's Integrated Forecast System (IFS) (Tiedtke, 1993; Nogherotto *et al*., 2016)	Cloud microphysics scheme by Lohmann and Roeckner (1996)

3.2.2.2 CMIP6 data

The Coupled Model Intercomparison Project Phase 6 (CMIP6) represents the latest state-of-the-art climate simulations for future projections based on Shared Socioeconomic Pathways (SSPs) (Eyring *et al*., 2016). The CMIP6 provide an opportunity to improve our understanding of climate change impacts resulting from exacerbated global warming. Policymakers and community workers are in dire need of timely information that will enable them to address pertinent issues such as those that pinpoint exact tendencies of historical changes, the magnitude of the shift, and future projections. Moreover, the new pathways representing a range of future greenhouse gas emissions and land use change scenarios promise a robust estimate of future projections of hydroclimate variables. They incorporate various assumptions about socio-economic growth, climate mitigation efforts, and global governance (O'Neill *et al*., 2016).

Table 3.4: The CMIP6 global climate models (GCMs) used as driving fields in the present CORDEX-CORE Ensemble

Name	Institution	Horizontal resolution	Vertical levels	References
HadGEM2-ES	MOHC	0.55° ×0.83°	38	(Andrews *et al*., 2020)
MPI-ESM-LR	MPI-M	0.932° ×0.937°	47	(Mauritsen *et al*., 2019; Müller *et al*., 2018)
NorESM1-M	NCC	0.947° ×1.25°	26	(Seland *et al*., 2020)

3.3 Methods of analysis

3.3.1 The correlation coefficient

The correlation coefficient (r) is used to measure the intensity of the linear connection between two variables. Between two variables OB and PR, it is obtained by the ratio:

$$r = \frac{cov(PR,OB)}{\sigma PR \times \sigma OB} \qquad \textbf{(3.1)}$$

where $\sigma PR, \sigma OB$ are the standard deviations of PR and OB respectively, and $cov(PR, OB)$ their covariance. Its value is between -1 and 1.

3.3.2 Mean Bias

The mean bias measures the difference between actual measured and expected physical quantities.

If M_i is the forecast on date i and O_i is the observation on date i, the bias between the forecast and the observation on date i is given by the following relation:

$$b_i = M_i - O_i \qquad \textbf{(3.2)}$$

The average bias over a long period of time is given by:

$$MB = \frac{1}{N}\sum_{i=1}^{N}(M_i - O_i) \qquad \textbf{(3.3)}$$

3.3.3 The Root Mean Square Error

The Root Mean Square Error (RMSE) is a commonly used statistic that provides a good overall measure of how close modelled values are to predicted values.

$$RMSE = \sqrt[2]{\frac{\sum_{i=1}^{n}(M_i - O_i)^2}{n}} \qquad \textbf{(3.4)}$$

where O_i represents the ith observed value and M_i represents the ith model value for a total of n observations.

3.3.4 The SWAT Model

The Soil and Water Assessment Tool (SWAT) is one of the most extensively used eco-hydrological models internationally, as documented by previous review studies and a wide literature collection that now exceeds 5000 studies (CARD, 2022). Since it was developed, it has undergone continuous expansion of capabilities and improvement of many of its modules leading to its latest reconstructed version "SWAT+" (Bieger *et al*., 2017). The new SWAT model generation SWAT+ was developed in order to overcome the restricted potential flexibility that the current SWAT structure reached after thirty years of thriving development. SWAT + provides a more flexible spatial representation of interactions and processes within a watershed. Although lacking in calibration support, SWAT + has a number of advantages over SWAT in terms of database management, coding flexibility, connectivity, reservoir operation and aquifer boundary (Yen *et al*., 2019). The SWAT model is physically semi-distributed. It operates through the discretization of the watershed into spatially connected sub-catchments through a hydrographic drainage network. The sub-catchments are further sub-divided into hydrologic response units (HRUs), which correspond to lumped homogeneous units in terms of land use, soil type, and slope class. Hydrological processes are evaluated at the scale of HRUs and summed up at the sub-catchment level. The surface runoff is then routed to the watershed global outlet through the channel network.
level. The surface runoff is then routed to the watershed global outlet through the channel network.
The hydrological balance at the scale of HRUs in the SWAT model is calculated based on Equation (3.9) (Neitsch *et al*., 2011):

$$SW_t = SW_0 + \sum_{i=1}^{t}\left(P_i + Q_{s,i} + ET_i + w_i + Q_{gw,i}\right) \tag{3.9}$$

where $SW_t$and SW_0 are the soil water content and the initial soil water content at the beginning

of day i, t is the elapsed time (in days), P_i is the daily rainfall, $Q_{s,i}$ is the daily surface runoff, ET_i is the daily actual evapotranspiration, w_i is the daily seepage loss entering the vadose zone under the soil profile, and $Q_{gw,i}$ is the return flow from the aquifer. All these quantities are expressed in millimeters (mm). Surface runoff is estimated in this study through the Soil Conservation Service Curve Number (SCS-CN) method (Mockus, 1972; Neitsch *et al.*, 2011), given by Equation (3.10)

$$Q_{s,i} = (P_i - I_a)^2/(P_i - I_a + S)\,, S = 245 \times (100/CN - 1) \quad (3.10)$$

where Ia (in mm) is the initial abstraction defined as the amount of rainfall interception by

plant canopy or to fill in soil surface depression storage, occurring at the onset of a rainfall

event, S is the soil water retention parameter (in mm), defined as a function of soil, slope,

and Land use and land cover (LULC) type, and the CN parameter relates to S. The surface runoff obtained at the sub-basin level is transmitted to the watershed outlet using the variable travel time method and converted to discharge (Neitsch *et al.*, 2011).

CHAPTER FOUR

RESULTS AND DISCUSSIONS

4.1 Climate trend over West Africa

4.1.1 The monthly precipitation

Simple statistical methods are used to evaluate simulations of monthly precipitation, evaporation, and air temperature from CORDEX regional climate models between 1970 and 2005 against observational data from ERA5. These include the correlation coefficient (R), mean bias (Mbias) and root mean square error (RMSE). To facilitate a comparison with the monthly data results, we changed the horizontal resolution of the original CORDEX RCMs from $0.22^\circ \times 0.22^\circ$ to a grid of $0.25^\circ \times 0.25^\circ$ to standardize the grids. We compared the precipitation of the RCMs of CORDEX to that of ERA5.

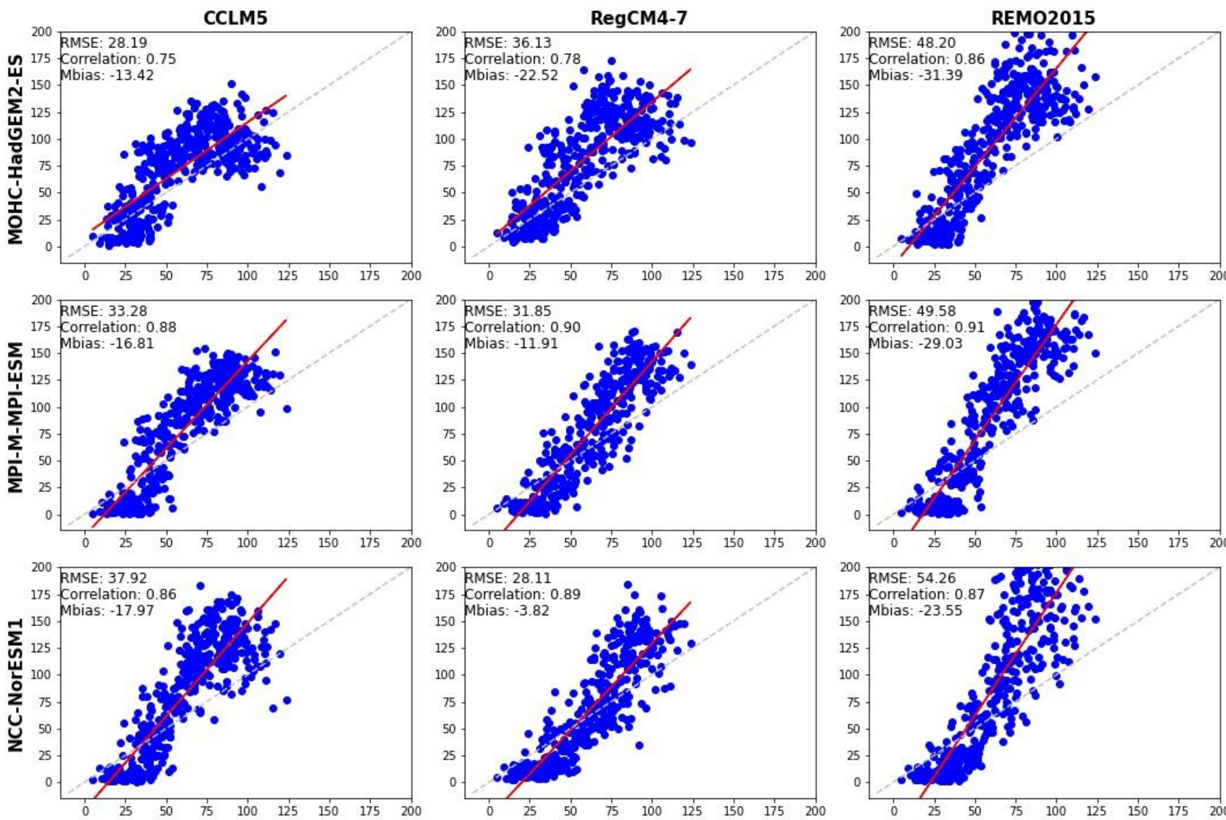

Figure 4.1: Statistical presentation of the ERA5 monthly mean precipitation and simulation of three RCMs driven by the three GCMs.

Figure 4.1 presents the statistical values of correlation coefficients (Rs), Root Mean Square Errors (RMSEs) and Mean Bias errors (Mbiases) between the ERA5 as observation and the simulations of the three RCMs: CCLM5 (in the first column); RegCM4.7 (in the second column); and REMO2015 (in the third column), while each of the three RCMs was driven by the three GCMs: MOHC-HadGEM2-ES in the first row; MPI-M-MPI-ESM (in the second row); and the NCC-NorESM1 (in the third row) over the entire west Africa from CORDEX . The statical values for Guines, Savanna and Sahel (and entire West Africa) are presented in Table 4.1.

Amongst the nine simulations metrics shown in Figure 4.1, the GCM with the highest correlation coefficient for all the three RCMs is the MPI-M-MPI-ESM (second row) with maximum values of 0.88 for CCLM, 0.90 for RegCM4.7, and 0.91 for REMO2015. The Mbias doesn't follow this pattern, as in there is no particular GCM or RCM with lowest/highest Mbias error but the Mbias is negative throughout. This implies that all the RCMs regardless of the driven GCM underestimate the mean monthly precipitation over West Africa sub-region. The RMSE values are lowest for RegCM4.7 driven by MPI-M-MPI-ESM and NCC-NorESM1 while CCLM5 has lowest with HadGEM2-ES as the driving GCM. All these values are tabulated in Table 4.1 with the worst and best for each of these statistical variables coloured in blue and red respectively.

Table 4.1: The correlation coefficients, Mbiases and RMSEs of monthly mean precipitation of ERA5 and simulated of the respective GCMs and RCMs.

		Guinea zone			Savannah			Sahel			West Africa		
RCM	**GCM**	**R**	**RMSE**	**Mbias**	**R**	**RMSE**	**Mbias**	**R**	**RMSE**	**Mbias**	**R**	**RMSE**	**Mbias**
	MOHC-HadGEM2-ES	0.71	87.71	-25.8	0.9	45.36	3.07	0.89	30.86	-12.53	0.75	28.19	-13.42
CCLM5	**MPI-M-MPI-ESM**	0.88	72.79	-17.64	0.92	43.09	-5.31	0.9	37.78	-19.4	0.88	33.28	-16.81
	NCC-NorESM1	0.85	99.65	-24.7	0.93	43.41	22.28	0.8	30.25	0.93	0.86	37.92	-17.97
	MOHC-HadGEM2-ES	0.68	151.53	-89.16	0.87	95.57	-49.36	0.78	33.9	-7.04	0.78	36.13	-22.52
RegCM4-7	**MPI-M-MPI-ESM**	0.81	84	-15.7	0.92	78.03	-30.48	0.84	42.15	-13.21	0.9	31.85	-22.91
	NCC-NorESM1	0.73	123.14	-25.64	0.9	53.97	-0.28	0.72	34.92	9.3	0.89	28.11	-3.82
	MOHC-HadGEM2-ES	0.82	137.68	-69.28	0.94	60.62	-24.37	0.91	27.34	-9.91	0.86	48.2	-31.39
REMO2015	**MPI-M-MPI-ESM**	0.88	101.89	-41.3	0.95	56.87	-24.02	0.9	31.13	-11.44	0.91	49.58	-29.03
	NCC-NorESM1	0.76	143.75	-37.45	0.94	38.54	12.56	0.83	30.39	11.77	0.87	54.26	-23.55

The results show that the values of R reach 0.91 in the Sahel, 0.95 in the savannah and 0.88 for the Guinea Coast (Table 4.5). The negative Mbias in the scatter plots show an underestimation of the monthly precipitation estimate from the RCMs compared to the ERA5 data in the three regions (Table 4.5). The RMSE oscillate between 84 and 151.53 in the coastal zone, in the savannah between 38.54 and 78.03 and in the Sahel zone between 27.34 and 42.15 (Table 4.5), these results are similar to those of (Ilori and Balogun., 2021; Akinsanola and Ogunjobi., 2017) over West Africa and (Mathewos *et al*., 2023) in the East Africa.

4.1.2 The monthly evaporation

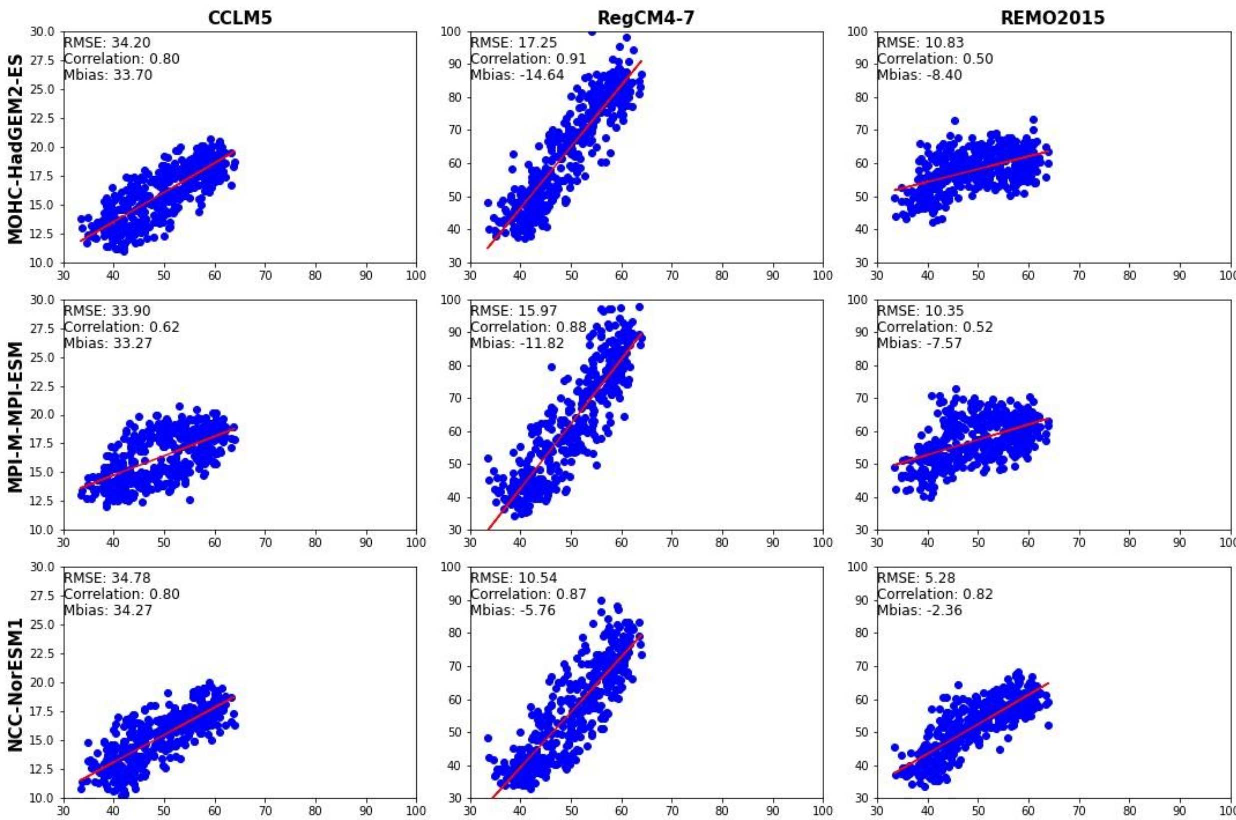

Figure 4.2: Statistical presentation of the ERA5 monthly mean evaporation and simulation of three RCMs driven by the three GCMs.

Figure 4.2 presents the statistical values of correlation coefficients (Rs), Root Mean Square Errors (RMSEs) and Mean Bias errors (Mbiases) between the ERA5 as observation and the simulations of the three RCMs of evaporation: CCLM5 (in the first column); RegCM4.7 (in the second column); and REMO2015 (in the third column), while each of the three RCMs was driven by the three GCMs: MOHC-HadGEM2-ES in the first row; MPI-M-MPI-ESM (in the second row); and the NCC-NorESM1 (in the third row) over the entire west Africa from CORDEX . The statical values for Guines, Savanna and Sahel (and entire West Africa) are presented in Table 4.2. RCMs driven by the three GCMs.

Figure 4.2 shows that the R values reach 0.80 for the CCLM5 simulations, 0.91 for the RegCM4-7 simulations and 0.82 for the REMO2015 simulations. The negative Mbias show an underestimation of the evaporation estimate overall, with the exception of the CCLM5 simulations which overestimate the evaporation compared to the ERA5 data. the RMSE values oscillate between 33.90 and 34.78 for the CCLM5 simulations, for the RegCM4-7 simulations between 10.54 and 17.25 and for the REMO2015 simulations between 5.28 and 10.83.

Table 4.2: The correlation coefficients, Mbiases and RMSEs of monthly mean evaporation of ERA5 and simulated of the respective GCMs and RCMs.

		Guinea zone			Savannah			Sahel			West Africa		
RCM	GCM	R	RMSE	Mbias	R	RCM	GCM	R	RMSE	Mbias	R	RCM	GCM
	MOHC-HadGEM2-ES	-0.1	60.75	59.72	0.82	57.57	54.81	0.93	33.62	29.47	0.8	34.2	33.7
CCLM5	MPI-M-MPI-ESM	-0.32	61.71	60.41	0.76	56.67	53.71	0.91	32.15	27.65	0.62	33.9	33.27
	NCC-NorESM1	0.81	24.27	-22.38	0.91	58.94	56.59	0.89	35.45	31	0.8	34.78	34.27
	MOHC-HadGEM2-ES	0.82	34.81	-33.16	0.87	39.99	-34.31	0.88	27.37	-16.05	0.91	17.25	-14.64
RegCM4-7	MPI-M-MPI-ESM	0.86	23.09	-20.33	0.9	37	-30.43	0.91	29.38	-18.53	0.88	15.97	-11.82
	NCC-NorESM1	0.81	24.27	-22.38	0.87	34.89	-23.73	0.8	19.52	0.31	0.87	10.54	-5.76
	MOHC-HadGEM2-ES	0	27.64	-21.88	0.69	23.31	-16.64	0.81	15.7	-7.25	0.5	10.83	-8.4
REMO2015	MPI-M-MPI-ESM	0.18	24.3	-17.37	0.78	20.89	-15.37	0.82	14.81	-6.92	0.52	10.35	-7.57
	NCC-NorESM1	0.58	19.02	-13.51	0.93	9.54	-2.86	0.89	15.6	11.56	0.82	5.28	-2.36

Comparison of the monthly evaporation of CORDEX RCMs to that of ERA5. To shows that R reaches 0.93 in the Sahel, 0.93 in the savannah and 0.86 for the Guinea Coast (Table 4.2). The Mbias are negative overall with the exception of the three CCLM5 simulations. The RMSE values oscillate between 23.09 and 61.41 in the coastal zone, in the savannah zone between 9.54 and 58.94 and in the Sahel zone between 14.81 and 35.45 (Table 4.2), this result is similar to that of (El-Mahdy *et al*., 2021) in Egypt.

4.1.3 The monthly air temperature

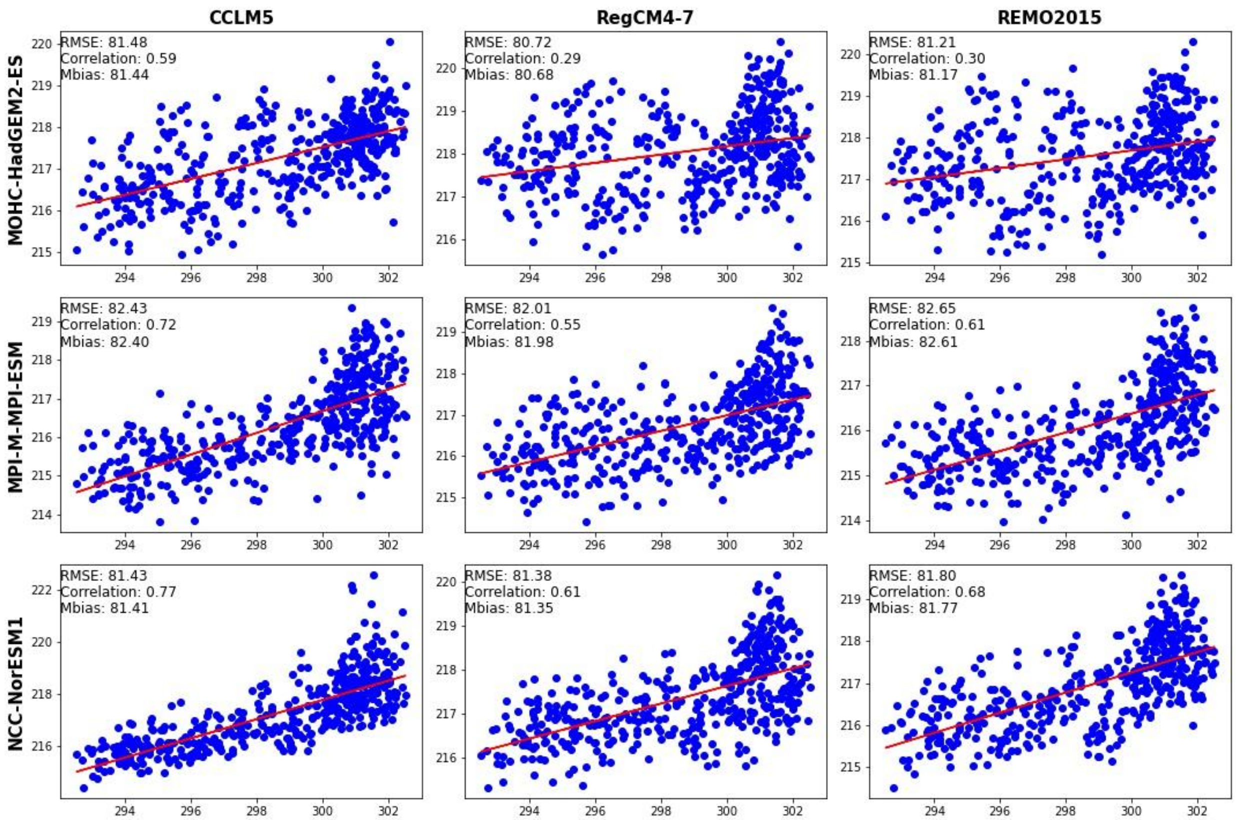

Figure 4.3: Statistical presentation of the ERA5 monthly mean air temperature and simulation of three RCMs driven by the three GCMs.

Figure 4.3 presents the statistical values of correlation coefficients (Rs), Root Mean Square Errors (RMSEs) and Mean Bias errors (Mbiases) between the ERA5 as observation and the simulations of the three RCMs of air temperature: CCLM5 (in the first column); RegCM4.7 (in the second column); and REMO2015 (in the third column), while each of the three RCMs was driven by the three GCMs: MOHC-HadGEM2-ES in the first row; MPI-M-MPI-ESM (in the second row); and the NCC-NorESM1 (in the third row) over the entire west Africa from CORDEX . The statical values for Guines, Savanna and Sahel (and entire West Africa) are presented in Table 4.3.

Figure 4.3 shows that correlation coefficients reach 0.77 for the CCLM5 simulations, 0.61 for the RegCM4-7 simulations and 0.68 for the REMO2015 simulations. The positive Mbias show an overestimation of the RCM's mean monthly air temperature as compared to the ERA5 data. The RMSEs range between 81.43 and 82.40 for the CCLM5 simulations, for the RegCM4-7 simulations between 80.72 and 82.01 and for the REMO2015 simulations between 81.21 and 82.61.

Table 4.3: The correlation coefficients, Mbiases and RMSEs of monthly mean air temperature of ERA5 and simulated of the respective GCMs and RCMs.

		Guinea zone			Savannah			Sahel			West Africa		
RCM	GCM	R	RMSE	Mbias	R	RCM	GCM	R	RMSE	Mbias	R	RCM	GCM
CCLM5	MOHC-HadGEM2-ES	0.22	81.75	81.74	0.43	82.87	82.52	0.59	84	83.96	0.59	81.48	81.44
	MPI-M-MPI-ESM	-0.07	82.52	82.51	0.01	83.56	83.54	0.51	84.73	84.69	0.72	82.43	82.4
	NCC-NorESM1	0.33	81.29	81.28	0.29	82.46	82.44	0.64	83.76	83.72	0.77	81.43	81.41
RegCM4-7	MOHC-HadGEM2-ES	0.22	80.88	80.87	0.06	82.15	82.13	0.08	83.44	83.38	0.29	80.72	80.68
	MPI-M-MPI-ESM	-0.2	82.2	82.19	-0.14	83.38	83.36	0.29	84.59	84.54	0.55	82.01	81.98
	NCC-NorESM1	0.3	81.04	81.03	0.11	82.5	82.48	0.42	84.03	83.99	0.61	81.38	81.35
REMO2015	MOHC-HadGEM2-ES	0.23	81.36	81.36	0.23	82.63	82.61	0.19	83.92	83.87	0.3	81,21	81.17
	MPI-M-MPI-ESM	-0.07	82.58	82.57	-0.03	83.73	83.71	0.36	85	84.96	0.61	82.65	82,61
	NCC-NorESM1	0.41	81.13	81.13	0.32	82.54	82.52	0.55	84.12	84.08	0.68	81.8	81.77

While comparing the air temperature of the RCMs of CORDEX to that of ERA5. The R values reach 0.86 in the Sahel, 0.93 for the savanna zone and the Guinea Coast zone as depicted in Table 4.3. The Mbias are positive overall which show an overestimation of the monthly air temperature estimate of the RCMs compared to the ERA5 data in the three regions (Table 4.3). The RMSE values oscillate between 81.04 and 84.96 in all the climatic zones of West Africa (Table 4.3), this result is similar to that of (Okafor *et al*., 2019) over the Volta basin, (Mostafa *et al.,* 2019) over Egypt, (Demissie *et al*., 2021) over southwest Ethiopia.

Table 4.4: The best simulation by variable and on each zone and the entire West Africa.

	Guinea zone			Savannah			Sahel			West Africa		
	Prec.	**Evap.**	**Air Temp.**	**Prec.**	**Evap.**	**Air Temp.**	**Prec.**	**Evap.**	**Air Temp.**	**Prec.**	**Evap.**	**Air Temp.**
RCM	**REMO2015**	**RegCM4-7**	**REMO2015**	**REMO2015**	**REMO2015**	**CCLM5**	**REMO2015**	**CCLM5**	**CCLM5**	**REMO2015**	**RegCM4-7**	**CCLM5**
GCM	**MPI-ESM**	**MPI-ESM**	**NorESM1**	**MPI-ESM**	**NorESM1**	**HadGEM2**	**HadGEM2**	**HadGEM2**	**NorESM1**	**MPI-ESM**	**HadGEM2**	**NorESM1**
R	**0.88**	**0.86**	**0.41**	**0.95**	**0.93**	**0.43**	**0.91**	**0.93**	**0.64**	**0.91**	**0.91**	**0.77**
RMSE	**101.89**	**23.09**	**81.13**	**56.87**	**9.54**	**82.87**	**27.34**	**33.62**	**83.76**	**49.58**	**17.25**	**81.43**
Mbias	**-41.3**	**-20.33**	**81.13**	**-24.02**	**-2.86**	**82.52**	**-9.91**	**29.47**	**83.72**	**-29**	**-14.6**	**81.41**

Table 4.4 presents the performance of regional climate models (RCMs) coupled with different global climate models (GCMs) evaluated according to the three major climatic zones of West Africa using statistical indicators (R, RMSE and Mbias). The objective is to determine which model couplings best reproduce observations according to the climatic characteristics specific to each zone. This approach is essential because the performance of a model can vary considerably depending on the geographical area due to the dominant physical processes specific to each climate. In the Guinean zone, characterized by a hot and very humid climate, the best precipitation simulation is the REMO2015 models coupled with MPI-ESM-LR with a correlation of 0.88, a root mean square error of 101.86 and an mean bias of -41.3, the best evaporation simulation is the RegCM4-7 models coupled with MPI-ESM-LR with a correlation of 0.86, a low root mean square error of 23.09 and a mean bias of -20.33, the best air temperature simulation is the REMO2015 models coupled with Nor-ESM1 with a correlation of 0.41, a root mean square error of 81.13 and a mean bias of 81.13,

The savannah zone shows the best overall performance, with an excellent correlation for the three variables (R = 0.95 for precipitation, 0.93 for evaporation, 0.43 for temperature). The REMO2015 model coupled with MPI-ESM-LR offers a very good representation of evaporation (RMSE = 56.87; Mbias = -24.02), the REMO2015 model coupled with Nor-ESM1 offers a very good representation of precipitation (RMSE = 9.54; Mbias = -2.86), the CCLM5 coupled with HadGEM2-ES offers a representation of air temperature (RMSE = 82.87; Mbias = -82.52). In the Sahel, a semi-arid zone marked by strong seasonal variability, the best precipitation simulation is the REMO2015 models coupled to HadGEM2-ES with a correlation of 0.91, a root mean square error of 27.34 and a mean bias of -9.91, the best evaporation simulation is the CCLM5 models coupled to HadGEM2-ES with a correlation of 0.93, a low root mean square error of 33.62 and a mean bias of 29.47, the best air temperature simulation is the CCLM5 models coupled to Nor-ESM1 with a correlation of 0.64, a root mean square error of 83.76 and a mean bias of 83.72. At the scale of all West Africa, the performances of the climate models remain generally satisfactory, with high correlations for all the variables studied, notably for precipitation and evaporation (R = 0.91). Air temperature is particularly well simulated, with a correlation coefficient of 0.77, a low RMSE (81.43) and a mean bias of (+81.41), which indicates a very good representation of thermal variability at the regional scale. This consistency is explained by the capacity of these models to represent the dominant climate processes at large scales, such as the monsoon.

4.2 Projected Climate changes over West Africa from CORDEX Experiment

4.2.1 The Projected changes in annual precipitation under RCP 2.6

The Figure 4.4 shows the analysis of changes in precipitation over West Africa for the near future under RCP 2.6 as simulated by three RCMs (CCLM5, RegCM4-7, REMO2015). The CCLM5 simulations driven by the three GCMs (MOHC-HadGEM2-ES, MPI-M-MPI-ESM, NCC-NorESM1) indicate moderate changes. In the simulation driven by the MOHC-HadGEM2-ES, a slight reduction in precipitation was observed, except for the western and eastern parts of the Sahel where small increases were projected, while the one driven by the MPI-M-MPI-ESM shows a reduction throughout the area with more moderate values in the Sahel and the one driven by NCC-NorESM1 mainly projected increase in all areas with a latitudinal zone of 10ºN and 15ºN. The RegCM4-7 model shows similar trends to CCLM, but with less pronounced variations according to the combinations. The simulation driven by the MOHC-HadGEM2-ES, projected a weak reduction in precipitation throughout.

The simulation driven by the MOHC-HadGEM2-ES displays a strong decrease overall with areas of maximum with significant values in all three climatic zones. The simulations driven by the MPI-M-MPI-ESM and NCC-NorESM1, show a dominant increase, but the coastal decreases become more visible. This model is distinguished by the variability in the projections, which could reflect an amplified response to changes in atmospheric circulations.

The figure 4.5 shows the changes in precipitation over West Africa for the far future under RCP 2.6 according to the regional climate models (CCLM5, RegCM4-7, REMO2015). CCLM5 model simulations (MOHC-HadGEM2-ES, MPI-M-MPI-ESM, NCC-NorESM1) indicate weak changes. In the simulation driven by the MOHC-HadGEM2-ES, a slight reduction in precipitation is observed overall, except for the western parts of the Sahel where small increases are projected from western Mali to the Ocean. The simulation driven by the MPI-M-MPI-ESM shows a reduction throughout the area with more moderate values in the western Sahel and small increases over Niger and Nigeria. In the simulation driven by the NCC-NorESM1, CCLM projects small increases throughout the area. The RegCM4-7 model shows similar trends to CCLM, but with less pronounced variations according to the combinations. The simulation driven by the MOHC-HadGEM2-ES, a weak reduction in precipitation is dominant overall except for the eastern part of the Sahel which projects a weak increase. The simulation driven by the MPI-M-MPI-ESM, RegCM shows a decrease in precipitation overall with an amplification of the decreases in the Sahel. The simulation driven by the NCC-NorESM1 highlights a weak increase in precipitation in all areas. REMO2015 projects a mixed variability, notably with reductions in the coastal areas and significant increases in the Sahel. The simulation driven by the MOHC-HadGEM2-ES displays a strong decrease overall with maximum areas with significant values between 7ºN and 12ºN. The simulations driven by the MPI-M-MPI-ESM and NCC-NorESM1, show a dominant increase in the Sahel and the Savannah but the decreases in the coastal zone become more visible. Our results are consistent with previous studies of (Tamoffo *et al*., 2023) over West Africa, (Dosio *et al*., 2021) over Africa, (Shiru *et al*., 2020) in Nigeria, (Gebrechorkos *et al*., 2020) in East Africa, (Gao *et al*., 2024) over Yellow River in China.

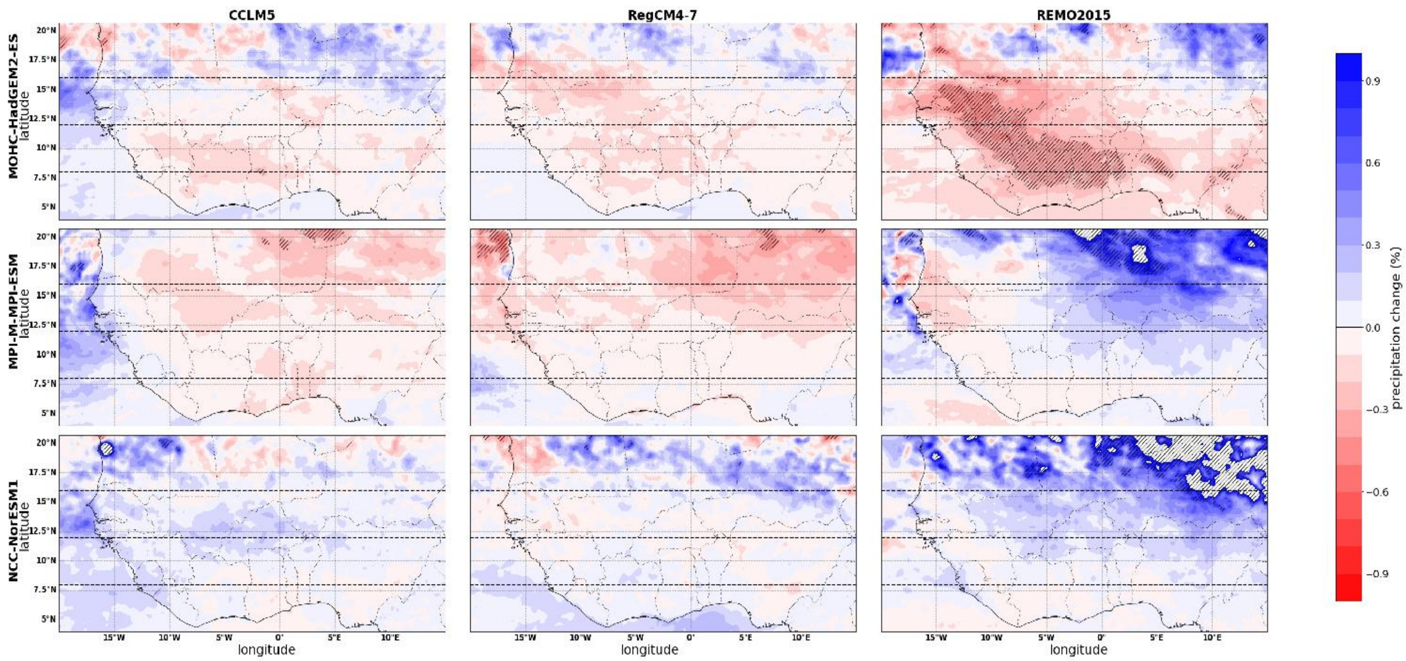

Figure 4.4: Projected changes in annual precipitation over the period 2021–2060 relative to the historical period 1970–2005 under the RCP 2.6 scenario. the areas with statistical significance at 95% confidence level are marked with black stippling.

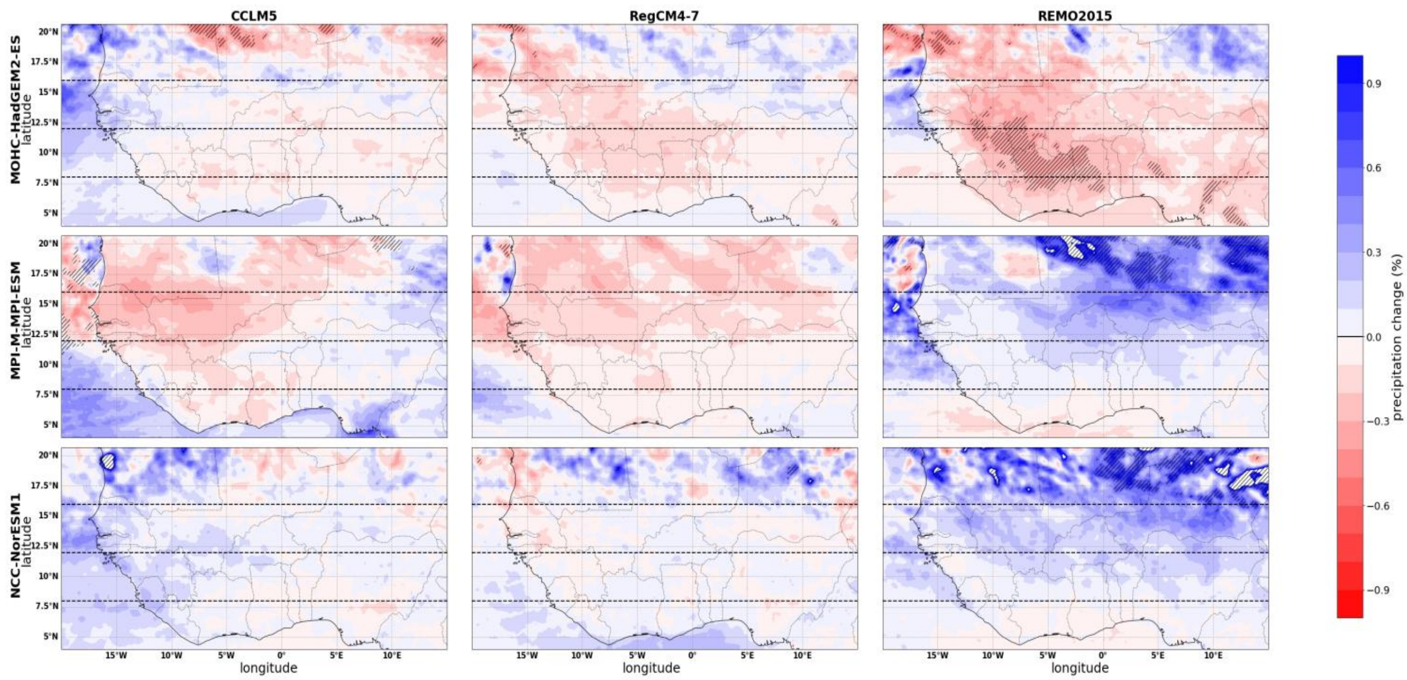

Figure 4.5: Projected changes in annual precipitation over the period 2061–2100 relative to the historical period 1970–2005 under the RCP 2.6 scenario. the areas with statistical significance at 95% confidence level are marked with black stippling.

4.2.2 The Projected changes in annual precipitation under RCP 8.5

The Figure 4.6 shows the changes in precipitation over West Africa for the near future under RCP 8.5. The CCLM5 model simulations indicated some mixed changes. In the simulation driven by the MOHC-HadGEM2-ES, a slight reduction in precipitation was observed throughout the entire West Africa, with the exception of the western parts of the Sahel where small increases were projected. The simulation driven by the MPI-M-MPI-ESM shows a reduction throughout the area with more moderate values in the Sahel. In the simulation driven by the NCC-NorESM1, CCLM5 projecteds small increases in all areas with a moderate zone in the Sahel. The RegCM4-7 model shows similar trends to CCLM5, but with less pronounced variations according to the combinations. In the simulation driven by the MOHC-HadGEM2-ES, a small reduction in precipitation is dominant overall. The RegCM4-7's simulation driven by the MPI-M-MPI-ESM, shows a decrease in precipitation overall with an amplification of the decreases in the Sahel. The simulation driven by the NCC-NorESM1 shows a small increase in precipitation in all areas. The REMO2015 model projects a mixed variability, notably with reductions in the coastal areas and significant increases in the Sahel. The simulation driven by the MOHC-HadGEM2-ES displays a strong decrease overall with significant values in the three climatic zones. The simulations driven by the MPI-M-MPI-ESM and NCC-NorESM1, show a dominant increase overall with the exception of the coastal zone which projects decreases.

The Figure 4.7 shows changes in West Africa precipitation for the far future under RCP 8.5 according to the regional climate models (CCLM5, RegCM4-7, REMO2015). CCLM5 model simulations (MOHC-HadGEM2-ES, MPI-M-MPI-ESM, NCC-NorESM1) project a precipitation. In the simulation driven by the MOHC-HadGEM2-ES, a slight reduction in precipitation is observed overall with significant values in all three climate zones. The simulation driven by the

MPI-M-MPI-ESM shows a reduction throughout the zone with the exception of the eastern part of West Africa which projects a slight increase in precipitation. In the simulation driven by the NCC-NorESM1, CCLM5 projects decreases overall with the exception of the eastern Sahel and the western Savannah which project increases. The RegCM4-7 model shows similar trends to CCLM5, but with less pronounced variations depending on the combinations. The simulation driven by the MOHC-HadGEM2-ES, a strong reduction in precipitation is dominant overall with significant values in the three climatic zones. The simulation driven by the MPI-M-MPI-ESM, RegCM4-7 shows a decrease in precipitation overall with an amplification of the decreases in the west of the Sahel. The simulation driven by the NCC-NorESM1 shows a decrease overall with the exception of the eastern part of the Sahel which projects a small increase in precipitation. REMO2015 projects a mixed variability, notably with reductions in the coastal areas and significant increases in the Sahel. The simulation driven by the MOHC-HadGEM2-ES displays a strong decrease overall with significant values in the three climatic zones. The simulations driven by the MPI-M-MPI-ESM and NCC-NorESM1, show a dominant increase in the Sahel and the Savannah, small decreases are localized in the coastal zone and western part of the Sahel. Our results are consistent with previous studies that of (Tamoffo *et al*., 2023) West Africa, (Koffi *et al*., 2023) in West-Central of Côte d'Ivoire, (Cook *et al*., 2022) over West Africa, (Bojer *et al*., 2024) on the Gilgel Gibe Watershed in Ethiopia, (Stanzel *et al*., 2018) over West Africa.

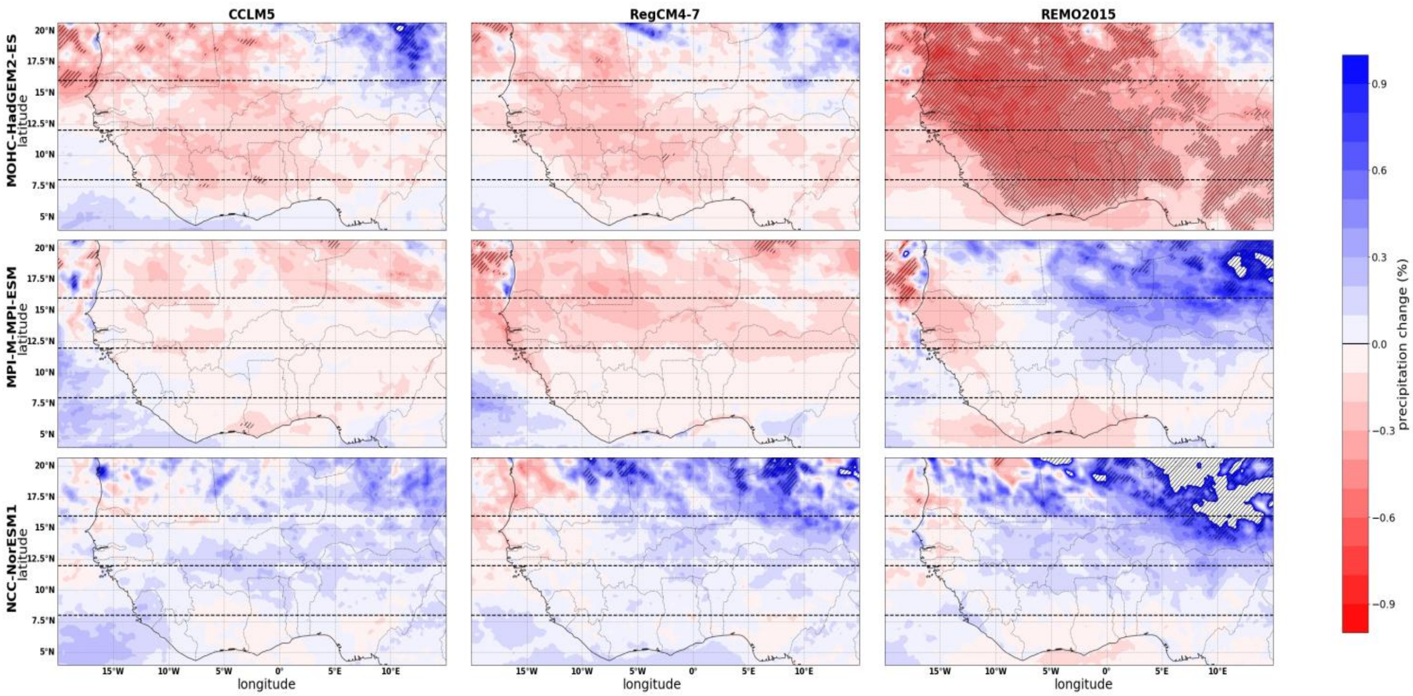

Figure 4.6: Projected changes in annual precipitation over the period 2021–2060 relative to the historical period 1970–2005 under the RCP 8.5 scenario. the areas with statistical significance at 95% confidence level are marked with black stippling.

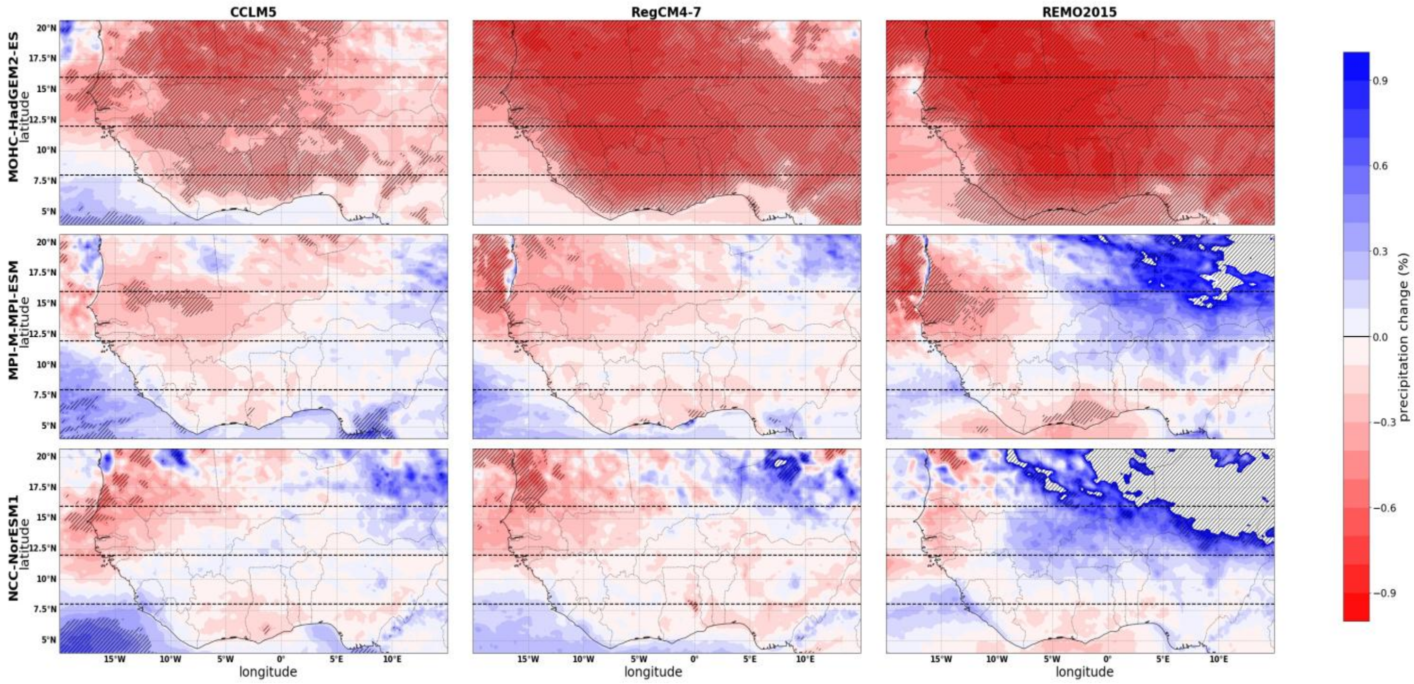

Figure 4.7: Projected changes in annual precipitation over the period 2061–2100 relative to the historical period 1970–2005 under the RCP 8.5 scenario. the areas with statistical significance at 95% confidence level are marked with black stippling.

4.2.3 The Projected changes in annual evaporation under RCP 2.6

The Figure 4.8 shows the changes in evaporation over West Africa for the near future under RCP 2.6 according to the regional climate models (CCLM5, RegCM4-7, REMO2015). CCLM5 model simulations (MOHC-HadGEM2-ES, MPI-M-MPI-ESM, NCC-NorESM1) show weak changes. In the simulation driven by the MOHC-HadGEM2-ES, a slight reduction in evaporation is observed overall, with the exception of the western and eastern parts of the Sahel where small increases are projected. The simulation driven by the MPI-M-MPI-ESM shows a small reduction throughout the area. In the simulation driven by the NCC-NorESM1, CCLM 5projects small increases in all areas except the coastal zone. The RegCM4-7 model shows similar trends to CCLM5, but with less pronounced variations according to the combinations. In the simulation driven by the MOHC-HadGEM2-ES, a small reduction in evaporation is dominant overall. The simulation driven by the MPI-M-MPI-ESM, RegCM shows a decrease in evaporation overall with an amplification of the decreases in the Sahel. The simulation driven by the NCC-NorESM1 shows a small increase in evaporation in all areas except the coastal zone which projects a decrease. The REMO2015 model projects a mixed variability, notably with reductions in the coastal zones and significant increases in the Sahel. The simulation driven by the MOHC-HadGEM2-ES displays a strong decrease overall with significant values in the three climatic zones. The simulations driven by the MPI-M-MPI-ESM and NCC-NorESM1, show a dominant increase in the Sahel and the Savannah, a decrease is projected in the coastal zone.

The Figure 4.9 shows the changes in evaporation over West Africa for the far future under RCP 8.5 according to the regional climate models (CCLM5, RegCM4-7, REMO2015). The CCLM5 model simulations (MOHC-HadGEM2-ES, MPI-M-MPI-ESM, NCC-NorESM1) indicate weak changes. In the simulation driven by the MOHC-HadGEM2-ES, a slight reduction in evaporation is observed overall, except for the western and eastern parts of the Sahel where small increases are projected. The simulation driven by the MPI-M-MPI-ESM shows a reduction throughout the area with significant decreases in the western Sahel. In the simulation driven by the NCC-NorESM1, CCLM5 projects small increases in all climate zones. The RegCM4-7 model shows similar trends to CCLM, but with less pronounced variations according to the combinations. In the simulation driven by the MOHC-HadGEM2-ES, a small reduction in evaporation is dominant overall. The simulation driven by the MPI-M-MPI-ESM, RegCM shows an overall decrease in evaporation with an amplification of the decreases in the Sahel. The simulation driven by the NCC-NorESM1 shows a dominant increase in the Sahel and the Savannah, a decrease is projected in the coastal zone. REMO2015 projects a mixed variability, notably with reductions in the coastal zones and significant increases in the Sahel. The simulation driven by the MOHC-HadGEM2-ES shows a small decrease overall with significant values in the three climatic zones. The simulations driven by the MPI-M-MPI-ESM and NCC-NorESM1, show a dominant increase in the Sahel and the Savannah, a decrease is projected in the coastal zone. Our results are consistent with previous studies that of (Soares *et al*., 2019) over Africa, (Gebrechorkos *et al*., 2020) in East Africa, (Bojer *et al*., 2024) on the Gilgel Gibe Watershed in Ethiopia, (La Fuente *et al*., 2022) over the lake Kinneret in Israel.

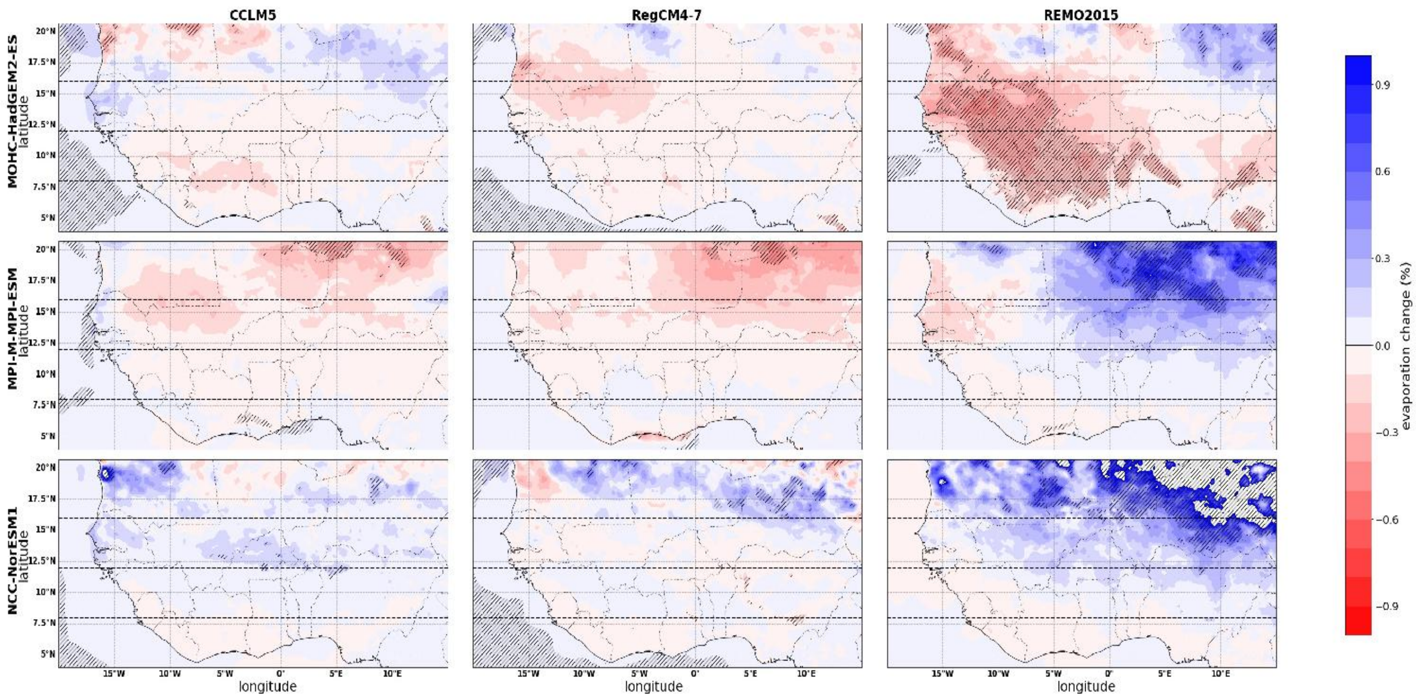

Figure 4.8: Projected changes in annual evaporation over the period 2021–2060 relative to the historical period 1970–2005 under the RCP 2.6 scenario. the areas with statistical significance at 95% confidence level are marked with black stippling.

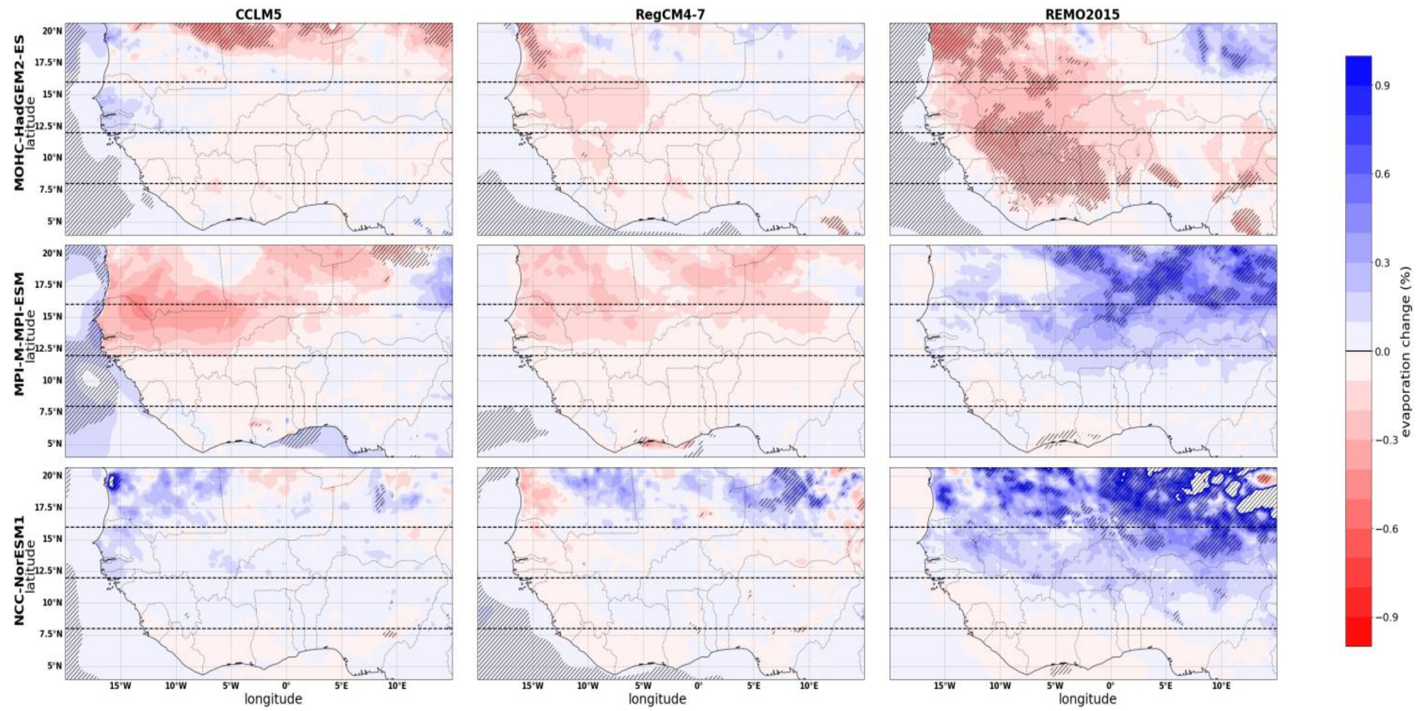

Figure 4.9: Projected changes in annual evaporation over the period 2061–2100 relative to the historical period 1970–2005 under the RCP 2.6 scenario. the areas with statistical significance at 95% confidence level are marked with black stippling.

4.2.4 The Projected changes in annual evaporation under RCP 8.5

The Figure 4.10 shows the changes in evaporation over West Africa for the near future under RCP 8.5 according to the regional climate models (CCLM5, RegCM4-7, REMO2015). The CCLM5 model simulations (MOHC-HadGEM2-ES, MPI-M-MPI-ESM, NCC-NorESM1) indicate weak changes. In the simulation driven by the MOHC-HadGEM2-ES, a slight reduction in evaporation is observed overall except for the eastern part of the Sahel where weak increases are projected. The simulation driven by the MPI-M-MPI-ESM shows a reduction throughout the area with more moderate values in the western part of the Sahel. In the simulation driven by the NCC-NorESM1, CCLM projects weak increases throughout the area. The RegCM4-7 model shows similar trends to CCLM5, but with less pronounced variations according to the combinations. In the simulation driven by the MOHC-HadGEM2-ES, a weak reduction in evaporation is dominant overall. The simulation driven by the MPI-M-MPI-ESM, RegCM4-7 shows an overall decrease in evaporation with an amplification of the decreases in the Sahel. The simulation driven by the NCC-NorESM1 shows a dominant increase in the Sahel and the Savannah, a decrease is projected in the coastal zone. The REMO2015 model projects a mixed variability, notably with reductions in the coastal zones and significant increases in the Sahel. The simulation driven by the MOHC-HadGEM2-ES displays a strong decrease overall with significant values in the three climatic zones. The simulations driven by the MPI-M-MPI-ESM and NCC-NorESM1 show a dominant increase in the Sahel and the Savannah, a decrease is projected in the coastal zone.

The Figure 4.11 shows the changes in evaporation over West Africa for the far future under RCP 8.5 according to the regional climate models (CCLM5, RegCM4-7, REMO2015). The CCLM5 model simulations (MOHC-HadGEM2-ES, MPI-M-MPI-ESM, NCC-NorESM1) indicate weak changes. In the simulation driven by the GCM "MOHC-HadGEM2-ES", a slight reduction in evaporation is observed overall with significant values in all three climate zones. The simulation driven by the MPI-M-MPI-ESM shows a reduction throughout the zone with more moderate values in the Sahel, with significant values in the Sahel. The simulation driven by the NCC-NorESM1, CCLM5 projects weak decreases throughout the zone with significant values in the Sahel and the coastal zone. The RegCM4-7 model shows similar trends to CCLM5. In the simulation driven by the MOHC-HadGEM2-ES, a weak reduction in evaporation is dominant overall with significant values in all three climate zones. The simulation driven by the MPI-M-MPI-ESM, RegCM4-7 shows a decrease in evaporation overall with an amplification of the decreases in the Sahel. The simulation driven by the NCC-NorESM1 shows a weak decrease in evaporation in all areas except the eastern part of the Sahel. The REMO2015 model projects a mixed variability. The simulation driven by the MOHC-HadGEM2-ES shows a strong decrease overall with significant values in the three climatic zones. The simulations driven by the MPI-M-MPI-ESM, show a decrease overall except for the eastern part of the Sahel. The simulation driven by the NCC-NorESM1, show a weak decrease overall with localized increases between 7ºN and 16ºN. Our results are consistent with previous studies that of (Cook *et al*., 2022) over West Africa, (Stanzel *et al*., 2018) over West Africa, (Gebrechorkos *et al*., 2020) in East Africa, (Bojer *et al*., 2024) on the Gilgel Gibe Watershed, Ethiopia, (La Fuente *et al*., 2022) over the lake Kinneret in Israel.

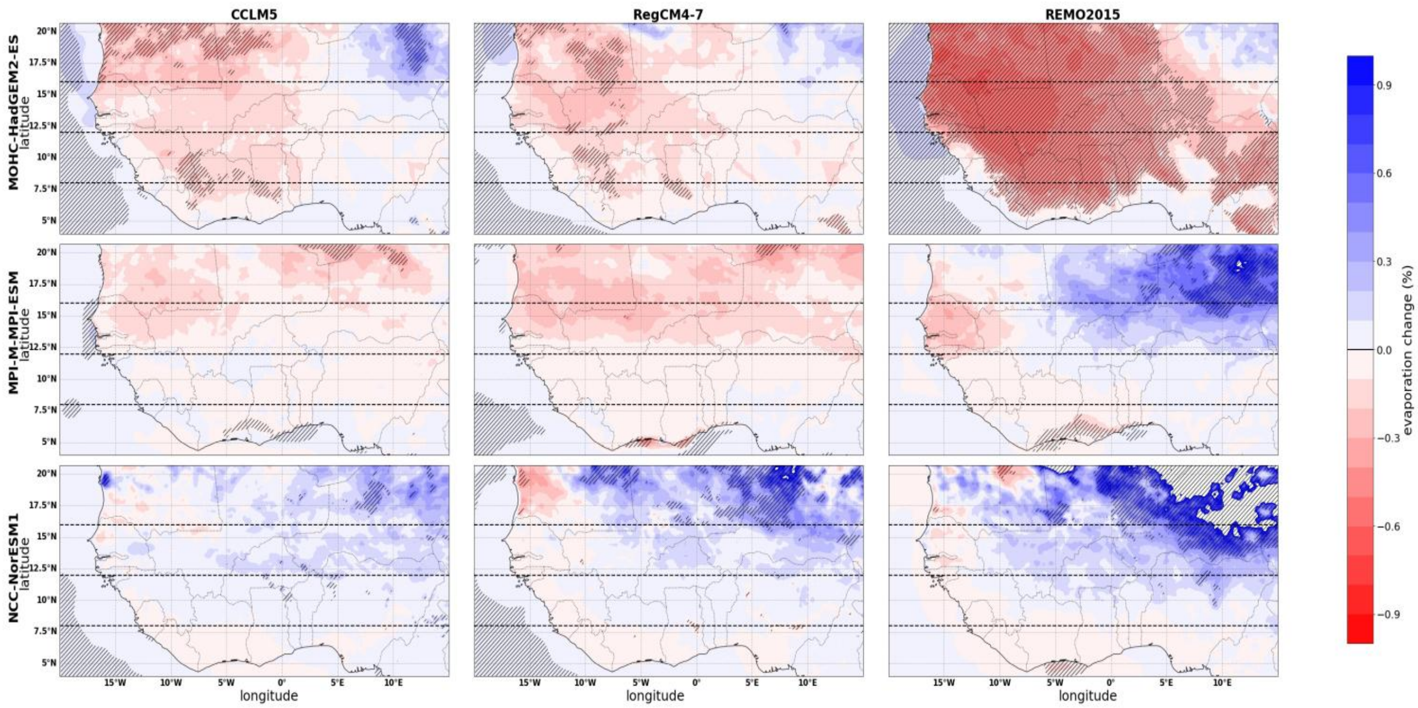

Figure 4.10: Projected changes in annual evaporation over the period 2021–2060 relative to the historical period 1970–2005 under the RCP 8.5 scenario. the areas with statistical significance at 95% confidence level are marked with black stippling.

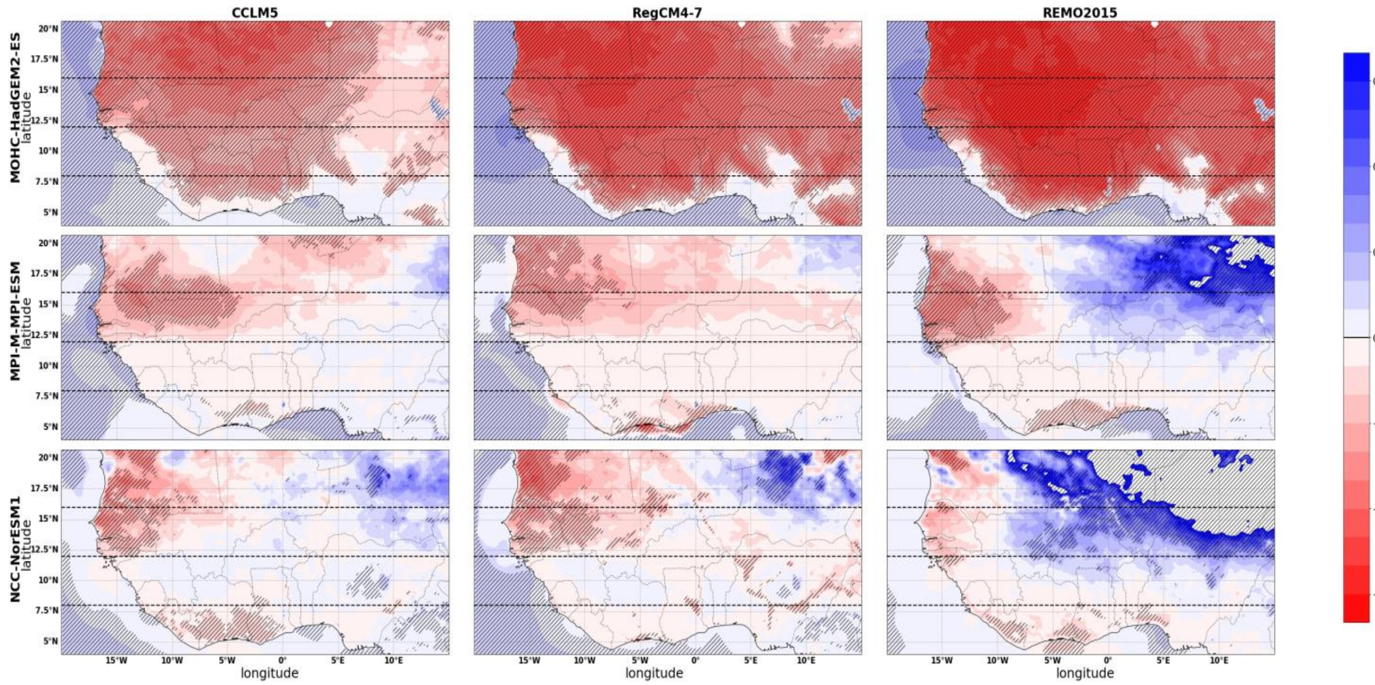

Figure 4.11: Projected changes in annual evaporation over the period 2061–2100 relative to the historical period 1970–2005 under the RCP 8.5 scenario. the areas with statistical significance at 95% confidence level are marked with black stippling.

4.2.5 The Projected changes in annual air temperature under RCP 2.6

The Figure 4.12 shows the changes in air temperature over West Africa for the near future under RCP 2.6 according to the regional climate models (CCLM5, RegCM4-7, REMO2015). The CCLM5 and RegCM4-7 model simulations (MOHC-HadGEM2-ES, MPI-M-MPI-ESM, NCC-NorESM1) show homogeneous increases in the three climatics zones with significant values throughout. The REMO2015 model projects low variability. The simulation driven by the MOHC-HadGEM2-ES shows an overall increase with significant values in the three climate zones. The simulations driven by the MPI-M-MPI-ESM, show a weak overall increase with an intensification in the Sahel. The simulations driven by the NCC-NorESM1, show a weak overall increase with an intensification in the western parts of the Sahel and the Savannah.

The Figure 4.13 shows the changes in air temperature over West Africa for the far future under RCP 2.6 according to the regional climate models (CCLM5, RegCM4-7, REMO2015). The CCLM5 and RegCM4-7 model simulations (MOHC-HadGEM2-ES, MPI-M-MPI-ESM, NCC-NorESM1) show homogeneous increases in the three climate zones with significant values overall. The REMO2015 model projects low variability. The simulation driven by the MOHC-HadGEM2-ES shows an overall increase with significant values in the three climate zones. The simulations driven by the MPI-M-MPI-ESM, show an overall increase with low intensity in the coastal zone. The simulations driven by the NCC-NorESM1, show an overall increase with a low value in the eastern parts of West Africa. Our results are consistent with previous studies that of (Gao *et al*., 2024) over Yellow River in China, (Shiru *et al*., 2020) in Nigeria, (Gebrechorkos *et al*., 2020) in East Africa.

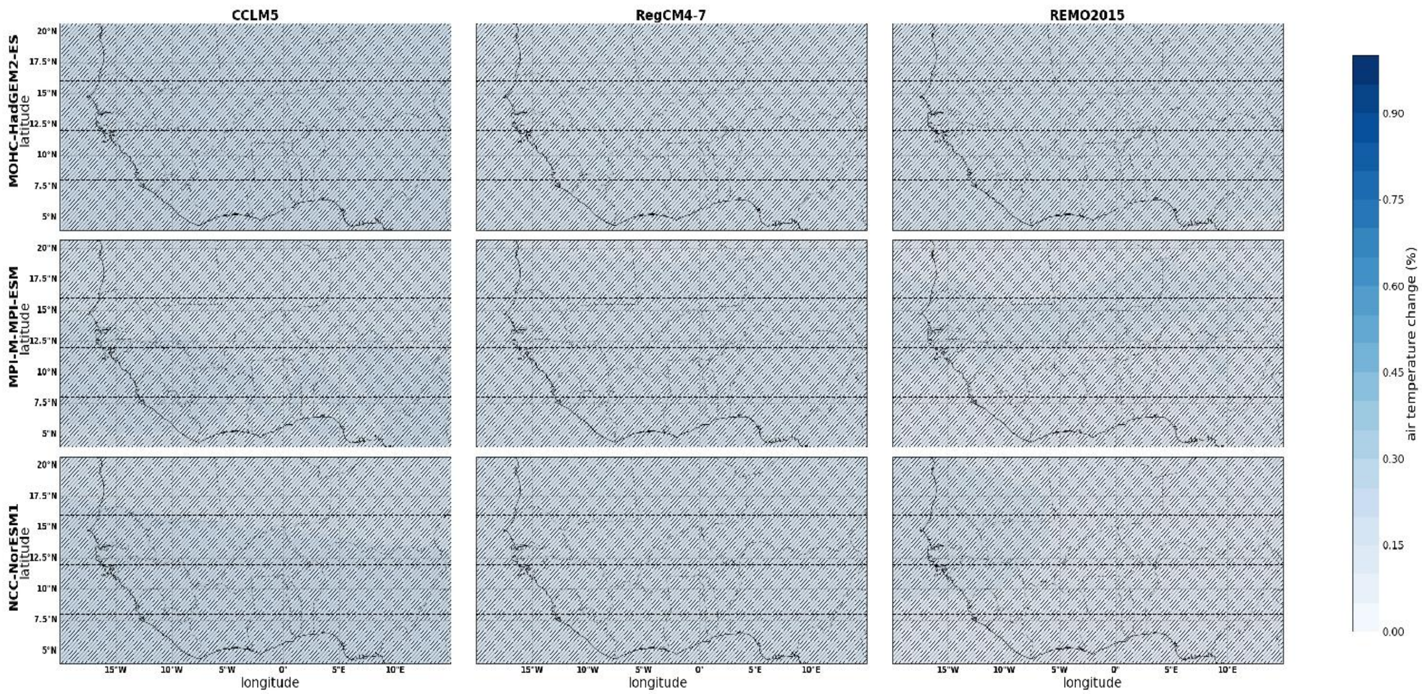

Figure 4.12: Projected changes in annual air temperature over the period 2021–2060 relative to the historical period 1970–2005 under the RCP 2.6 scenario. the areas with statistical significance at 95% confidence level are marked with black stippling.

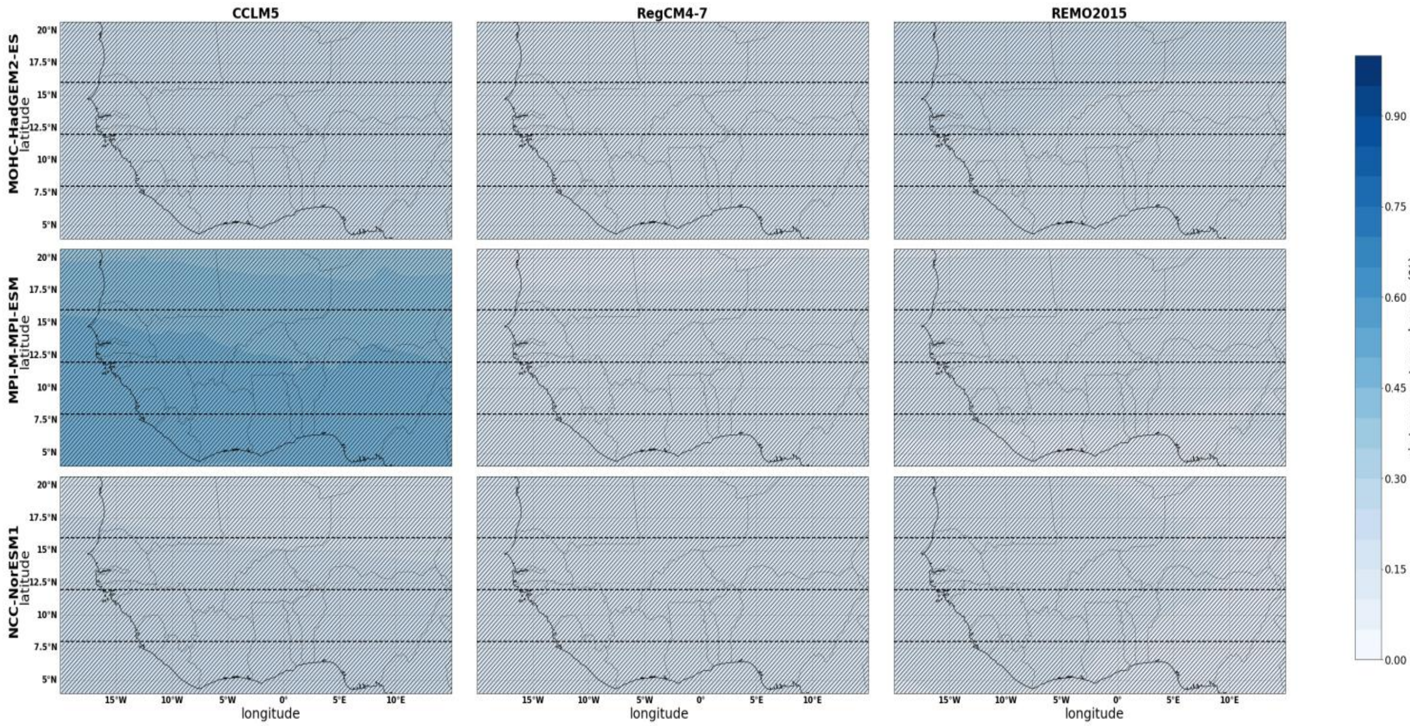

Figure 4.13: Projected changes in annual air temperature over the period 2061–2100 relative to the historical period 1970–2005 under the RCP 2.6 scenario. the areas with statistical significance at 95% confidence level are marked with black stippling.

4.2.6 The Projected changes in annual air temperature under RCP 8.5

The figure 4.14 shows the changes in air temperature over West Africa for the near future under RCP 8.5 according to the regional climate models (CCLM5, RegCM4-7, REMO2015). The CCLM5 model simulations (MOHC-HadGEM2-ES, MPI-M-MPI-ESM, NCC-NorESM1) show homogeneous increases in the three climate zones with significant values overall.

The RegCM4-7 model projects low variability. The simulations driven by the MOHC-HadGEM2-ES and NCC-NorESM1 show an overall increase with significant values in the three climate zones. The simulations driven by the MPI-M-MPI-ESM, show a weak overall increase. The REMO2015 model simulations (MOHC-HadGEM2-ES, MPI-M-MPI-ESM, NCC-NorESM1) show weak homogeneous increases in the three climate zones with significant values overall.

The Figure 4.15 shows the changes in West African air temperature for the far future under RCP 8.5 according to the regional climate models (CCLM5, RegCM4-7, REMO2015). The CCLM5 model simulations (MOHC-HadGEM2-ES, MPI-M-MPI-ESM, NCC-NorESM1) show homogeneous increases in the three climate zones with significant values overall. The RegCM4-7 model (MOHC-HadGEM2-ES, MPI-M-MPI-ESM, NCC-NorESM1) projects an overall increase with significant values in the three climate zones. The REMO2015 model simulations (MOHC-HadGEM2-ES, MPI-M-MPI-ESM, NCC-NorESM1) show small homogeneous increases in the three climate zones with significant values overall. Our results are consistent with previous studies that of (Gao *et al*., 2024) over Yellow River in China, (Shiru *et al*., 2020) in Nigeria, (Gebrechorkos *et al*., 2020) in East Africa, (Amoussou *et al*.,2020) in the Mono River Basin (West Africa).

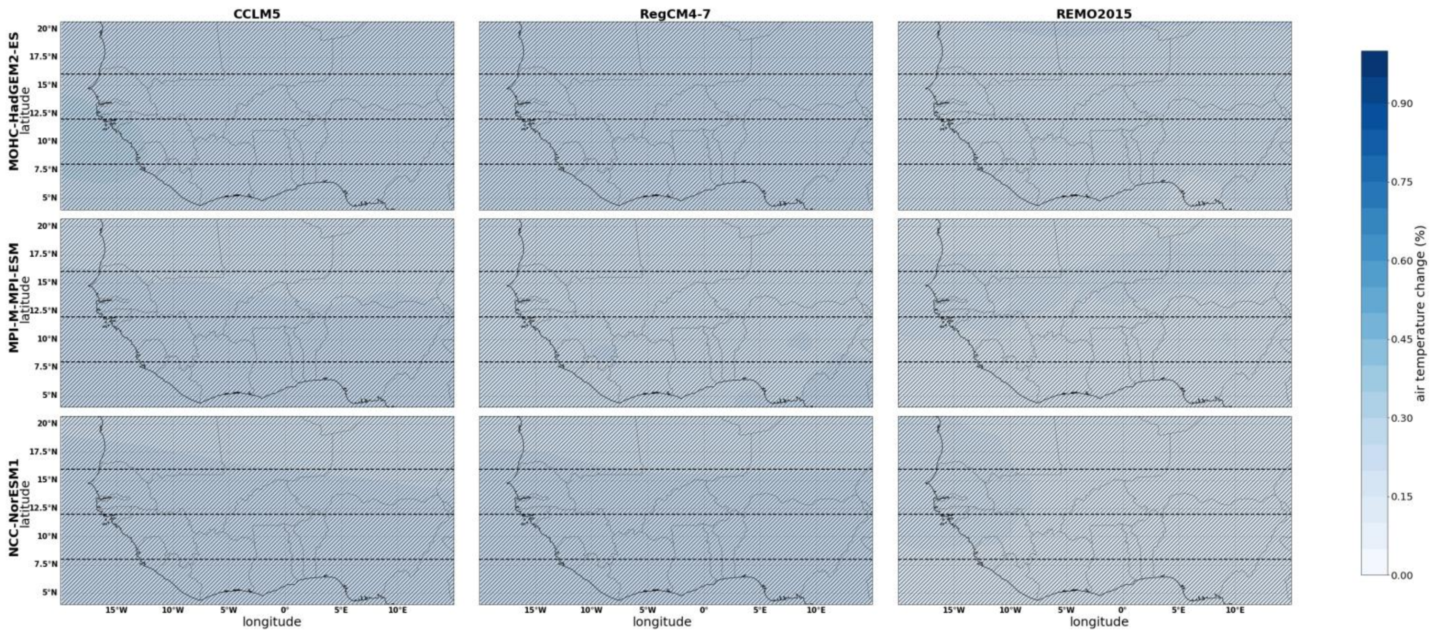

Figure 4.14: Projected changes in annual air temperature over the period 2021–2060 relative to the historical period 1970–2005 under the RCP 8.5 scenario. the areas with statistical significance at 95% confidence level are marked with black stippling.

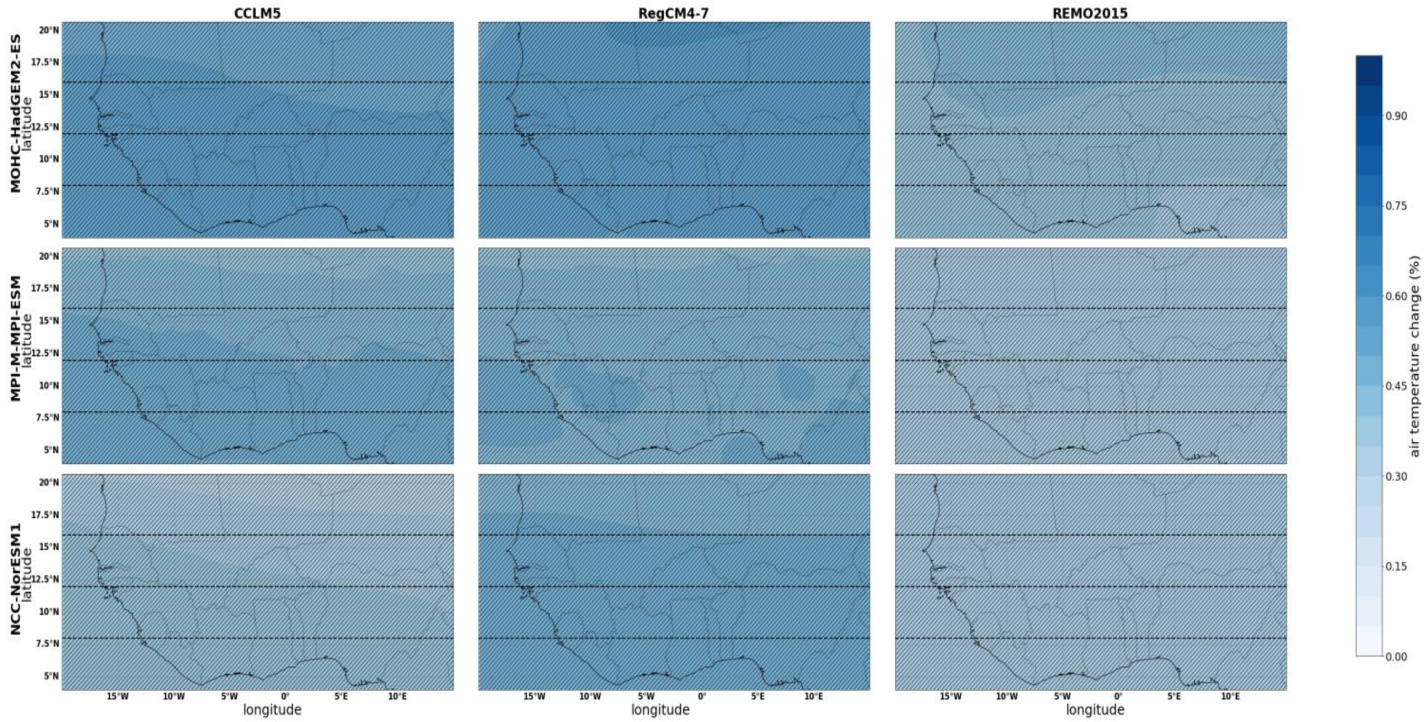

Figure 4.15: Projected changes in annual air temperature over the period 2061–2100 relative to the historical period 1970–2005 under the RCP 8.5 scenario. the areas with statistical significance at 95% confidence level are marked with black stippling.

4.2.7 The Projected changes in annual total runoff under RCP 2.6

The Figure 4.16 shows changes in the West African total runoff for the near future under RCP 2.6 according to the regional climate models (CCLM5, RegCM4-7, REMO2015). The CCLM5 model simulations (MOHC-HadGEM2-ES, MPI-M-MPI-ESM, NCC-NorESM1) indicate mixed changes. In the simulation driven by the MOHC-HadGEM2-ES, a slight reduction in the total runoff is observed overall, with the exception of the western and eastern parts of the Sahel where small increases are projected. The simulation driven by the MPI-M-MPI-ESM shows a reduction throughout the area with isolated increases in the Sahel. In the simulation driven by the NCC-NorESM1, CCLM5 projects mainly increases throughout the area with isolated decreases in the Sahel and coastal areas. The RegCM4-7 model shows similar trends to CCLM5. In the simulation driven by the MOHC-HadGEM2-ES, a small reduction in the total runoff is dominant overall. The simulation driven by the MPI-M-MPI-ESM, RegCM4-7 shows a decrease in the total runoff overall with isolated increases in the eastern Sahel. The simulation driven by the NCC-NorESM1 shows a weak increase in total runoff in all zones with isolated increases overall. The REMO2015 model projects a mixed variability. The simulation driven by the MOHC-HadGEM2-ES displays a strong decrease overall with significant values in the three climatic zones. The simulations driven by the MPI-M-MPI-ESM and NCC-NorESM1, show an increase overall with isolated increases in three climatic zones.

The Figure 4.17 shows changes in the West African total runoff for the far future under RCP 2.6 according to the regional climate models (CCLM5, RegCM4-7, REMO2015). The CCLM5 model simulations (MOHC-HadGEM2-ES, MPI-M-MPI-ESM, NCC-NorESM1) indicate moderate changes. In the simulation driven by the MOHC-HadGEM2-ES, a slight reduction in the total runoff is observed overall, with the exception of the western and eastern parts of the Sahel where small increases are projected. The simulation driven by the MPI-M-MPI-ESM shows a reduction in the western part and increases in the eastern part of the three climatic zones. In the simulation driven by the NCC-NorESM1, CCLM projects increases in all zones with isolated areas of increases in three climatic zones. The RegCM4-7 model projects mixed trends, with less pronounced variations according to the combinations. In the simulation driven by the MOHC-HadGEM2-ES, a small reduction in the total runoff is dominant overall. The simulation driven by the MPI-M-MPI-ESM, RegCM shows an overall decrease in total runoff with an amplification of the decreases in the Sahel. The simulation driven by the NCC-NorESM1 shows overall decreases with small isolated increases in all zones. The REMO2015 model projects a mixed variability. The simulation driven by the MOHC-HadGEM2-ES shows an overall decrease with significant values in the three climatic zones. The simulations driven by the MPI-M-MPI-ESM and NCC-NorESM1, show an overall increase with isolated decreases, with significant values in the Sahel and Guinea zone. Our results are consistent with previous studies that of (Kim *et al*., 2021) in Burundi, (Cook *et al*., 2022) over West Africa, (Stanzel *et al.,* 2018) over West Africa.

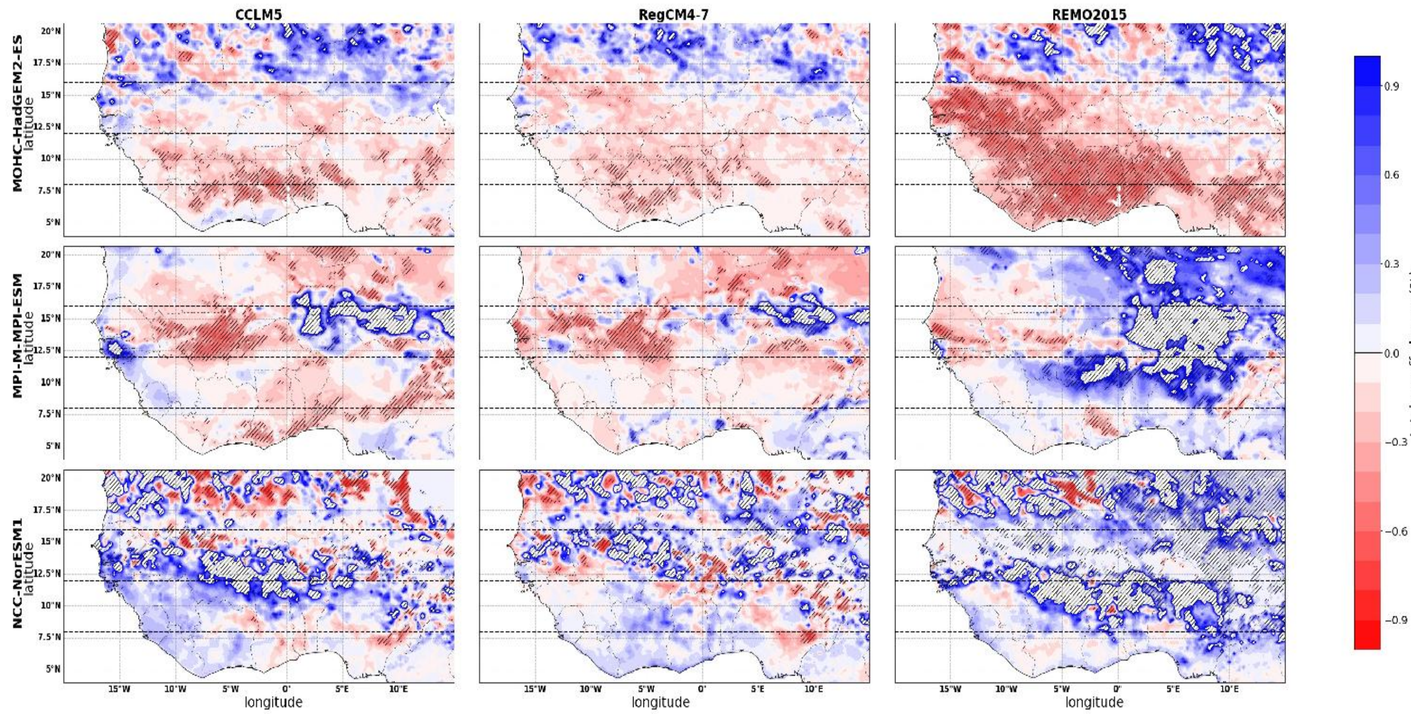

Figure 4.16: Projected changes in annual total runoff over the period 2021–2060 relative to the historical period 1970–2005 under the RCP 2.6 scenario. the areas with statistical significance at 95% confidence level are marked with black stippling.

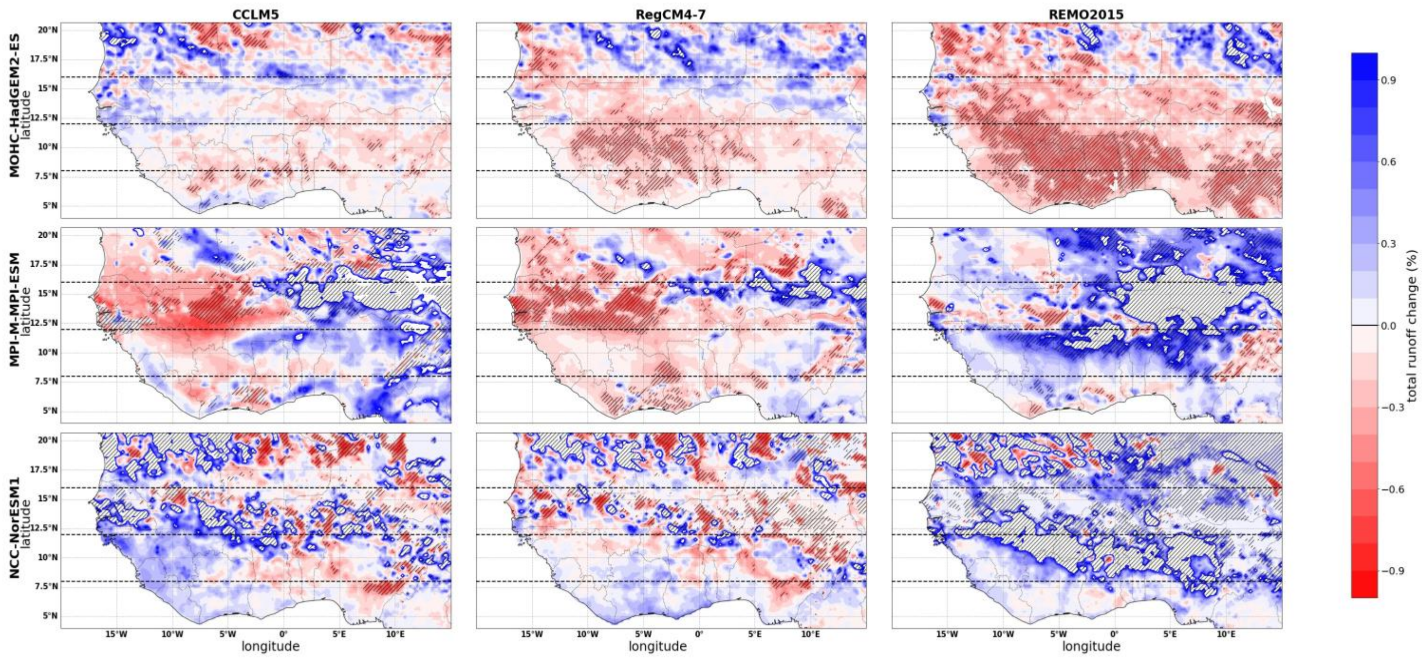

Figure 4.17: Projected changes in annual total runoff over the period 2061–2100 relative to the historical period 1970–2005 under the RCP 2.6 scenario. the areas with statistical significance at 95% confidence level are marked with black stippling.

4.2.8 The Projected changes in annual total runoff under RCP 8.5

The Figure 4.18 shows changes in the West African total runoff for the near future under RCP 8.5 according to the regional climate models (CCLM5, RegCM4-7, REMO2015). The CCLM5 and RegCM4-7 model simulations indicate small and mixed changes. In the simulations driven by the MOHC-HadGEM2-ES, a slight reduction in the total runoff is observed overall, with the exception of the eastern part of the Sahel where small increases are projected with significant values in all three climate zones. The simulations driven by the MPI-M-MPI-ESM show a reduction throughout the area with increases in the eastern Sahel. The simulations driven by the NCC-NorESM1, CCLM project increases in all areas with isolated decreases in the Sahel and Guinea zone. The REMO2015 model projects a mixed variability, notably with reductions in coastal areas and significant increases in the Sahel. The simulation driven by the MOHC-HadGEM2-ES shows a strong decrease overall with significant values in the three climatic zones. The simulations driven by the MPI-M-MPI-ESM and NCC-NorESM1, show an increase overall and isolated decreases located in the three zones, with significant values in the Sahel and in the Guinea zone.

The Figure 4.19 shows changes in the West African total runoff for the far future under RCP 8.5 according to the regional climate models (CCLM5, RegCM4-7, REMO2015). CCLM5 model simulations (MOHC-HadGEM2-ES, MPI-M-MPI-ESM, NCC-NorESM1) indicate moderate changes. In the simulation driven by the MOHC-HadGEM2-ES, a slight reduction in total runoff is observed overall with significant values in all the three climatics zones. The simulation driven by the MPI-M-MPI-ESM shows an overall reduction with increases to the east of the three zones. In the simulation driven by the NCC-NorESM1, CCLM projects increases in all zones with isolated decreases in all the three climatics zones.

The RegCM4-7 and REMO2015 models project mixed trends, notably with reductions in coastal areas and significant increases in the Sahel. Simulations driven by the MOHC-HadGEM2-ES, a strong reduction in total runoff is dominant overall with significant values in all the three climatics zones. Simulations driven by the MPI-M-MPI-ESM, show decreases in total runoff overall with isolated localized increases in all three zones. Simulations driven by the NCC-NorESM1 show increases in total runoff overall with isolated localized decreases in all the three climatics zones, with significant values in the Sahel and Savannah. Our results are consistent with previous studies that of (Bojer *et al*., 2024) on the Gilgel Gibe Watershed in Ethiopia, (Koffi *et al*., 2023) in West-Central of Côte d'Ivoire, (Cook *et al*., 2022) over West Africa, (Stanzel *et al*., 2018) over West Africa.

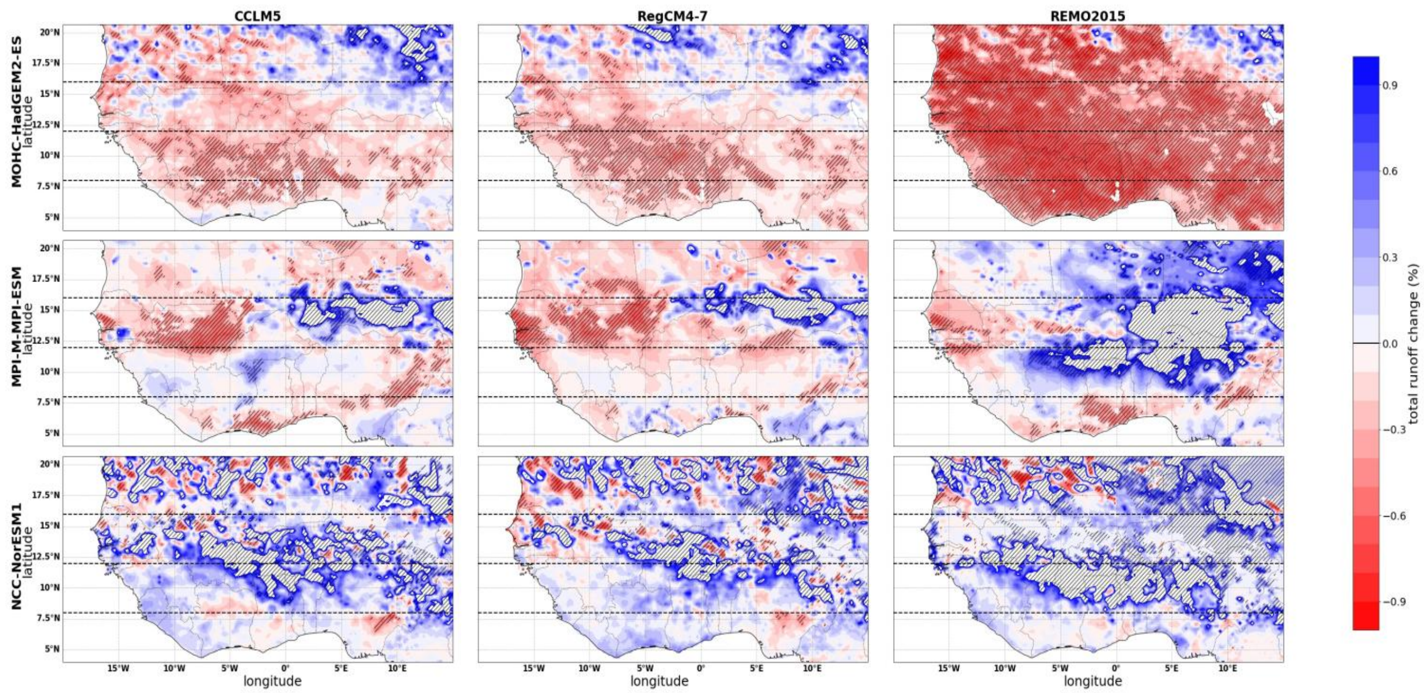

Figure 4.18: Projected changes in annual total runoff over the period 2021–2060 relative to the historical period 1970–2005 under the RCP 8.5 scenario. the areas with statistical significance at 95% confidence level are marked with black stippling.

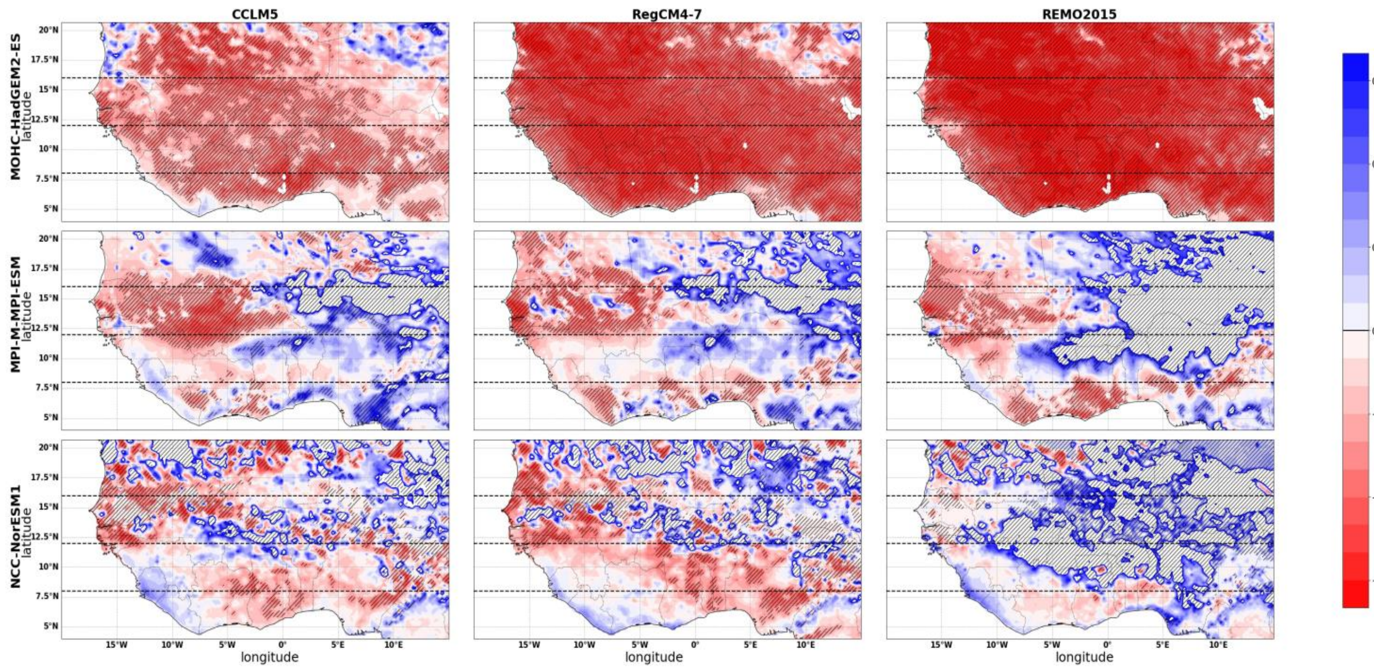

Figure 4.19: Projected changes in annual total runoff over the period 2061–2100 relative to the historical period 1970–2005 under the RCP 8.5 scenario. the areas with statistical significance at 95% confidence level are marked with black stippling.

4.3 Projected Climatic changes impact over Inner-Niger-Delta by CORDEX model

4.3.1 The Projected changes in mean seasonal precipitation over IND under the RCP 2.6 scenario

Figure 4.20 shows that future precipitation changes differ considerably between regional and underlying global models, highlighting the uncertainties associated with climate projections. The CCLM5 model shows notable reductions in precipitation in the DJF season when coupled with MOHC-HadGEM2-ES and MPI-M-MPI-ESM models, while it projects an increase with NCC-NorESM1. In contrast, this CCLM5 model tends to show smaller changes in the JJA (main rainy season) and SON seasons, regardless of the global model used. This highlights that interactions between global and regional models strongly influence seasonal outcomes. The RegCM4-7 shows similar trends, but with varying intensities. When coupled with MOHC-HadGEM2-ES, precipitation shows a slight decrease overall, but moderate in the MAM season. When coupled with MPI-M-MPI-ESM, precipitation shows a slight change overall, but with the exception in the DJF season for the near future and the MAM season for the far future. While coupled RegCM4-7 with NCC-NorESM1, the simulations projected an increase in all seasons, with the exception of the DJF season which shows a decrease in precipitation. The REMO model, when coupled with MOHC-HadGEM2-ES and MPI-M-MPI-ESM, projecteds small changes for all seasons, with the exception of the DJF season that shows a more significant decrease in precipitation. However, combined with NCC-NorESM1, it shows a slight increase for some wet seasons (JJA and SON) and a decrease for dry seasons (DJF and MAM). These inter-model differences highlight the importance of considering multiple configurations to better understand and reduce the uncertainty associated with climate projections, as each model combination provides a different perspective on the potential impacts of climate change on precipitation. The results here are consistent with previous studies of (Tamoffo *et al*., 2023) over West Africa, (Dosio *et al*., 2021) over Africa, (Shiru *et al*., 2020) in Nigeria, (Gebrechorkos *et al*., 2020) in East Africa, (Gao *et al*., 2024) over Yellow River in China.

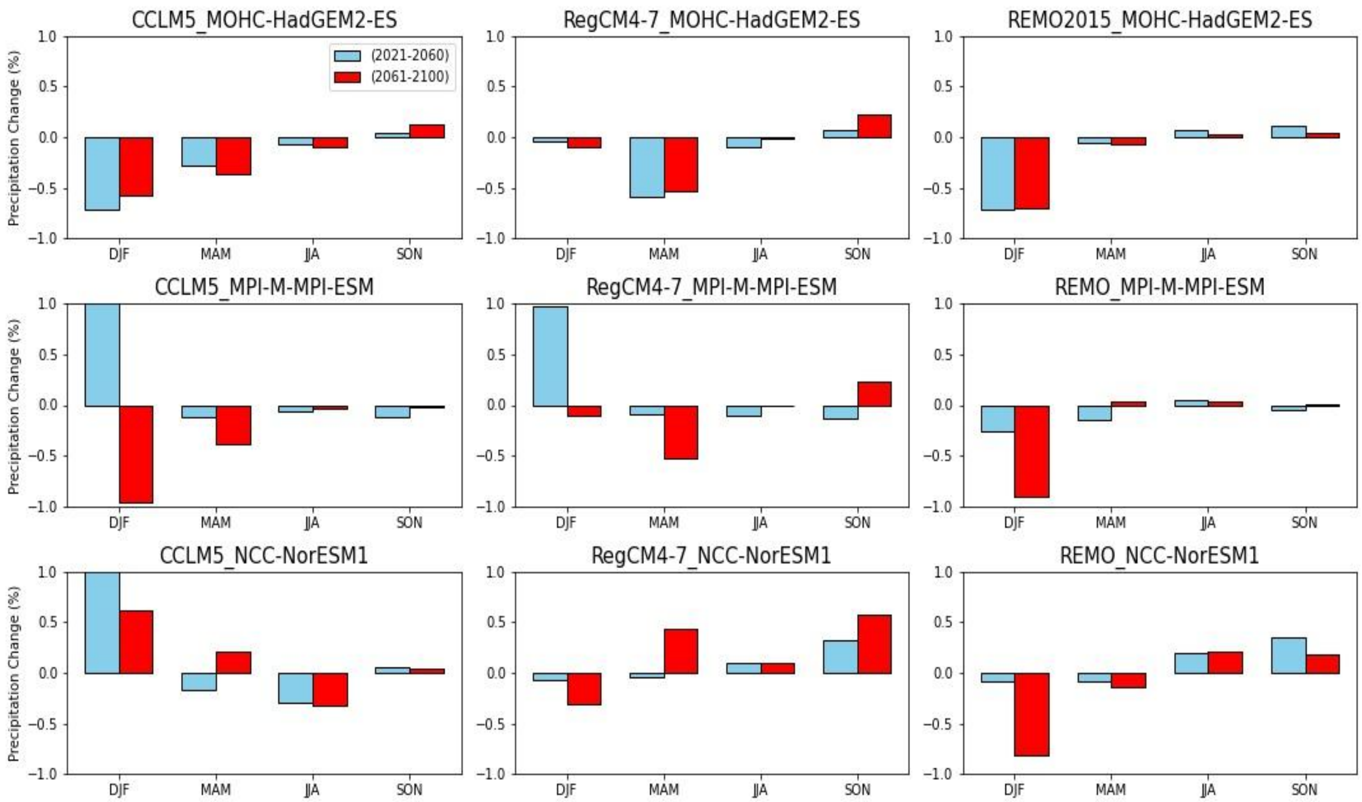

Figure 4.20: The changes in seasonal mean between historical and future values for precipitation of IND under the RCP 2.6 scenario.

4.3.2 The Projected changes in mean seasonal precipitation over IND under the RCP 8.5 scenario

The Figure 4.21 shows the precipitation projections from regional climate models (CCLM5, RegCM4-7, REMO2015) and global coupled models (MOHC-HadGEM2-ES, MPI-M-MPI-ESM, NCC-NorESM1), significant variations are observed between scenarios and seasons. For the CCLM5 model, a marked decrease in precipitation for the MAM, JJA and SON seasons is observed in all simulations and an increase in precipitation in the DJF season. For the RegCM4-7 model, precipitation shows a notable decrease during the DJF, MAM and JJA seasons and an increase is projected in the SON season in all model simulations. This model also highlights substantial reductions in the MAM and JJA seasons in the both of scenarios, reflecting a potentially drier trend during the periods. The REMO2015 model projects a decrease in precipitation in the DJF and MAM seasons. However, slight increases in SON season are observed for MOHC-HadGEM2-ES and MPI-M-MPI-ESM simulations, more intense for NCC-NorESM1 simulations. These results highlight significant inter-model variability, highlighting the need to use multiple projections to assess regional climate impacts. Our results are consistent with previous studies that of (Tamoffo *et al*., 2023) West Africa, (Koffi *et al*., 2023) in West-Central of Côte d'Ivoire, (Cook *et al*., 2022) over West Africa, (Bojer *et al*., 2024) on the Gilgel Gibe Watershed in Ethiopia, (Stanzel *et al*., 2018) over West Africa.

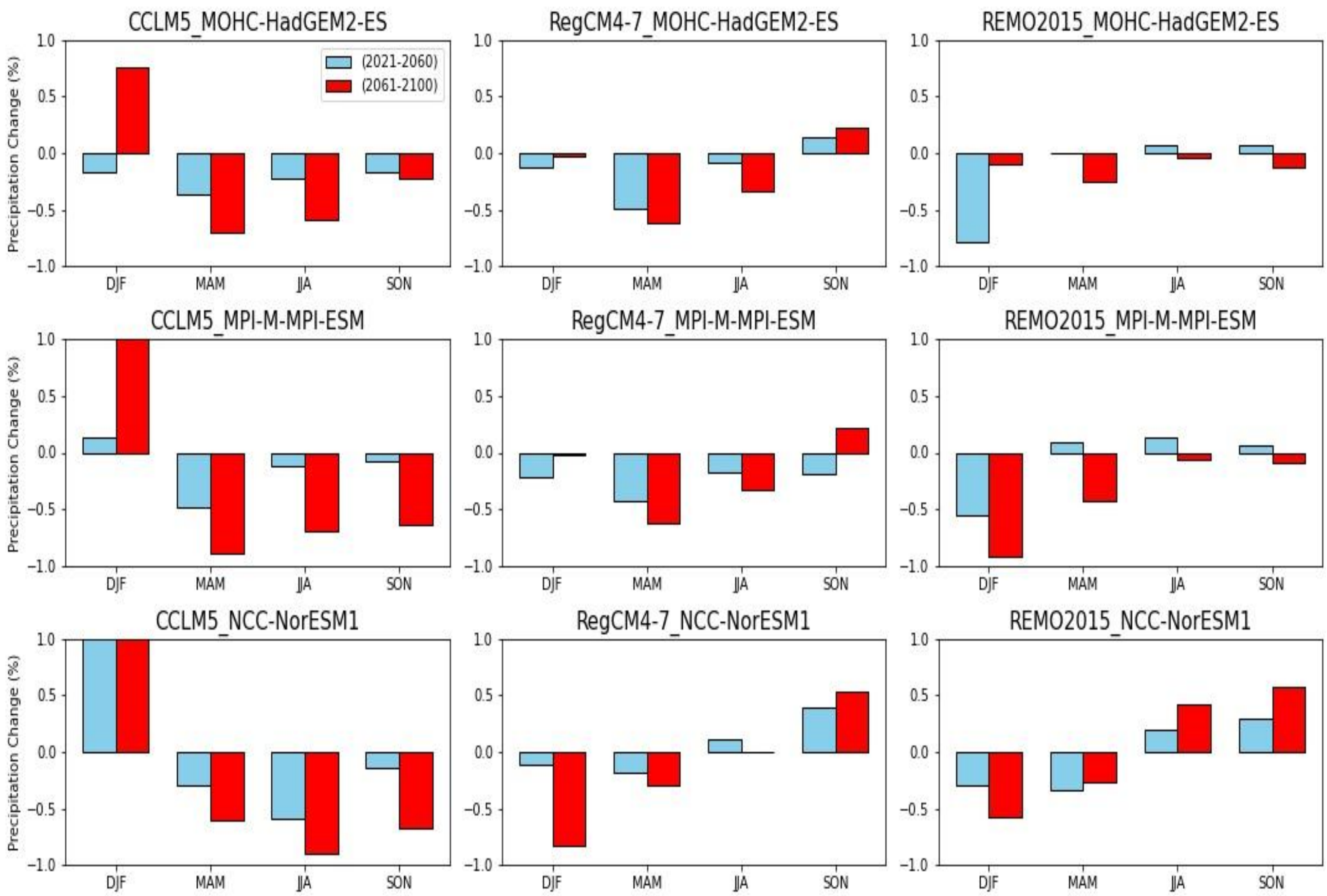

Figure 4.21: The changes in seasonal mean between historical and future values for precipitation of IND under the RCP 8.5 scenario.

4.3.3 The Projected changes in mean seasonal evaporation over IND under the RCP 2.6 scenario

The Figure 4.22 shows the variations of future evaporations under RCP 2.6 according to the regional models and the underlying global models, highlighting the uncertainties associated with climate projections. The CCLM5 model shows reductions in all seasons and simulations, evaporations reach the maximum in MAM season when coupled with MOHC-HadGEM2-ES and MPI-M-MPI-ESM models, in JJA season when coupled with NCC-NorESM1 models, this model shows smaller changes in SON season, independently of the global model used. The RegCM4-7 model shows mixed trends, but with variable intensity. When coupled with the MOHC-HadGEM2-ES and MPI-M-MPI-ESM models, evaporations show a slight decrease overall, more moderate in the MAM season, with the exception of the DJF and SON seasons which show an increase in evaporation for the distant future. While with NCC-NorESM1, the simulations project an increase in all seasons, evaporations reach the maximum in the SON season. The REMO2015 model, when coupled with the MOHC-HadGEM2-ES and MPI-M-MPI-ESM models, they project small increases for all seasons, with the exception of the DJF season (MPI-M-MPI-ESM) which shows a small decrease in evaporation. However, when associated with NCC-NorESM1, it shows a slight increase overall and reaches in the SON season. These inter-model differences highlight the importance of considering multiple configurations to better understand the uncertainty associated with climate projections, as each combination of models provides a different perspective on the potential impacts of climate change on evaporation. Our results are consistent with previous studies that of (Soares *et al*., 2019) over Africa, (Gebrechorkos *et al*., 2020) in East Africa, (Bojer *et al*., 2024) on the Gilgel Gibe Watershed in Ethiopia, (La Fuente *et al*., 2022) over the lake Kinneret in Israel.

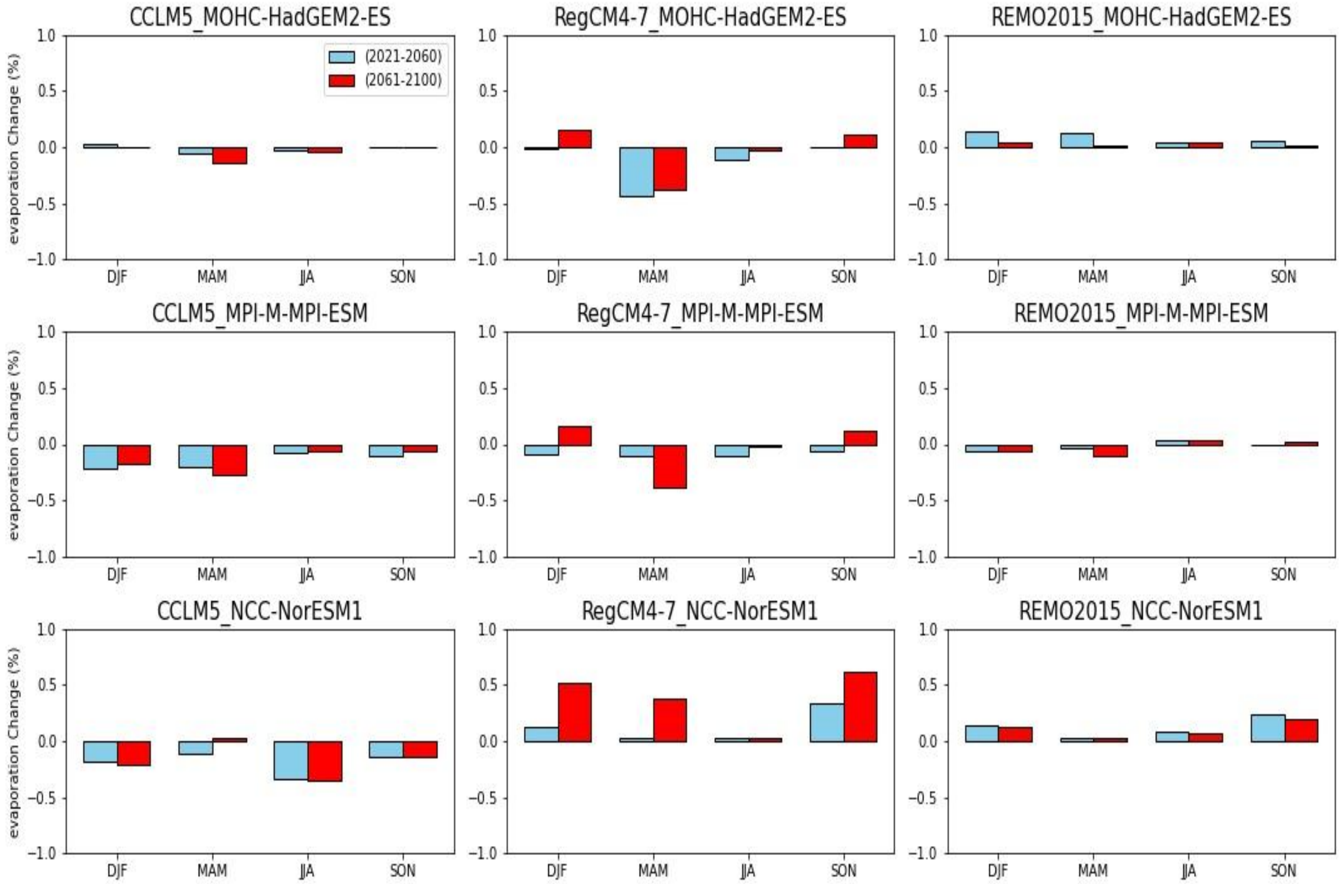

Figure 4.22: The changes in seasonal mean between historical and future values for evaporation of IND under the RCP 2.6 scenario.

4.3.4 The Projected changes in mean seasonal evaporation over IND under the RCP 8.5 scenario

The Figure 4.23 shows the variations of future evaporation under RCP 8.5 according to the regional models and the underlying global models, highlighting the uncertainties associated with climate projections. The CCLM5 model shows notable reductions in evaporation across all simulations and seasons and the maximum in the MAM season when coupled with the MOHC-HadGEM2-ES and MPI-M-MPI-ESM models, in the JJA season with NCC-NorESM1. The RegCM4-7 model shows similar trends, but with varying intensity. When coupled with the MOHC-HadGEM2-ES and MPI-M-MPI-ESM model, evaporation shows a slight decrease overall, more moderate in the MAM season. While with NCC-NorESM1, the simulations project an increase for the DJF and SON seasons, a decrease in evaporation for the MAM and JJA seasons. The REMO2015 model, when coupled with the MOHC-HadGEM2-ES and MPI-M-MPI-ESM models, it projects small increases for all seasons in the near future, reaching their maxima in the MAM season and shows small decreases for all seasons in the far future, reaching their maxima in the MAM season. However, when associated with NCC-NorESM1, it displays a slight increase for all seasons, more moderate in the MAM season. These inter-model differences highlight the importance of considering several configurations to better understand the uncertainty associated with climate projections, because each combination of models provides a different perspective on the potential impacts of climate change on evaporation. Our results are consistent with previous studies that of (Cook *et al*., 2022) over West Africa, (Stanzel *et al*., 2018) over West Africa, (Gebrechorkos *et al*., 2020) in East Africa, (Bojer *et al*., 2024) on the Gilgel Gibe Watershed, Ethiopia, (La Fuente *et al*., 2022) over the lake Kinneret in Israel.

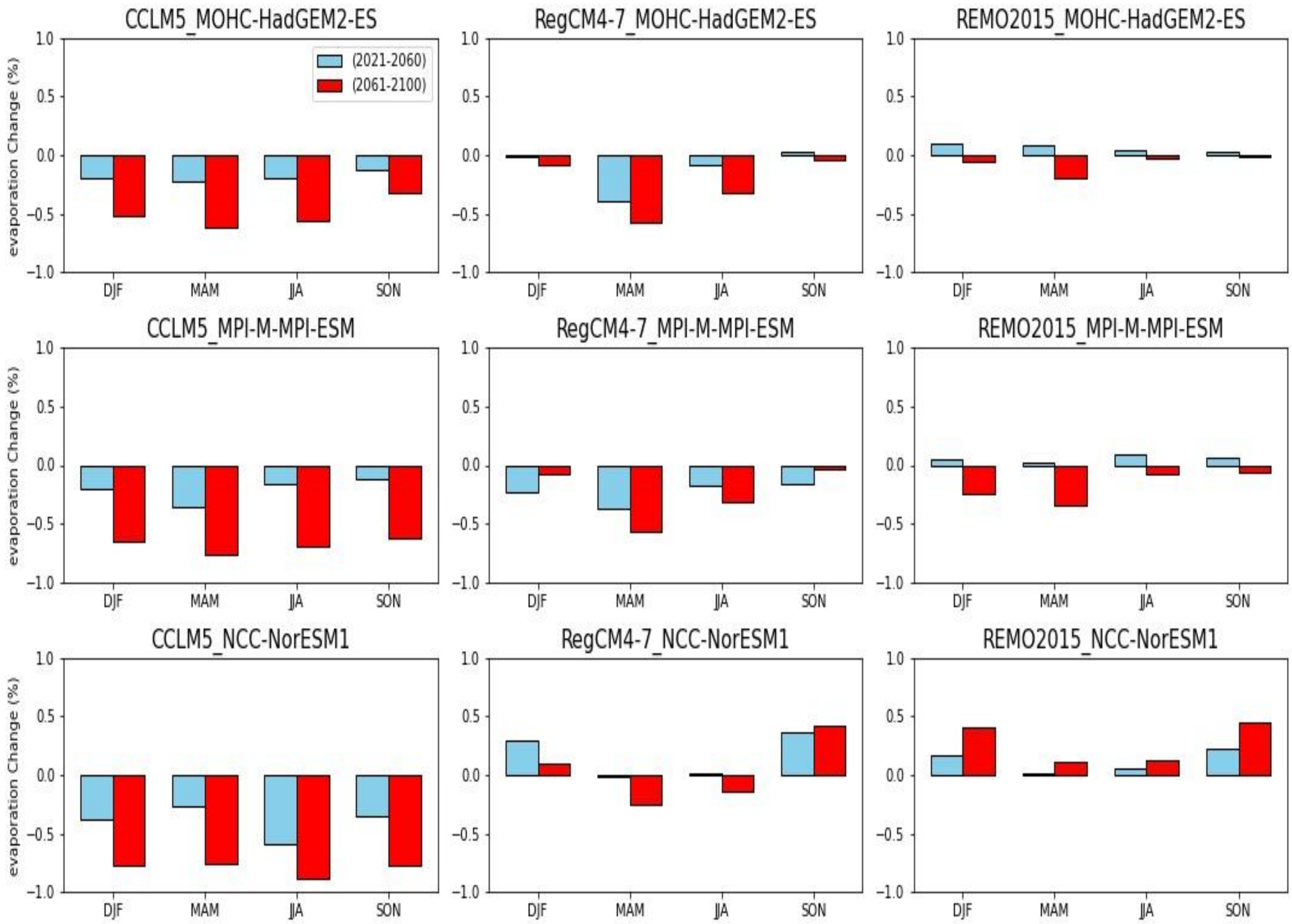

Figure 4.23: The changes in seasonal mean between historical and future values for evaporation of IND under the RCP 8.5 scenario.

4.3.5 The Projected changes in mean seasonal air temperature over IND under the RCP 2.6 scenario

The Figure 4.24 shows future air temperature variations under RCP 2.6 according to the underlying regional and global models, highlighting the uncertainties associated with climate projections. The CCLM5 model shows small increases in air temperature for all simulations and all seasons, more moderate when coupled with the MOHC-HadGEM2-ES and NCC-NorESM1 models. The RegCM4-7 model shows similar trends, but with a weak intensity. It shows small increases in air temperature for all simulations and all seasons, more moderate when coupled with the MOHC-HadGEM2-ES and MPI-M-MPI-ESM models. The REMO2015 model shows small increases in air temperature for all simulations and all seasons, more moderate when coupled with the MOHC-HadGEM2-ES and MPI-M-MPI-ESM models. Our results are consistent with previous studies that of (Gao *et al*., 2024) over Yellow River in China, (Shiru *et al*., 2020) in Nigeria, (Gebrechorkos *et al*., 2020) in East Africa.

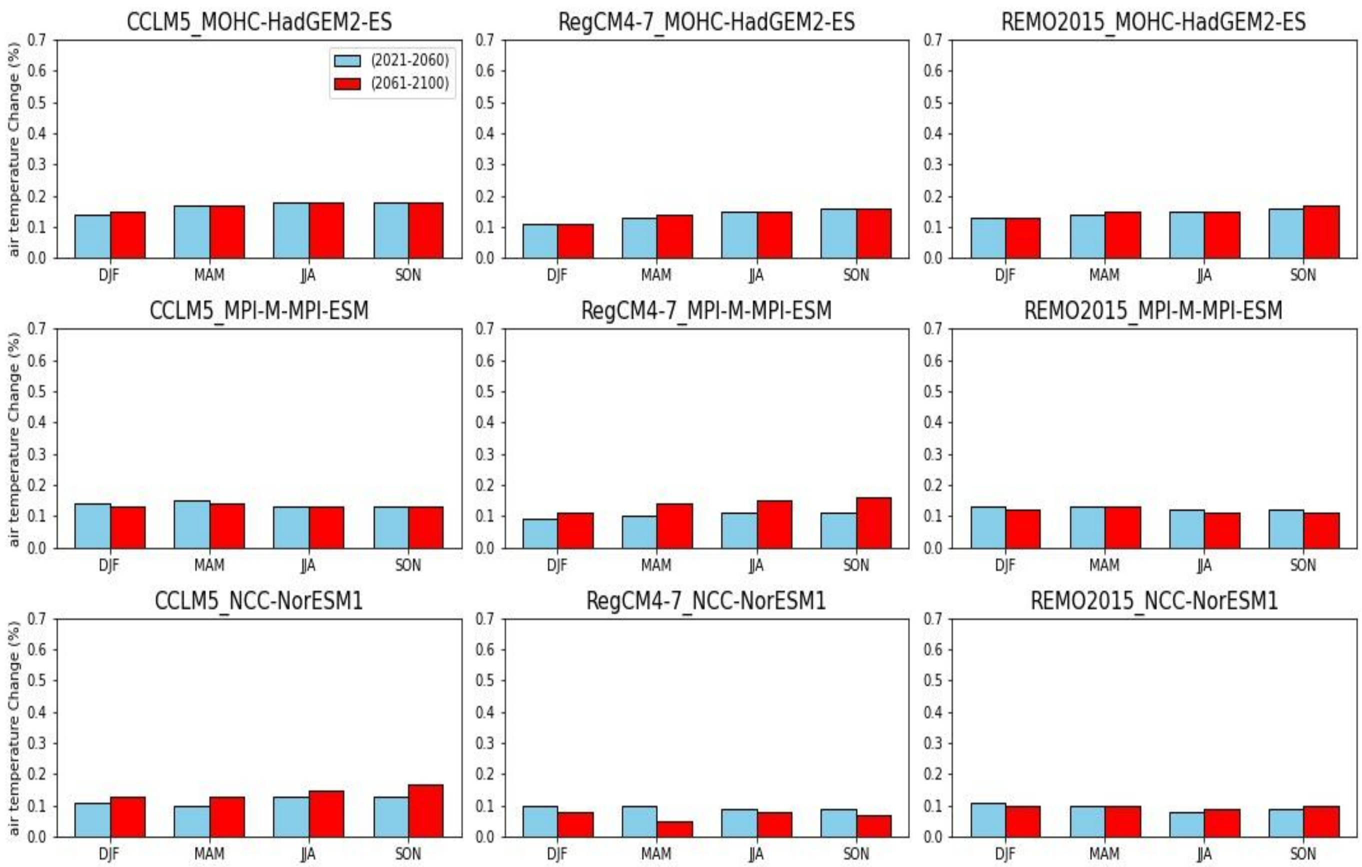

Figure 4.24: The changes in seasonal mean between historical and future values for air temperature of IND under the RCP 2.6 scenario.

4.3.6 The Projected changes in mean seasonal air temperature over IND under the RCP 8.5 scenario

The Figure 4.25 shows future air temperature variations under RCP 8.5 according to the underlying regional and global models, highlighting the uncertainties associated with climate projections. The CCLM5 model shows strong increases in air temperature for all simulations and all seasons, more moderate for the long-term simulations that reach +0.5% of the air temperature. The RegCM4-7 model shows similar trends, but with a weak intensity. It shows increases in air temperature for all simulations and all seasons, more moderate for the long-term simulations that reach +0.4% of the air temperature. The REMO2015 model, shows increases in air temperature for all simulations and all seasons, more moderate for the long-term simulations that reach +0.4% of the air temperature. Our results are consistent with previous studies that of (Gao *et al*., 2024) over Yellow River in China, (Shiru *et al*., 2020) in Nigeria, (Gebrechorkos *et al*., 2020) in East Africa, (Amoussou *et al*.,2020) in the Mono River Basin (West Africa).

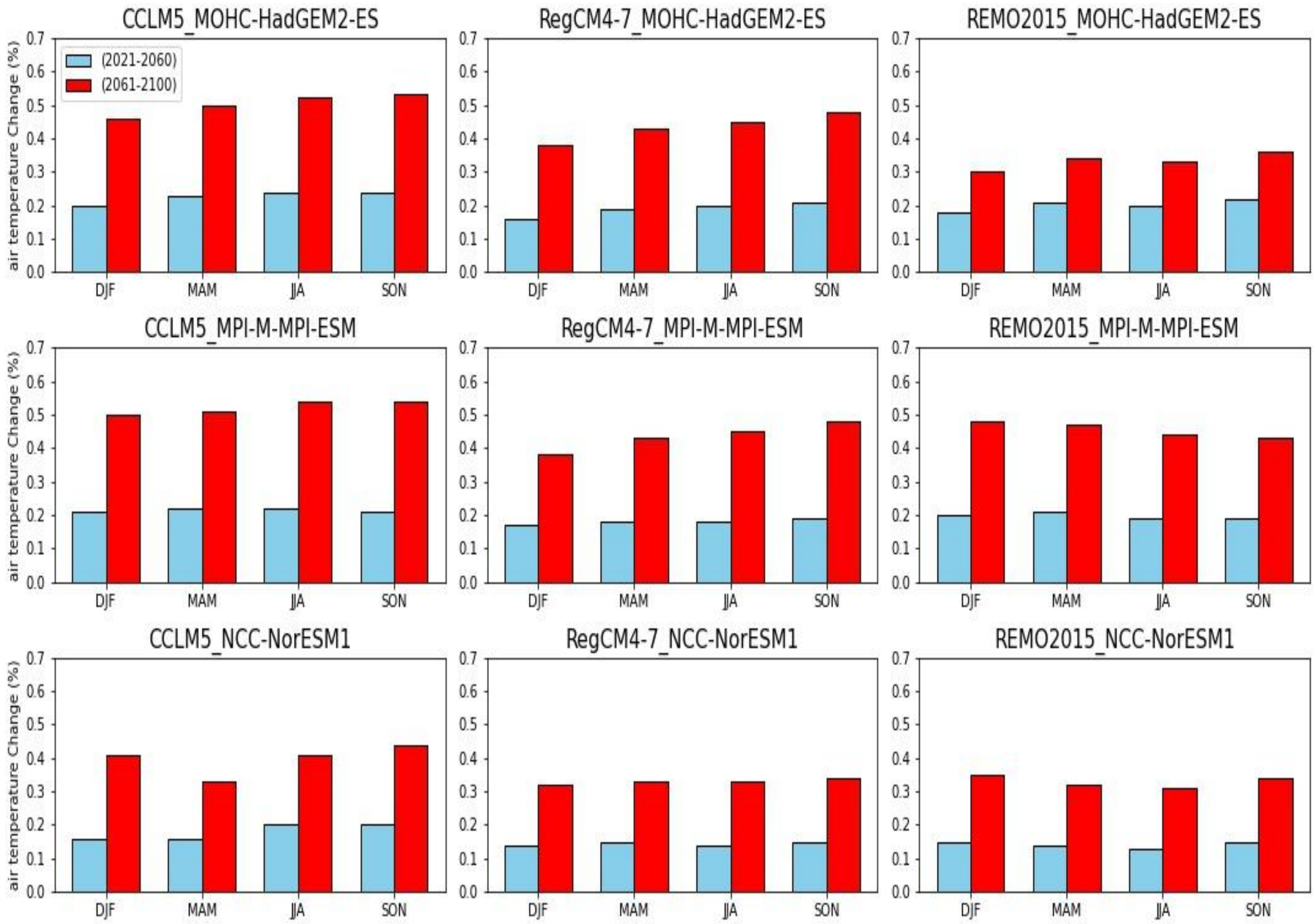

Figure 4.25: The changes in seasonal mean between historical and future values for air temperature of IND under the RCP 8.5 scenario.

4.3.7 The Projected changes in mean seasonal total runoff over IND under the RCP 2.6 scenario

The analysis of simulated total runoff changes (Figure 4.26), based on different regional climate models (RCMs) and seasons, reveals significant variations between time horizons and models. The results for the CCLM5_MOHC-HadGEM2-ES model indicate a significant increase in total runoff for all seasons, particularly the DJF and SON seasons. The CCLM5_MPI-M-MPI-ESM model shows less marked variations, with decreases close to zero, particularly for the JJA and SON seasons. This indicates that the choice of the model-forcing combination strongly affects the sensitivity of the total runoff simulations. However, the CCLM5_NCC-NorESM1 model shows mixed variations, with increases for the near future except for the JJA season and for the far future small decreases during the DJF and JJA seasons. The RegCM4-7_MOHC-HadGEM2-ES models project an increase in total runoff for all seasons for the near future, a reduction in total runoff in the far future especially for the DJF and MAM seasons. The RegCM4-7_MPI-M-MPI-ESM models project a decrease in total runoff for all seasons and periods, except for the DJF season for the near future. The RegCM4-7_NCC-NorESM1 models project an increase in total runoff for all seasons and periods, except for the DJF season for the far future. The REMO2015 model simulations show more stable and limited trends in amplitude, changes during the DJF and SON seasons are modest, with slight increases. The results show a more conservative response to climate variability compared to CCLM5 and RegCM4-7. Our results are consistent with previous studies that of (Kim *et al*., 2021) in Burundi, (Cook *et al*., 2022) over West Africa, (Stanzel *et al*., 2018) over West Africa.

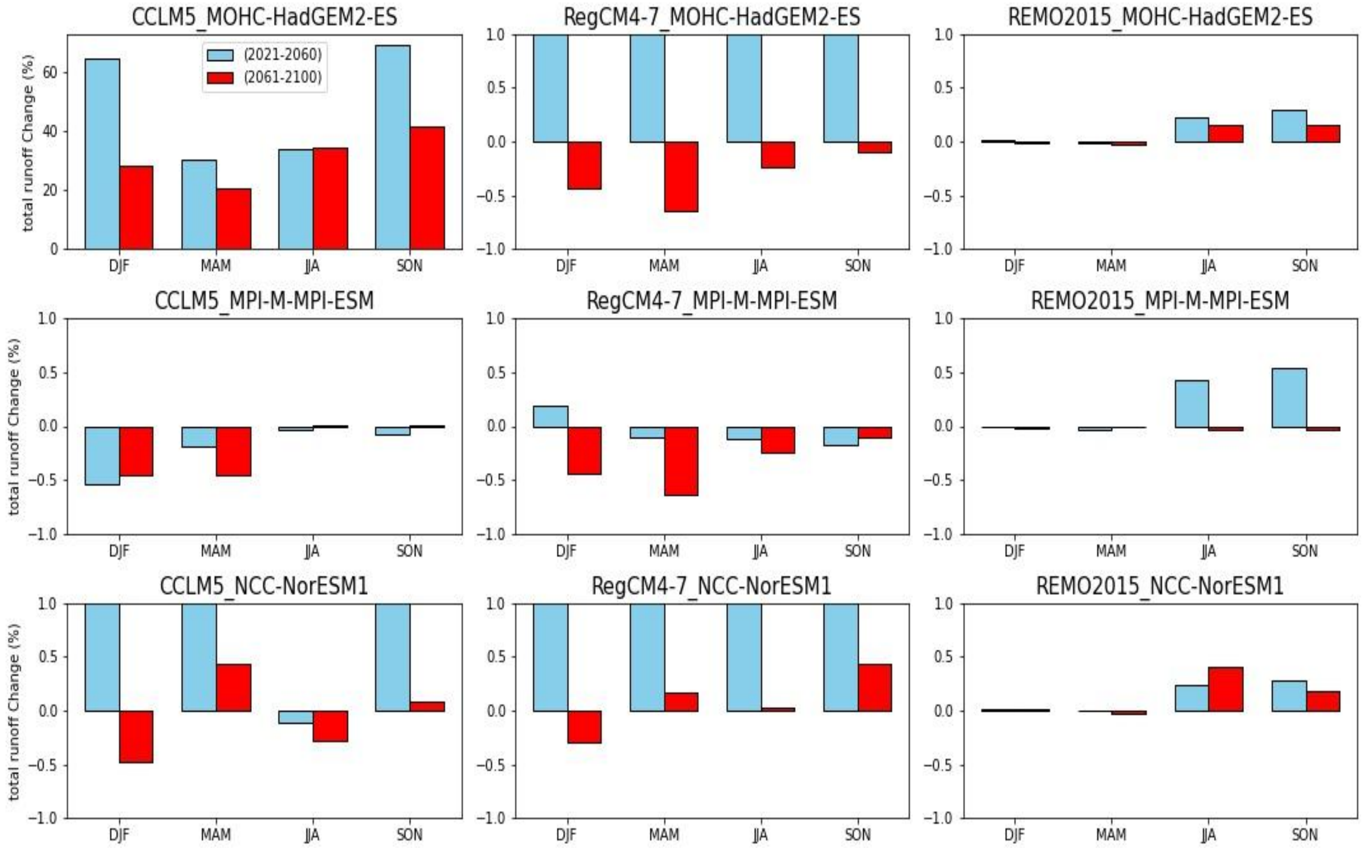

Figure 4.26: The changes in seasonal mean between historical and future values for total runoff of IND under the RCP 2.6 scenario.

4.3.8 The Projected changes in mean seasonal total runoff over IND under the RCP 8.5 scenario

The analysis of simulated total runoff changes (Figure 4.27), based on different regional climate models (RCMs) and seasons, reveals significant variations between time horizons and models. The results for the CCLM5_MOHC-HadGEM2-ES model indicate a significant increase in total runoff for all seasons, particularly the JJA and SON seasons. The CCLM5_MPI-M-MPI-ESM model shows small decreases for all seasons, particularly for the JJA and SON seasons. However, the CCLM5_NCC-NorESM1 model shows small reductions for all seasons, more moderate for the DJF and JJA seasons. The RegCM4-7_MOHC-HadGEM2-ES model projects a reduction in total runoff for all periods and seasons with the exception of the SON season during which a small increase in total runoff is observed. The RegCM4-7_ MPI-M-MPI-ESM models project a small decrease in runoff for all seasons and periods, more moderate in the MAM and JJA seasons. The RegCM4-7_ NCC-NorESM1 models project a decrease in total runoff for all seasons and periods, except for the JJA and SON seasons for the near future and the DJF season in the far future. The REMO2015_MOHC-HadGEM2-ES models project a mixed variation, with increases for the near future more moderate in the JJA and SON seasons, for the far future small decreases are observed for all seasons, more moderate during the JJA and SON seasons. The REMO2015_ MPI-M-MPI-ESM models project an increase in total runoff for all seasons, more moderate in the JJA and SON seasons for the near future, during the far future a small decrease is observed for all seasons. The REMO2015_NCC-NorESM1 model shows weak reductions for all periods and all seasons, more moderate for the JJA and SON seasons. Our results are consistent with previous studies that of (Bojer *et al*., 2024) on the Gilgel Gibe Watershed in Ethiopia, (Koffi *et al*., 2023) in West-Central of Côte d'Ivoire, (Cook *et al*., 2022) over West Africa, (Stanzel *et al*., 2018) over West Africa.

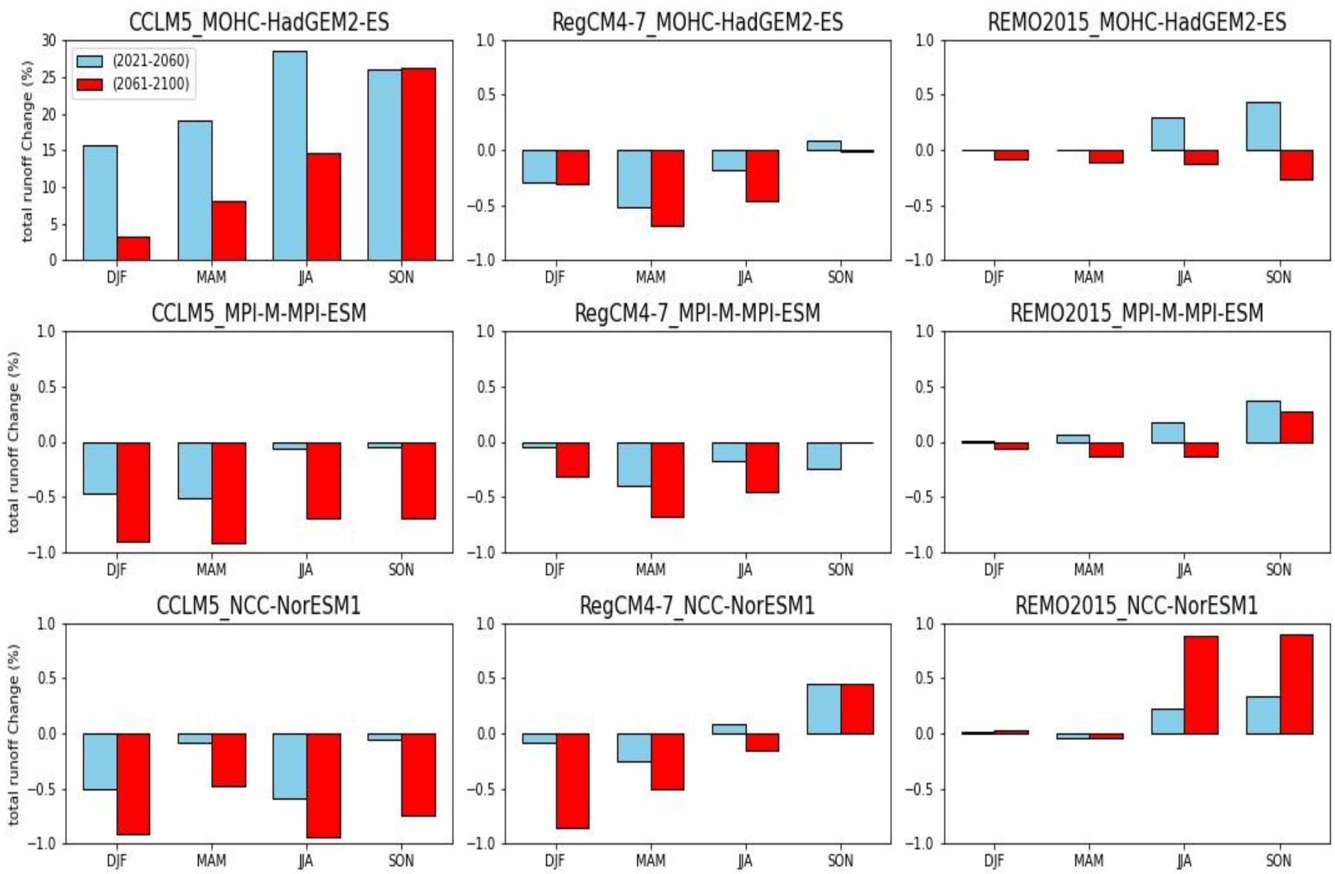

Figure 4.27: The changes in seasonal mean between historical and future values for total runoff of IND under the RCP 8.5 scenario.

4.4 Projected Climatic changes Impact on Hydrology over IND by SWAT model

4.4.1 Calibration and validation of SWAT model in streamflow simulation of IND

The Figure 4.28(A) shows the calibration and validation of the streamflow rate for the Mopti station by comparing observed and simulated streamflow over two distinct periods: the calibration phase (1990-2004) and the validation phase (2005-2010). During the calibration, the correlation coefficient R=0.79 indicates a good match between the observed and simulated data, although the root means square error (RMSE = 745.99) and the mean bias (MBias = -61.57) show an underestimation of the model for some periods of heavy rainfall. During the validation, the correlation coefficient remains high (R=0.78), demonstrating that the model maintains a stable performance even over different periods of time. However, a slight increase in the RMSE (747.35) indicated that the overall error remains similar to that of the calibration, with reduced underestimation of MBias = -40.16. These results show that the model captures the general trend of the streamflow, although it has difficulties in reproducing the streamflow peaks with perfect accuracy.

The Figure 4. 28 (B) shows the calibration and validation of the streamflow rate for the Dire station by comparing observed and simulated streamflow over two distinct periods: the calibration phase (1990-2004) and the validation phase (2005-2010). During the calibration phase, the correlation between simulated and observed values is R=0.60, indicating a moderate relationship. However, the root mean square error (RMSE) is relatively high (926.32mm), reflecting significant differences between simulated and measured values. In addition, the average bias (MBias=-80.80) indicates a slight underestimation of the model. These results show that, although the model reproduces the general trend of streamflow, adjustments are necessary to improve the accuracy. For the validation phase (2005-2010), the model performance remains similar with a slightly lower correlation (R=0.54) and an increase in the root mean square error (RMSE=1036.40 mm), suggesting a reduced accuracy. However, the mean bias decreases in absolute value (MBias=-72.52), which means that the underestimation of the model is reduced compared to the calibration. Visually, we notice that the streamflow peaks are often underestimated or poorly captured by the simulation, especially during extreme events.

The figure 4.28(C) shows the calibration and validation of the streamflow rate for the Tombouctou station by comparing observed and simulated streamflow over two distinct periods: the calibration phase (1990-2004) and the validation phase (2005-2010). During the calibration phase, the correlation between simulated and observed values is R=0.57, indicating a moderate relationship. However, the root mean square error (RMSE) is relatively high (739.16 mm), reflecting significant differences between simulated and measured values. In addition, the average bias (MBias=-60.55) indicates a slight underestimation of the model. These results show that, although the model reproduces the general trend of streamflow, adjustments are necessary to improve the accuracy. For the validation phase (2005-2010), the model performance remains similar with a slightly lower correlation (R=0.54) and an increase in the root mean square error (RMSE=899.34 mm), suggesting a loss of accuracy. However, the mean bias decreases in absolute value (MBias=-34.86), which means that the underestimation of the model is reduced compared to the calibration. Visually, it is noted that the peak streamflow are often underestimated or poorly captured by the simulation, especially during extreme events. Although the model performance is satisfactory with a good level of correlation, the relatively high error and the underestimation of maximum streamflow could limit its use for analyses requiring increased accuracy, especially in water resources management and flood forecasting.

Ebodé *et al*., (2024) obtained an identical result in their study carried out in the in the Nyong basin catchment in Cameroon and Naik *et al*., (2024) in the Western Cape in South Africa.

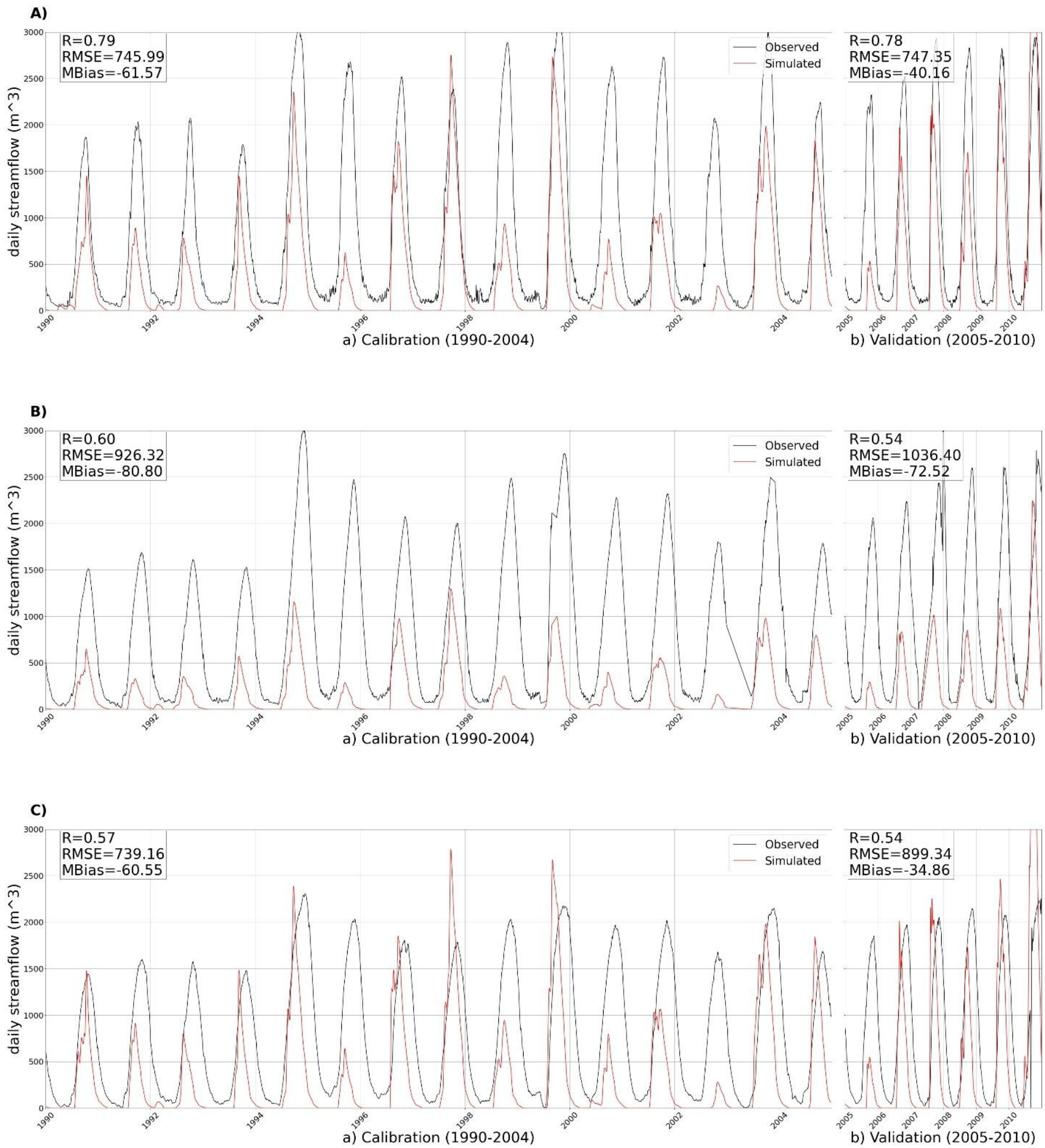

Figure 4.28: Comparisons and statistical values of the observed and simulated surface streamflow at stations (A) Mopti; (B) Dire; and (C) Tombouctou for calibration and validation periods.

4.4.2 The Projected Climate Changes Impact on the seasonal streamflow over Mopti as simulated by SWAT model

The three models (CCLM5_NCC-NorESM1-M, RegCM4-7_MOHC-HadGEM2-ES and REMO2015_MPI-M-MPI-ESM) with the best performance from the historical study were chosen to perform future simulations with the SWAT model. The figure 4.29 shows the changes in streamflow in Mopti according to the climate models presented in columns, highlighting notable variations according to the scenarios and seasons. The CCLM5_NCC-NorESM1-M model projects a significant increase in streamflow, particularly in winter (DJF) and autumn (SON) under both emission scenarios. Under RCP 2.6, the increase reaches about 78% for the period 2020-2060, with a slightly lower trend for 2061-2100. On the other hand, under RCP 8.5, the increases are even lower, with values lower than 60% in SON and 40% in JJA in the near future and far future respectively. This indicates a strong impact of global warming on the intensification of streamflow. The RegCM4-7_MOHC-HadGEM2-ES model shows a more moderate increase in streamflow, spread over all seasons. Under RCP 2.6, the increases remain below 30% except for the DJF season which reaches 75%, with a relatively constant increase between the two periods (2021-2060 and 2061-2100). Under RCP 8.5, the increase is more marked in summer (DJF) and autumn (SON), but it remains lower than that of the CCLM5 model for the near future. In the long-term period, the change remains below 30%. This model shows a more gradual response of the streamflow to climate change, which could be associated with more distributed precipitation over time. The REMO2015_MPI-M-MPI-ESM model projects similar trends to those of CCLM5, a strong increase in streamflow is expected. Under RCP 2.6, the increase reaches about 80% for the period 2061-2100, with a slightly lower trend for 2020-2060. In contrast, under RCP 8.5, the increases are even lower, with values below 40% except for the MAM season for all periods. The model highlights an increased risk of intense streamflow towards the end of the century, particularly in response to heavier rainfall and extreme rain events. All models indicate an increase in streamflow in Mopti in the coming decades, with a more marked intensity under RCP 2.6. Our results are consistent with previous studies that of (Iradukunda *et al*., 2024) in Rwanda, (Ndhlovu *et al*., 2021) in the Zambezi River Basin of Southern Africa, (Naik *et al*., 2024) in the Western Cape in South Africa, (Dai *et al*., 2022) in the Hanjiang River basin in China.

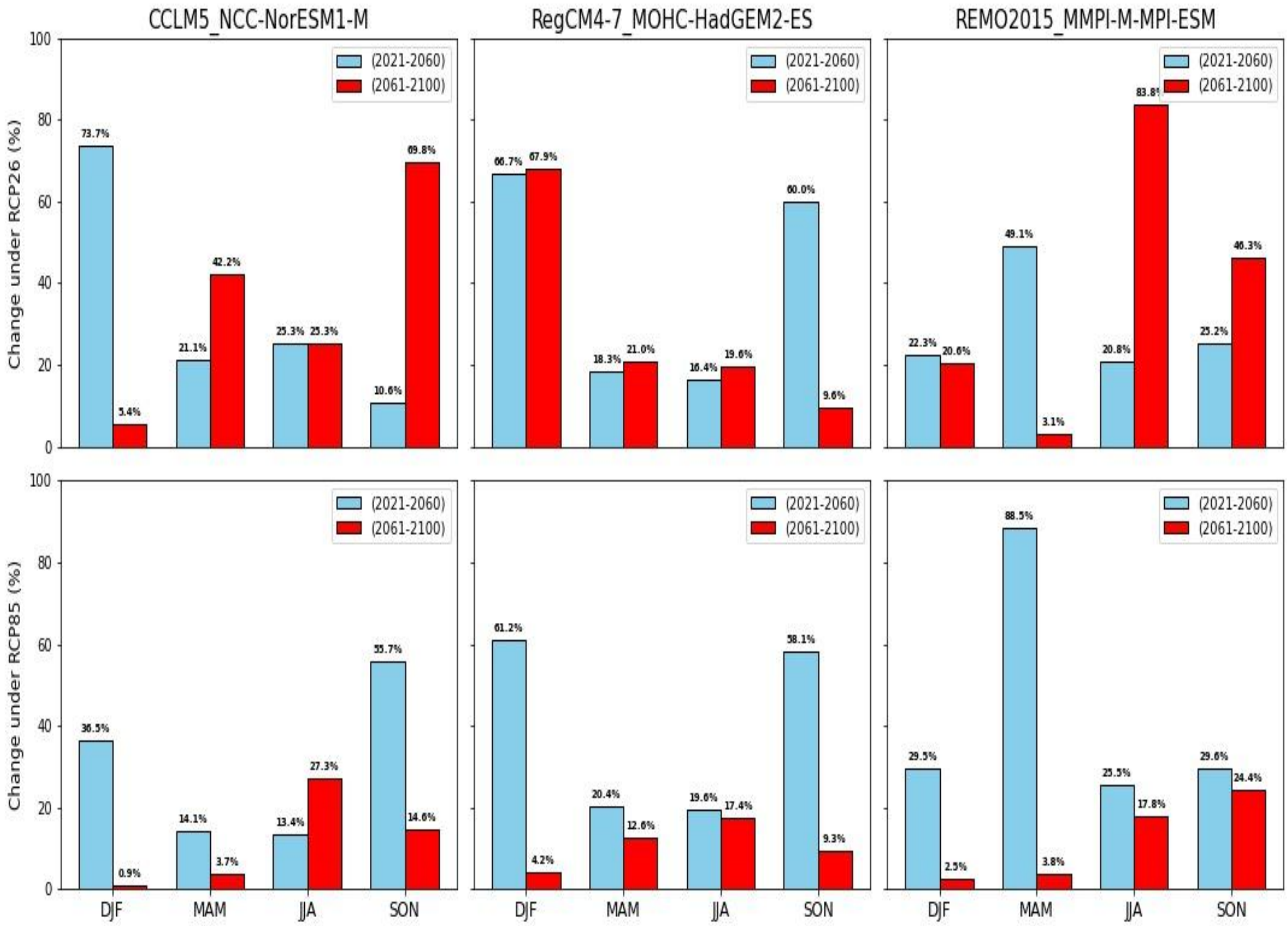

Figure 4.29: The changes in seasonal mean between historical and future values for streamflow of Mopti under the RCP 2.6 and 8.5 scenarios.

4.4.3 The Projected Climate Changes Impact on the seasonal streamflow over Dire as simulated by SWAT model

The figure 4.30 shows the changes in streamflow in Dire according to the climate models presented in columns, highlighting notable variations according to scenarios and seasons. The CCLM5_NCC-NorESM1-M model projects a significant increase in streamflow, especially in summer (JJA) and autumn (SON) under both emission scenarios. Under RCP 2.6, the increase reaches about 78% for the period 2020-2060, with a slightly lower trend for 2061-2100. In contrast, under RCP 8.5, the increases are even lower, with values below 70% in JJA and 20% in SON in the near and far future, respectively. This indicates a strong impact of global warming on discharge intensification. The RegCM4-7_MOHC-HadGEM2-ES model shows a more moderate increase in discharge, spread over all seasons. Under RCP 2.6, the increases remain below 50% except for the MAM and JJA season which reaches 75% for the period 2020-2060, the long-term projection period is below 50% for all seasons. Under RCP 8.5, the increase is more marked in the MAM and JJA seasons, but it remains lower than that of the CCLM5 model for the near future. In the long-term period the change remains below 40% This model shows a more gradual response of the streamflow to climate change, which could be associated with more distributed precipitation over time. The REMO2015_MPI-M-MPI-ESM model projects similar trends to those of CCLM5, a strong increase in streamflow is expected. Under RCP 2.6 and RCP 8.5, the increase reaches about 80% for the period 2020-2060, with a slightly lower trend for 2061-2100. The model highlights an increased risk of intense streamflow towards the end of the century, particularly in response to heavier precipitation and extreme rainfall events. All models indicate an increase in streamflow at Dire in the coming decades, with a greater intensity in the JJA and SON seasons. Our results are consistent with previous studies that of (Iradukunda *et al*., 2024) in Rwanda, (Ndhlovu *et al*., 2021) in the Zambezi River Basin of Southern Africa, (Naik *et al*., 2024) in the Western Cape in South Africa, (Dai *et al*., 2022) in the Hanjiang River basin in China.

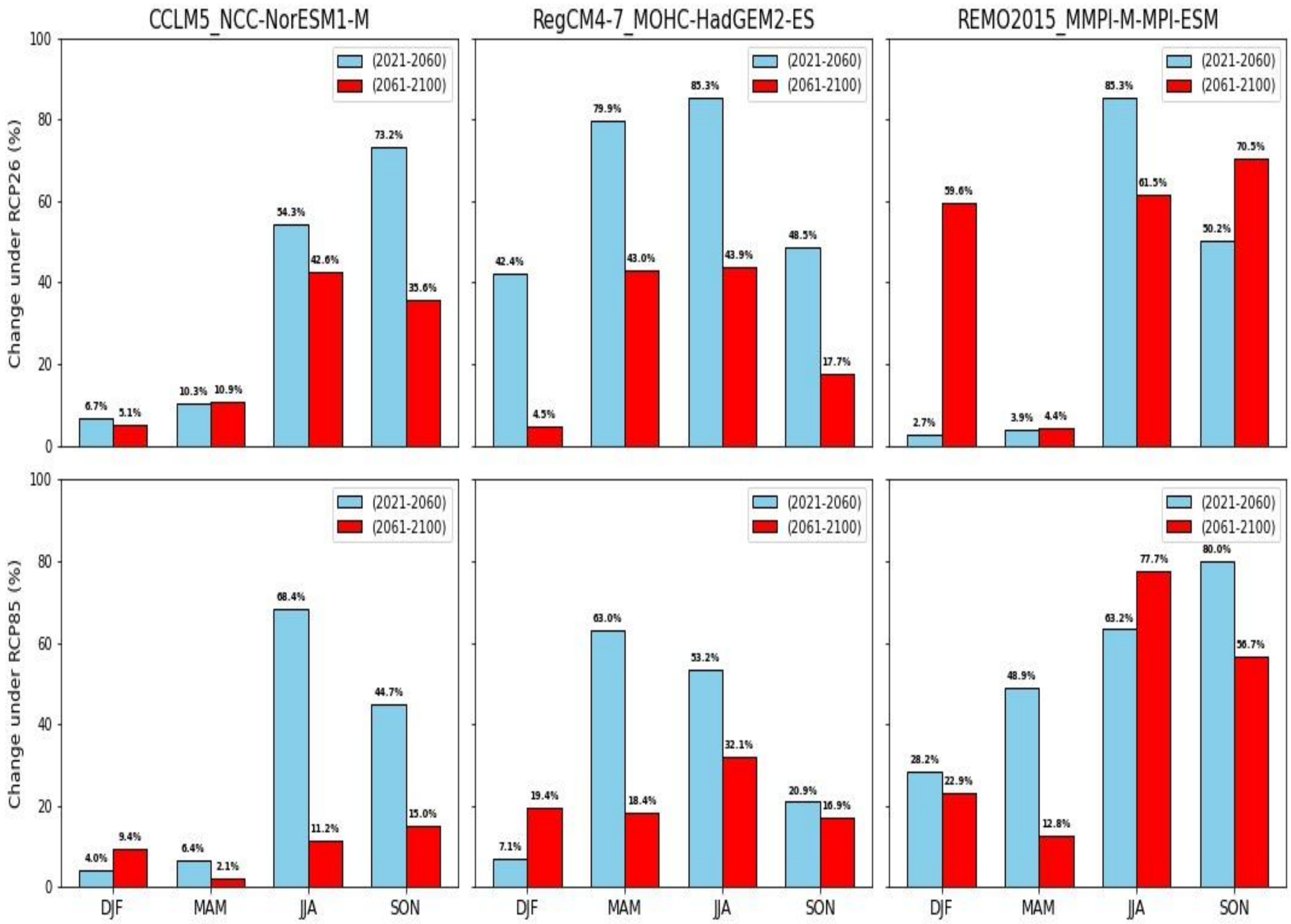

Figure 4.30: The changes in seasonal mean between historical and future values for streamflow of Dire under the RCP 2.6 and 8.5 scenarios.

4.4.4 The Projected Climate Changes Impact on the seasonal streamflow over Tombouctou as simulated by SWAT model

The figure 4.31 shows the changes in the streamflow in Tombouctou according to the climate models presented in columns, highlighting notable variations according to the scenarios and seasons.

The CCLM5_NCC-NorESM1-M model projects a significant increase in streamflow, particularly in winter (JJA) and autumn (SON) under both emission scenarios. Under RCP 2.6, the increase reaches about 90% in the JJA season for the period 2061-2100, with a slightly lower trend for 2020-2060. In contrast, under RCP 8.5, the increases are even lower, with values lower than 50% in JJA and 80% in SON in the near and far future, respectively. This indicates a strong impact of global warming on the intensification of streamflow. The RegCM4-7_MOHC-HadGEM2-ES model shows a more moderate increase in streamflow, spread over all seasons, particularly the MAM and JJA seasons. Under RCP 2.6, the increases reach 30% in the MAM and JJA seasons, 50% in the SON season and less than 30% in the DJF season for both periods (2021-2060 and 2061-2100). Under RCP 8.5, the increase reaches 90% in the MAM and JJA seasons for the near future. In the long term, the change reaches 90% in the JJA season and 70% in the MAM season. This model shows a more gradual response of discharge to climate change. The REMO2015_MPI-M-MPI-ESM model projects similar trends to those of CCLM5, a strong increase in streamflow is expected in the JJ and SON seasons in the long term. Under RCP 2.6, the increase reaches about 90% for the period 2061-2100, with a trend below 20% for 2020-2060. In contrast, under RCP 8.5, the increase reaches 90% in the JJA seasons and 50% in the SON seasons for the near future. In the long term, the change reaches 80% in the SON season and 70% in the JJA season. The model highlights an increased risk of intense discharge towards the end of the century, particularly in response to heavier precipitation and extreme rainfall events. All models indicate an increase in streamflow in Tombouctou in the coming decades, with a more marked intensity under RCP 2.6. Our results are consistent with previous studies that of (Iradukunda *et al*., 2024) in Rwanda, (Ndhlovu *et al*., 2021) in the Zambezi River Basin of Southern Africa, (Naik *et al*., 2024) in the Western Cape in South Africa, (Dai *et al*., 2022) in the Hanjiang River basin in China.

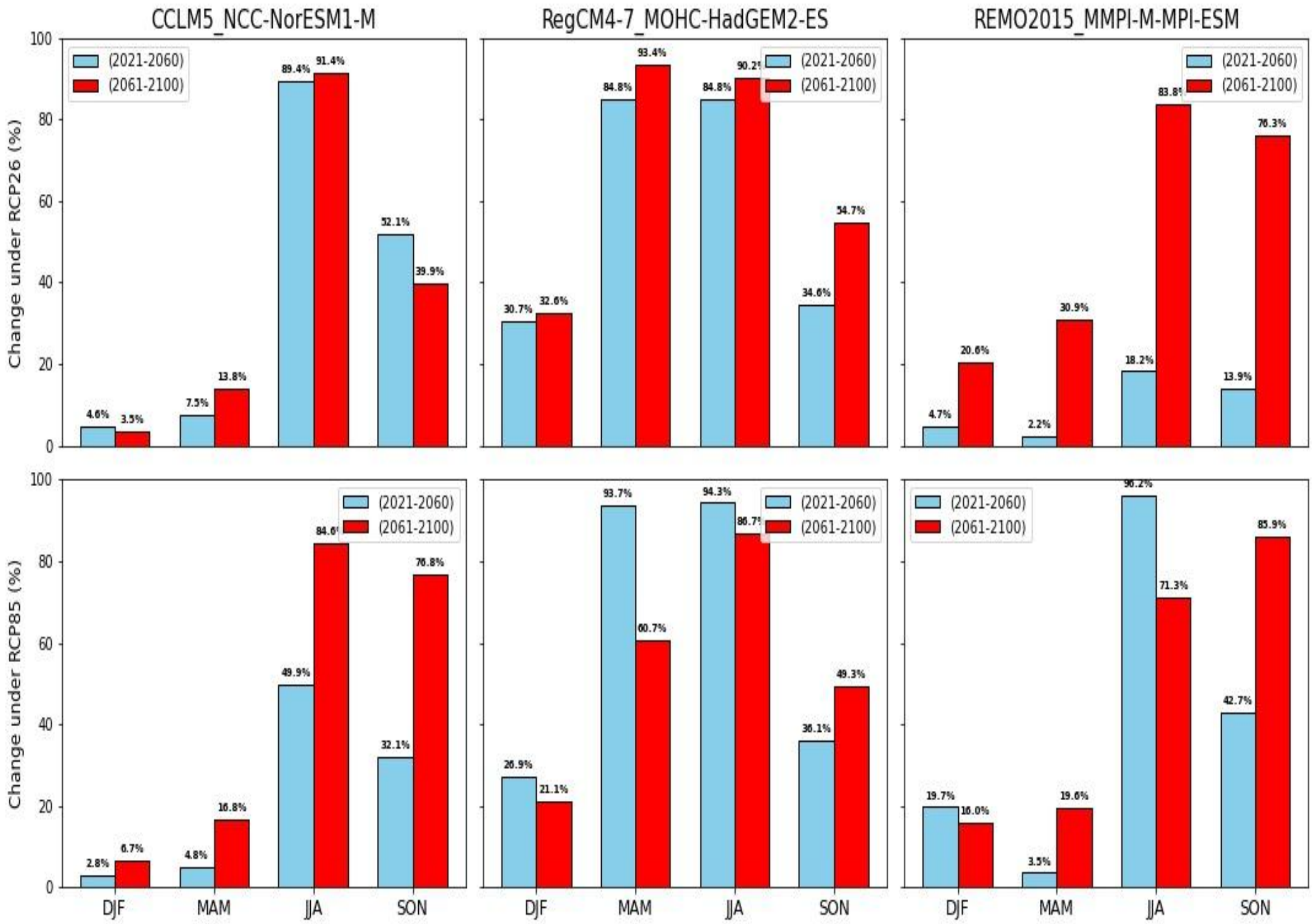

Figure 4.31: The changes in seasonal mean between historical and future values for streamflow of Tombouctou under the RCP 2.6 and 8.5 scenarios.

4.4.5 The Projected Climate Changes Impact on the seasonal surface runoff over Mopti as simulated by SWAT model

The figure 4.32 shows the changes in runoff in Mopti according to the climate models presented in columns, highlighting notable variations according to the scenarios and seasons. The CCLM5_NCC-NorESM1-M model projects an increase in runoff, particularly in summer (JJA) and autumn (SON) under both emission scenarios. Under RCP 2.6, the increase reaches around 50% for the period 2061-2100, with a slightly lower trend for 2021-2060. On the other hand, under RCP 8.5, the increases are less marked, with values lower than 30% for both periods. This indicates a strong impact of global warming on the intensification of runoff. The RegCM4-7_MOHC-HadGEM2-ES model shows a more moderate increase in runoff, spread over all seasons, particularly in the MAM and JJA seasons under both scenarios. Under RCP 2.6, the increases remain below 30%, with a relatively constant increase between the two periods (2021-2060 and 2061-2100). Under RCP 8.5, the increase is more pronounced in the MAM and JJA seasons, but it remains lower than that of the CCLM5 model. The model shows a more gradual response of runoff to climate change. The REMO2015_MPI-M-MPI-ESM model projects similar trends to those of CCLM5. Under RCP 2.6, the increase reaches 40% in the SON season for the period 2061-2100, with a slightly lower trend for 2020-2060. In contrast, under RCP 8.5, the increases are even lower, with values below 40% and 35% in the SON JJA season in the near and far future, respectively. The model highlights an increased risk of intense runoff towards the end of the century, particularly in response to heavier precipitation and extreme rainfall events. Our results are consistent with previous studies that of (Yonaba *et al*., 2023) in burkina faso, (Naik *et al*., 2024) in the Western Cape in South Africa, (Ebodé *et al*., 2023) in the Nyong River Basin (equatorial Central Africa), (Abie *et al*., 2024) in Agewmariyam watershed in Northern Ethiopia, (Ebodé *et al*., 2022) in the So'o River Basin (south of Cameroon).

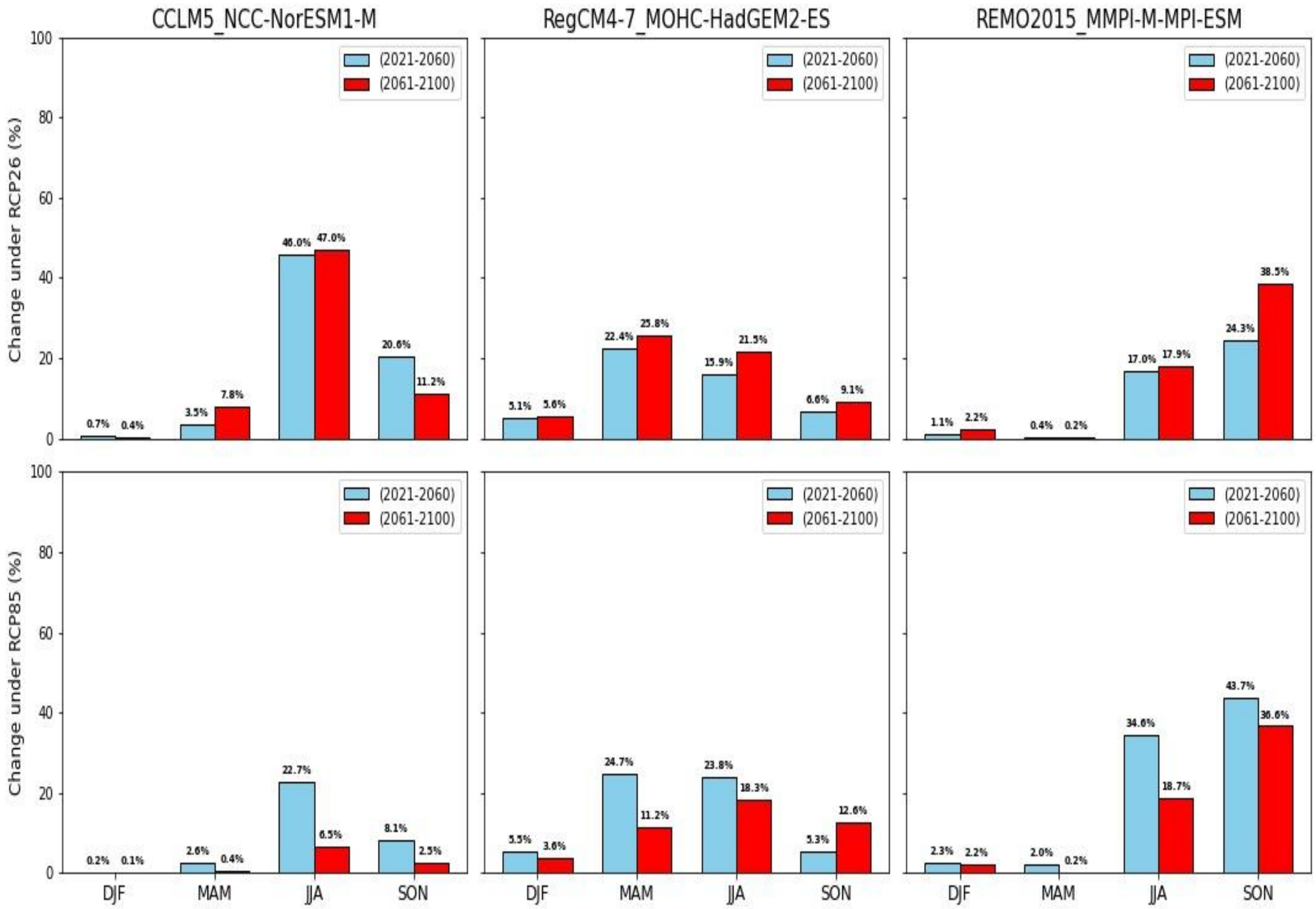

Figure 4.32: The changes in seasonal mean between historical and future values for surface runoff of Mopti under the RCP 2.6 and 8.5 scenarios.

4.4.6 The Projected Climate Changes Impact on the seasonal surface runoff over Dire as simulated by SWAT model

The figure 4.33 shows the changes in runoff in Dire according to the climate models presented in columns, highlighting notable variations according to the scenarios and seasons. The CCLM5_NCC-NorESM1-M model predicts an increase in runoff, particularly marked in summer (JJA) under the RCP 2.6 scenario, with an increase of more than 30% over the period 2021-2060 and a similar trend for 2061-2100. On the other hand, under RCP 8.5, the increase is small, with values lower than 20% for both periods, although runoff in the DJF and SON seasons remains almost unchanged. The RegCM4-7_MOHC-HadGEM2-ES model shows a more uniform increase in runoff across all seasons, although the MAM and JJA seasons experience the largest increases of less than 20% for all periods and scenarios. Indicating a gradual impact of climate change on runoff. The REMO2015_MPI-M-MPI-ESM model projects an increase in runoff especially in summer (JJA) and autumn (SON) under both emission scenarios. Under RCP 2.6 and RCP 8.5, the increase reaches 35% in JJA seasons for the period 2020-2060, with a slightly lower trend for 2061-2100. This indicates a strong impact of global warming on runoff intensification. Our results are consistent with previous studies that of (Yonaba *et al.*, 2023) in burkina faso, (Naik *et al.*, 2024) in the Western Cape in South Africa, (Ebodé *et al.*, 2023) in the Nyong River Basin (equatorial Central Africa), (Abie *et al.*, 2024) in Agewmariyam watershed in Northern Ethiopia, (Ebodé *et al.*, 2022) in the So'o River Basin (south of Cameroon).

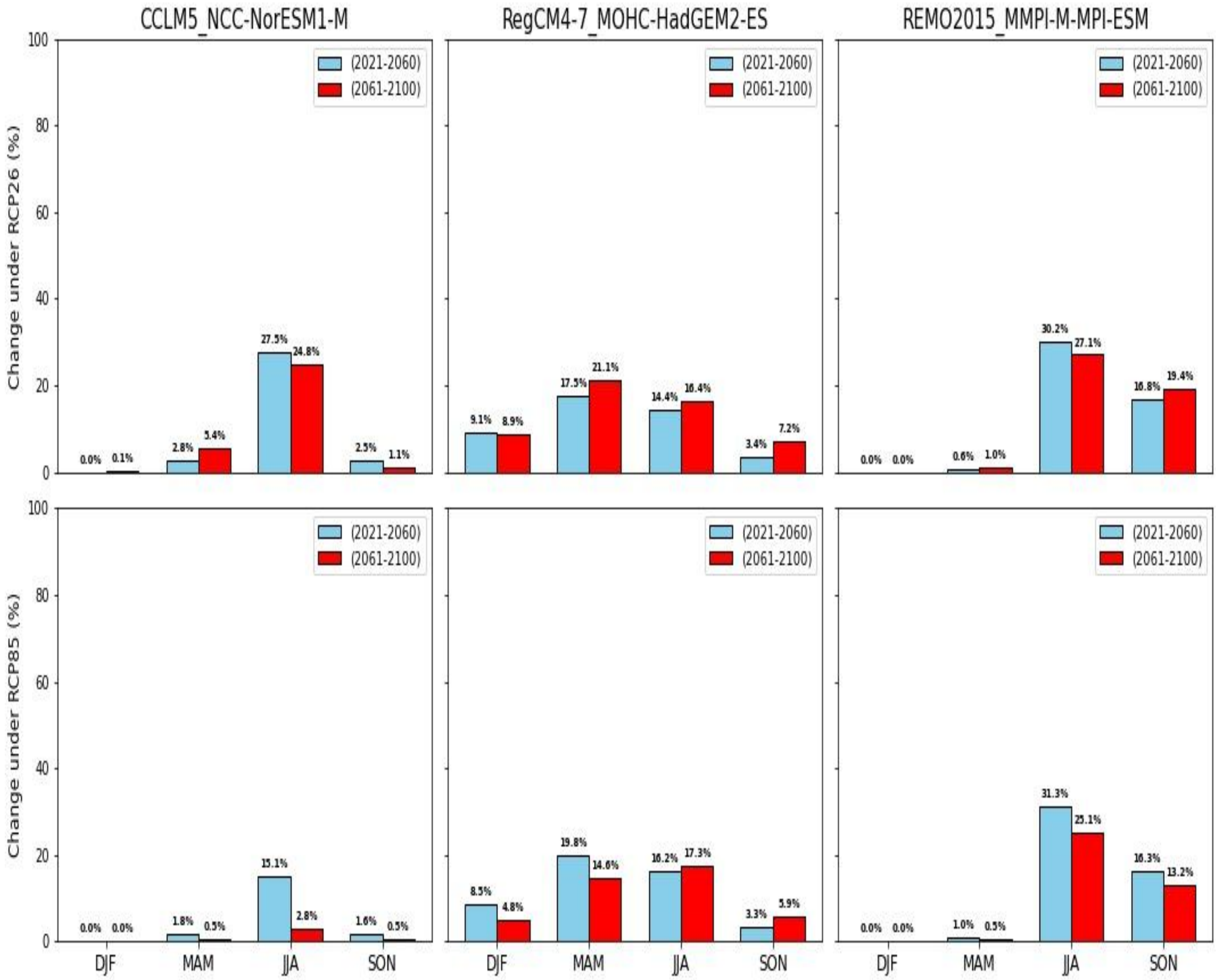

Figure 4.33: The changes in seasonal mean between historical and future values for surface runoff of Dire under the RCP 2.6 and 8.5 scenarios.

4.4.7 The Projected Climate Changes Impact on the seasonal surface runoff over Tombouctou as simulated by SWAT model

The figure 4.34 shows the changes in runoff in Tombouctou according to the climate models presented in columns, highlighting notable variations according to the scenarios and seasons.

The CCLM5_NCC-NorESM1-M model projects an increase in runoff, particularly in summer (JJA) and autumn (SON) under both emission scenarios. Under RCP 2.6, the increase reaches its maximum of 20% in the JJA season for both periods. On the other hand, under RCP 8.5, the increases are less marked, with values lower than 10% for both periods. This indicates a strong impact of global warming on the intensification of runoff. The RegCM4-7_MOHC-HadGEM2-ES model shows a more moderate increase in runoff, distributed over all seasons, particularly in the MAM and JJA seasons under both scenarios. Under RCP 2.6, the increases remain below 30%, with a relatively constant increase between the two periods (2021-2060 and 2061-2100). Under RCP 8.5, the increase is more pronounced in the MAM and JJA seasons, but it remains higher than that of the CCLM5 model. The model shows a more gradual response of runoff to climate change. The REMO2015_MPI-M-MPI-ESM model projects similar trends to those of CCLM5. Under RCP 2.6, the increase reaches about 35% in the SON season for both periods. In contrast, under RCP 8.5, the increases are even lower, with values below 35% and 30% in the SON season in the near and far future, respectively. The model highlights an increased risk of intense runoff towards the end of the century, particularly in response to heavier precipitation and extreme rainfall events. Our results are consistent with previous studies that of (Yonaba *et al*., 2023) in burkina faso, (Naik *et al*., 2024) in the Western Cape in South Africa, (Ebodé *et al*., 2023) in the Nyong River Basin (equatorial Central Africa), (Abie *et al*., 2024) in Agewmariyam watershed in Northern Ethiopia, (Ebodé *et al*., 2022) in the So’o River Basin (south of Cameroon).

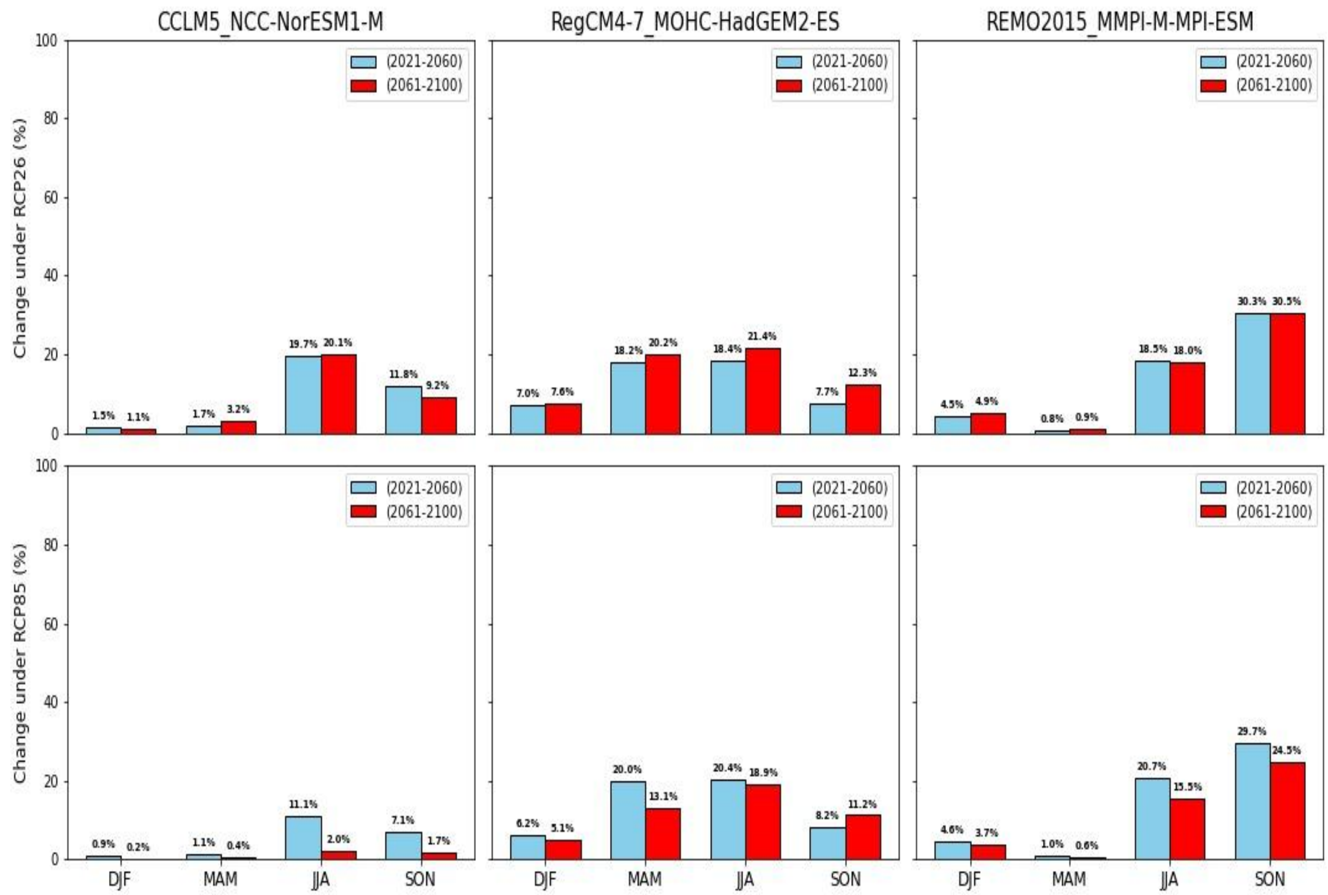

Figure 4.34: The changes in seasonal mean between historical and future values for surface runoff of Tombouctou under the RCP 2.6 and 8.5 scenarios.

CHAPTER FIVE

SUMMARY, CONCLUSION AND RECOMMENDATION

5.1 Summary

The main aim of this study was to assess the performance of some CORDEX RCMs driven by a set of the same GCMs in simulating of the precipitation, the air temperature and the evaporation by comparing with ERA5 over West Africa and hence, use the best combination metrics to analyze the impacts of climate change on the Inner-Niger-Delta (IND) wetland in Mali. The best combination metric for simulating means monthly precipitation showed that R reached 0.91 in the Sahel, 0.95 in the savannah and 0.88 for the Guinea Coast. The negative Mbias depicted an underestimation in the three regions. The RMSE values are between 84mm and 151.53mm in the coastal zone, in the savannah between 38.54mm and 78.03mm and in the Sahel zone between 27.34mm and 42.15mm. Evaluation of these models for reproducing monthly mean evaporation presented another combinational metrics of R reaching 0.93 in the Sahel, 0.93 in the savannah and 0.86 for the Guinea Coast. The RMSE values oscillate between 23.09mm and 61.41mm in the coastal zone, in the savannah zone between 9.54mm and 58.94mm and in the Sahel zone between 14.81mm and 35.45mm. Compared the monthly mean air temperature, the R values reach 0.86 in the Sahel, 0.93 for the savanna zone and the Guinea Coast zone. The Mbias are positive overall which show an overestimation of the monthly air temperature estimate of the RCMs compared to the ERA5 data in the three regions. The RMSE values are between 81.04 ºC and 84.96 ºC in all the climatic zones of West Africa. This study shows that the CORDEX RCMs underestimate the precipitation overall, underestimate the evaporation expected from the three CCLM5 simulations and overestimate the temperature of the area, with a strong correlation coefficient for all the variables.

The analysis of seasonal climate projections from the regional models CCLM5, RegCM4 and REMO, coupled with the global models MOHC-HadGEM2-ES, MPI-M-MPI-ESM and NCC-NorESM1, showed some significant seasonal variations in precipitation, evaporation, air temperature and runoff in the Inner Niger Delta. These changes varied according to time horizons and emission scenarios, highlighting the uncertainties related to climate projections and the need for a multi-model approach to better understand future developments.

5.2 Conclusion

Analysis of climate projections from CORDEX regional models for West Africa reveals high variability in the trends of precipitation, evaporation, temperature and total runoff across two emission scenarios (RCP 2.6 and RCP 8.5) and time periods (near and far future).

The results indicate that:

(i) CCLM, RegCM and REMO climate models show some disagreements in their projections, due to their sensitivity to boundary conditions and atmospheric physics;

(ii) the precipitation projection showed mixed changes, with dominant reductions in coastal areas and possible increases in some regions of the Sahel, depending on the model and scenario considered;

(iii) the evaporation projection followed a similar trend to precipitation, influenced by local climate conditions and temperature variations;

(iv) a general trend of increasing temperatures was observed in all simulations, with more pronounced variations under the RCP 8.5 scenario; and

(v) the total runoff projection reflected variations in precipitation and evaporation, with a general decreasing trend, particularly in coastal areas, while some increases are projected in the Sahel.

These results further highlighted the uncertainty of climate projections in West Africa and the importance of using a multi-model approach to better understand and project future climate change. Effective adaptation to climate change will require a detailed assessment of local-scale impacts and appropriate strategies for water resource management and the resilience of agricultural and hydrological systems.

The precipitation projections showed a large inter-model and inter-seasonal variability. During the dry season (DJF), a general trend towards decreasing precipitation was observed, particularly with the CCLM5 and RegCM4 models with most couplings showed an accentuation of arid conditions in winter. However, some REMO model couplings (notably with NCC-NorESM1) projected moderate increases, highlighting the uncertainty associated with this season. In spring (MAM), a notable decrease in precipitation was projected, particularly under the RCP 8.5 scenarios and with the CCLM5 and RegCM4 models. This decrease was particularly marked in the long-term simulations, showing a reduction in groundwater recharge and a decrease in runoff at the beginning of the rainy season. In contrast, in summer (JJA), the models showed contrasting results, while CCLM5 and RegCM4 predicted reductions in precipitation under several configurations, REMO, coupled with NCC-NorESM1, projected a slight increase, showing differentiatial impacts on the hydrological regime of the Inner Niger Delta. During SON, some models such as RegCM4 showed a slight increase in precipitation, particularly under NCC-NorESM1, while others (CCLM5) predicted a stable or moderately decreasing trend.

The evaporation projections also varied according to seasons and climate model couplings. Under RCP 2.6, a slight increase in evaporation was observed in DJF and SON with RegCM4 and REMO, while CCLM5 showed a generalized decrease across all seasons. On the other hand, under RCP 8.5, a marked increase in evaporation was projected, particularly in MAM and JJA, which could aggravate water deficits during the transition to the rainy season. In particular, REMO simulations coupled with NCC-NorESM1 predicted maximum evaporation during SON, indicating an increased risk of late summer season drought.

Increased air temperature was a general trend across all projections, with increasing intensity under RCP 8.5. Under RCP 2.6, the increase remained moderate with limited seasonal differences. In contrast, under RCP 8.5, a more pronounced increase (+0.3 to +0.5 %) was projected for all seasons, with higher peaks in DJF and SON, which could have a significant impact on evapotranspiration and the water balance of the region.

Projected changes in total runoff followed similar trends to precipitation and evaporation. Under RCP 2.6, projections showed relatively stable runoff in DJF and SON, with limited variation between models. However, under RCP 8.5, notable runoff reductions were observed in MAM and JJA in several configurations (notably with RegCM4 and CCLM5), which could lead to a decrease in streamflow at the beginning and middle of the rainy season. Conversely, some REMO simulations coupled with NCC-NorESM1 predicted an increase in runoff in SON, which could partly compensate for summer water loss.

Analysis of hydrological projections from the SWAT model highlighted some significant impacts of climate change on the Inner Niger Delta wetland both in the short and long term. Overall, the results showed an increase in streamflow and runoff, with disparities depending on the scenarios and climate models used.

Under the RCP 2.6 scenario, the increases were more pronounced, particularly in the dry season, which could lead to an intensification of flooding and a modification of the hydrological cycle in the region. On the other hand, under RCP8.5, although the increases were less, the interannual variability of precipitation could make water management more complex, with an alternation of extreme flood episodes and periods of low streamflow.

The differences between regional climate models highlighted uncertainties in predicting hydrological changes, but the general trend remains an increase in water availability, with increased risks for hydrologic infrastructure, ecosystems and local populations.

5.3 Recommendation

The implications of these changes require adaptive water resource management, integrating climate projections into development strategies and water management policies. In this context, several adaptation measures should be considered, including strengthening water control infrastructure, improving flood forecasting and warning systems, and implementing sustainable wetland management strategies in the delta. Integrating climate scenarios into hydrological planning will be essential to minimize risks and optimize water resource use in the Inner Niger Delta by 2100. The Inner Niger Delta Wetland is an area sensitive to hydrological variations, influenced by climate change and human activities. The use of the SWAT model has made it possible to obtain results on the hydrological dynamics of the delta, but some limitations remain. To deepen these analyses and improve the accuracy of the projections, several research perspectives can be considered:

a) improving the accuracy of hydrological simulations: refining the model calibration by integrating higher-resolution data and testing other automatic calibration methods;

b) studying the ecological and socio-economic impacts of hydrological changes: analyzing the effects of changes in streamflow and runoff on ecosystems and local activities;

c) developing adaptation scenarios for flood and water resource management by proposing sustainable solutions to mitigate the risks associated with increased runoff and streamflow; and

d) comparison with other hydrological and climate models: compare the results of the SWAT model with other models to refine predictions and reduce uncertainties.

5.4 Contribution to Knowledge

As contribution to knowledge, this research contributes to:

i. reveal the reliability of CORDEX models simulations in capturing key climatic variables across West Africa; and

ii. enhance understanding of how climate change affects the hydrology and ecosystem dynamics of the Inner Niger Delta wetland.

REFERENCES

Achite M., Caloiero T., Wał˛ega A., Krakauer N. and Hartani T. (2021). Analysis of the Spatiotemporal Annual Rainfall Variability in the Wadi Cheliff Basin (Algeria) over the Period 1970 to 2018. Water 2021, 13, 1477. https://doi.org/10.3390/w13111477

Adejokun J. A., (1965). The three-dimensional structure of the Inter-Tropical Discontinuity over Nigeria.*Nigerian Meteorological Service Technical Note* 39, 9pp.

Adnan M.S.G., Haque A. and Hall J.W. (2019). Have coastal embankments reduced flooding in Bangladesh? Sci. Total Environ. 682, 405–416. doi:10.1016/j.scitotenv.2019.05.048.

AFDB, 2005. Mali country strategy paper 2005–2009. Technical Report African Development Bank, African Development Fund.

Agricultural and Rural Development, Iowa State University, Ames, IA, USA.

Ajay O. C., Diakite N., Konate A.B. and Catacutan D. (2012). Rapid assessment of the Niger Delta of Mali. ICRAF Working Paper n0 no 144. nairobi : worldnAgroforestry centre.

Akinsanola A.A. and Ogunjobi K.O. (2017). Evaluation of present-day rainfall simulations over West Africa in CORDEX regional climate models. Environ Earth Sci. https://doi.org/10.1007/s12665-017-6691-9

Allen M.R. and Ingram W.J. (2002). Constraints on future changes in climate and the hydrologic cycle. Nature 419, 224-232.

Amoussou E., Awoye H., Vodounon H.S.T., Obahoundje S., Camberlin P., Diedhiou A., Kouadio K., Mahé G., Houndénou C. and Boko M. (2020). Climate and extreme rainfall events in the mono river basin (West Africa): investigating future changes with regional climate models. Water 2020, 12, 833; doi:10.3390/w12030833

Andrews M.B., Ridley J.K., Wood R. A., Andrews T., Blockley E. W., Booth B., *et al*. (2020). Historical simulations with HadGEM3-GC3.1 for CMIP6. Journal of Advances in Modeling Earth Systems, 12, e2019MS001995. https://doi.org/10.1029/2019MS001995

Ardoin-Bardin S. (2004). Hydroclimatic variability and impacts on water resources of large hydrographic basins in the Sudano-Sahelian zone. Doctoral thesis in Water Sciences, University of Montpellier II, France

Asfaw A., Simane B., Hassen A. and Bantider A. (2018). Variability and time series trend analysis of rainfall and temperature in northcentral Ethiopia: a case study in Woleka sub-basin, Weather Clim. Extrem. 19 (December 2017) (2018) 29–41, https://doi.org/10.1016/j.wace.2017.12.002.

Ayugi B., Tana G., Gnitoua G.T., Ojaraa M. and Ongoma V. (2020). Historical evaluations and simulations of precipitation over East Africa from Rossby centre regional climate model. J Atmos Res 232:104705. https://doi.org/10.1016/j.atmosres.2019.104705

Baas J., Schotten M., Plume A., Côté G. and Karimi R. (2020). Scopus as a curated, high-quality bibliometric data source for academic research in quantitative science studies. Quantitative Sci Stud 1(1):377–386. https:// doi. org/ 10. 1162/ qss_a_00019

Bacmeister, J. T., M. Wehner, R. B. Neale, A. Gettelman, C. Hannay, P. Lauritzen, and J. Caron, 2014: Exploratory high-resolution climate simulations using the Community Atmosphere Model (CAM). J. Climate, 27, 3073–3099, doi:10.1175/JCLI-D-13-00387.1.

Baker C., Koning P., and Diallo M. (2023). Sustaining the Inner Niger Delta Lifeline. https://www.alliance4water.org/wr4er-cases/sustaining-the-inner-niger-delta-lifeline (accessed on 13 september 2024).

Baker C., Koning P., and Diallo M. (2023). Sustaining the Inner Niger Delta Lifeline. https://www.alliance4water.org/wr4er-cases/sustaining-the-inner-niger-delta-lifeline

Bamba F., Diabate M., Mahé G. and Diarra M. (1996). Rainfall and runoff decrease of five river bassins of the tropical upstream part of the Niger river over the period 1951-1989. In Roald L. A. (éd.): Global hydrological change, EGS XXIth gen. ass., La Haye, Pays Bas, 6-10 Mayi 1996, 16 p.based on CORDEX-Africa. Journal of Geophysical Research: Atmospheres, 124, 11,118–11,142. https://doi.org/10.1029/2018JD029473

Bathily C. B. (1991). Master plan for the development of water resources.

Bentsen M., Bethke I., Debernard J.B., Iversen T., Kirkevåg A., Seland Ø., Drange H., Roelandt C., Seierstad I.A., Hoose C. and Kristjansson, J.E. (2013). The Norwegian Earth System Model, NorESM1-M—part 1: description and basic evaluation of the physical climate. Geoscientific Model Development, 6, 687–720. https://doi.org/10.5194/gmd-6-687-2013.

Berge-Nguyen M., Cretaux J.F., (2015). Inundations in the inner Niger delta: monitoring and analysis using MODIS and global precipitation datasets. Rem. Sens. 7, 2127–2151.

Bertoli-Barsotti L. and Lando T. (2017). The *h*-index as an almost-exact function of some basic statistics. Scientometrics 113(2):1209–1228. https:// doi. org/ 10. 1007/ s11192- 017- 2508-6

Bieger K., Arnold J.G., Rathjens H., White M.J., Bosch D.D., Allen P.M., Volk M., *et al*., (2017). Introduction to SWAT+, a completely restructured version of the soil and water assessment tool. J. Am. Water Resour. Assoc. 53, 115–130. https://doi.org/10.1111/1752-1688.12482.

BojerA. K., Woldetsadik M. and Biru B. H. (2024). Machine learning and CORDEX-Africa regional model for assessing the impact of climate change on the Gilgel Gibe Watershed, Ethiopia.

Journal of Environmental Management 363 (2024) 121394. https://doi.org/10.1016/j.jenvman.2024.121394

Bollasina M. A., Y. Ming. and V. Ramaswamy. (2011). Anthropogenic aerosols and the weakening of the South Asian summer monsoon. Science, 334, 502–505, doi:10.1126/science.1204994.

Bony S., Stevens B., Frierson D.M.W., Jakob C., Kageyama M., Pincus R., Shepherd T. G., Sherwood S.C., Siebesma A. P., Sobel A. H., Watanabe M. and Webb M. J. (2015). Clouds, circulation and climate sensitivity, Nat. Geosci., 8, 261–268, 2015.

Brasseur G., and D. Carlson. (2015). Future directions for the World Climate Research Programme, Eos, 96, doi:10.1029/2015EO033577. Published on 30 July 2015.

Bricquet J.P., Bamba F., Mahé G., Toure M., Olivry J.C, (1997). Recent developments in water resources in Atlantic Africa. Rev. Sci. Eau, 3 : 321-337.

Brunet-Moret Y., Chaperon P., Lamagat J. P. and Molinier M. (1986). Hydrological monograph of the Niger River. Volume II. Lake Basin and Middle Niger. Ed. ORSTOM, Paris, France.

C. Dai., X.S. Qin., X.L. Zhang., B.J. Liu. (2022). Study of climate change impact on hydro-climatic extremes in the Hanjiang River basin, China, using CORDEX-EAS data. Weather and Climate Extremes 38 (2022) 100509. https://doi.org/10.1016/j.wace.2022.100509

Caloiero T., Coscarelli R., Ferrari E. and Sirangelo B. (2015). Analysis of dry spells in southern Italy (Calabria). Water 7:3009–3023

CARD, (2022). SWAT Literature Database for Peer-Reviewed Journal Articles. Center for

Chen J., Brissette FP., Leconte R. (2012). Coupling statistical and dynamical methods for spatial downscaling of precipitation. Clim Change. 2012 Apr 20; 114(3):509–26.

CityMayors. (2010). The World’s Fastest Growing Cities and Urban Areas from 2006 to 2020.

Clement A. R, (2013). An application of Geographic Information System in mapping flood risk zones in a north central city in Nigeria. Afr. J. Environ. Sci. Technol. 7 (6), 365–371.

Cook P.A., Black E.C.L., Verhoef, Macdonald D.M.J., Sorensen J.P.R. (2022). Projected increases in potential groundwater recharge and reduced evapotranspiration under future climate conditions in West Africa. Journal of Hydrology: Regional Studies 41 (2022) 101076. https://doi.org/10.1016/j.ejrh.2022.101076

Cubry P., Tranchant-Dubreuil C., Thuillet A. C., *et al*., (2018). The Rise and Fall of African Rice Cultivation Revealed by Analysis of 246 New Genomes. Current Biology 28, 2274–2282, July 23, 2018

Dadson S.J., Ashpole I., Harris P., Davies H.N., Clark D.B., Blyth E., Taylor C.M., (2010). Wetland inundation dynamics in *a* model of land surface climate: evaluation in the Niger inland delta region. J. Geophys. Res. 115, D23114. https://doi.org/ 10.1029/2010JD014474.

Daron J.D., (2014). Regional Climate Messages: East Africa. Scientifc report from the CARIAA Adaptation at Scale in Semi-Arid Regions (ASSAR) Project. Collaborative Adaptation Research Initiative in Africa and Asia, Africa and Asia

Davies T. (2014). Lateral boundary conditions for limited area models. Quarterly Journal of the Royal Meteorological Society. 2014 Jun 5; 140(678):185–96.

De Noray M.L. (2003). Inland Niger River Delta in Mali – When Floods Rule: Human Organization and Resource Sharing in a Highly Contrasting Floodplain. VertigO-la Rev. électron. Sci. l'environ. 4 (3), 1–9.

Dee D., Uppala S.M., Simmons A., Berrisford P., Poli P., Kobayashi S., Andrae U. *et al*., (2011) The ECMWF-ERAINT reanalysis: configuration and performance of the data assimilation system. Quarterly Journal of the Royal Meteorological Society, 137, 553–597.

Deptuck M. E., Steffens G. S., Barton M. and Pirmez C. (2003). Architecture and evolution of upper fan channel-belts on the Niger Delta slope and in the Arabian Sea. Marine and Petroleum Geology 20 (2003) 649–676

Devak M. and Dhanya C.T. (2014). Downscaling of Precipitation in Mahanadi Basin, India. Int. J. Civ. Eng. Res. 2014, 5, 111–120.

Dezfuli A.K. and Nicholson, S.E. (2013). The relationship of rainfall variability in western equatorial africa to the tropical oceans and atmospheric circulation. Part II Boreal Autumn. J. Clim. 26, 66–84. https://doi.org/10.1175/JCLI-D-11-00686.1.

Di Baldassarre G., (2012). *Floods In a Changing Climate: Inundation Modelling* (International Hydrology Series). Cambridge University Press, Cambridge. https://doi.org/10.1017/CBO9781139088411.

Diallo I., Sylla M.B., Camara M. and Gaye A.T. (2012) Interannual variability of rainfall and circulation features over the Sahel based on multiple regional climate models simulations. Appl Climatol Theor. https://doi.org/10.1007/s00704-012-0791-y

DIARRA D. Z. (2020). MALI NATIONAL DROUGHT PLAN 2021-2025. July 2020

Dieppois B., Diedhiou A., Durand A., Fournier M., Massei N., Sebag D., Xue Y. and Fontaine B. (2013). Quasi-decadal signals of Sahel rainfall and West African monsoon since the mid-twentieth century. J. Geophys. Res. Atmos. 118, 12587–12599. https://doi.org/10.1002/2013JD019681.

Dieppois B., Durand A., Fournier M., Diedhiou A., Fontaine B., Massei N., Nouaceur Z. and Sebag, D. (2015). Low-frequency variability and zonal contrast in Sahel rainfall and Atlantic Sea surface temperature teleconnections during the last century. Theor. Appl. Climatol. 121, 139–155. https://doi.org/10.1007/s00704-014-1229-5.

Doms G. and Baldauf M. (2013) A description of the nonhydrostatic regional COSMO-model part I: dynamics and numerics. Offenbach: COSMO. Technical report https://doi.org/10.5676/DWD_pub/nwv/cosmo-doc_5.00_I.

Dosio A., Jury M.W., Almazroui M., Ashfaq M., Diallo I., Engelbrecht F., Klutse N.A.B., Lennard C.J., Pinto, I., Sylla, M.B. *et al.,* (2021). Projected Future Daily Characteristics of African Precipitation Based on Global (CMIP5, CMIP6) and Regional (CORDEX, CORDEX-CORE) Climate Models. Clim. Dyn. 2021, 57, 3135–3158. https://doi.org/10.1007/s00382-021-05859-w

Druyan LM. (2011). Studies of 21st-century precipitation trends over West Africa. Int J Climatol 31:1415–1424

Ebodé V. B, Onana J. Y. N., Dzana J. G., Amougou J. A, Batha R. A. S., Boyomo T. M. S, Mbeih G. E. N. (2024). Availability of the current and future water resources in Equatorial Central Africa: case of the Nyong forest catchment in Cameroon. Environ Monit Assess (2024) 196:298. https://doi.org/10.1007/s10661-024-12471-y

Ebodé V. B. (2023). mpact of climate and anthropogenic changes on current and future variability in flows in the Nyong River Basin (equatorial Central Africa). Journal of Hydroinformatics Vol 00 No 0,1 DOI:10.2166/hydro.2023.116

Ebodé V. B., Dzana J. G., Nkiaka E., Nka N. B., Braun J. J. and Riotte J. (2022). Effects of climate and anthropogenic changes on current and future variability in flows in the So'o River Basin (south of Cameroon). Hydrology Research 53 (9), 1203–1220. doi:10.2166/nh.2022.047.

ECMWF. https://www.ecmwf.int/en/forecasts/dataset/ecmwf-reanalysis-v5. (9 Jan 2025)

Emerton L. and Bos E. (2004). Value. Counting ecosystems as water infrastructure. IUCN, Gland, Switzerland and Cambridge, United Kingdom. 88pp. http://data. iucn.org/dbtw-wpd/edocs/2004-046.pdf

Esch M., Ghosh R., Haak H., Ilyina T., Kleine T., Kornblueh L., Li H., Modali K., Notz D., Pohlmann H., Roeckner E., Stemmler I., Tian F., Marotzke J., (2018). A higher-resolution version of the Max Planck Institute Earth System Model (MPI-ESM1.2-HR). J. Adv. Model Earth Syst. 10, 1383–1413.

Eyring V., Bony S., Meehl G.A., Senior C.A., Stevens B., Stouffer R.J., Taylor K.E. (2016). Overview of the coupled model intercomparison project phase 6 (CMIP6) experimental design and organization. Geosci. Model Dev. 9, 1937–1958. https://doi.org/10.5194/gmd-9-1937-2016.

Flato G., Marotzke j., Abiodun B., Braconnot P., Chou SC., Collins W., *et al.,* (2013). Evaluation of Climate Models. Climate Change 2013: The physical Science Basis. Contribution of Working Group 1 to the Fifth Assessment Report of the Intergovernmental Panel on Climate Change. Cambridge University Press;2013 Apr.

Fleischmann A., Siqueira V., Parisb A., Collischonn W., Rodrigo Paiva., Paulo Pontes. and Jean-François Crétaux. (2018). Modelling hydrologic and hydrodynamic processes in basins with large semi-arid wetlands. Journal of Hydrology 561 (2018) 943–959

Flint LE. and Flint AL. (2012). Downscaling future climate scenarios to fine scales for hydrologic and ecological modeling and analysis. Ecol Process. 2012 Apr 20; 1(1):2.

Food and Agriculture Organization of the United Nations (FAO). (1997). Irrigation Potential in Africa. A Basin Approach; FAO Land and Water Bulletin: Roma, Italy, 1997; Volume 4.

Funk C., Michaelsen J. and Marshall M. (2012). Mapping recent decadal climate variations in precipitation and temperature across Eastern Africa and the Sahel, chap. 14 in Wardlow, B., Anderson, M., and Verdin, J., eds., Remote sensing of drought, Innovative monitoring approaches: Taylor and Francis, 25 pgs.

Gallais J. (1967). The Inner Niger Delta: A Study in Regional Geography*. Paris: Institute of African Studies. https://books.google.com.ng/books?hl=fr&lr=&id=L8MAEQAAQBAJ&oi=fnd&pg=PP1&dq=Le+Delta+Int%C3%A9rieur+du+Niger:+%C3%89tude+de+g%C3%A9ographie+r%C3%A9gionale*.+Paris:+Institut+d%E2%80%99%C3%89tudes+Africaines.&ots=KWTD3MTkCg&sig=mCDj0KoW7yz7lWHeLa5OdmrEC9M&redir_esc=y#v=onepage&q&f=false

Gao Y., Zhou M., Yu Z., Ju Q, Jin J., Dawei Zhang (2024). Climate change impacts on seasonal runoff in the source region of the Yellow River: Insights from CORDEX experiments with uncertainty analysis. Journal of Hydrology 645 (2024) 132132. https://doi.org/10.1016/j.jhydrol.2024.132132

Gebrechorkos S. H., Bernhofer C. and Hülsmann S. (2019). Impacts of projected change in climate on water balance in basins of East Africa. Science of The Total Environment, 682, 160–170. https://doi.org/10.1016/j.scitotenv.2019.05.053

Geen R., Bordoni S., Battisti D. S. and Hui K. (2020). Monsoons, ITCZs, and the concept of the global monsoon. Reviews of Geophysics, 58, e2020RG000700. https://doi.org/10.1029/2020RG000700

Gensini, V. A., Haberlie, A. M., and Ashley, W. S. (2023). Convection-permitting simulations of historical and possible future climate over the contiguous United States. Climate Dynamics, 60(1), 109–126. https://doi.org/10.1007/s00382-022-06306-0

Giorgetta M.A., Jungclaus J., Reick C.H., Legutke S., Bader J., Böttinger M., Brovkin V. *et al*., (2013). Climate and carbon cycle changes from 1850 to 2100 in MPI-ESM simulations for the Coupled Model Intercomparison Project phase 5. Journal of Advanced Modeling Earth Systems, 5, 572–597. https://doi.org/10.1002/jame.20038.

Giorgi (2019). Thirty Years of Regional Climate Modeling: Where Are We and Where Are We Going next? Journal of Geophysical Research: Atmospheres. 2019 Apr 20; 124(11):5696–723.

Giorgi F. and Gao X. (2018). Regional earth system modeling: review and future directions. Atmospheric and Oce-anic Science Letters. 2018 Apr 20; 11(2):189–97.

Giorgi F., Ciarlo J.M., Raffaele F., Giuliani G., Xuejie G., Sines T., Torres-Alavez J., Das S., Di Sante F., Pichelli E., Glazer R., Ashfaq M., Bukovsky M. and Im E.S. (2021). Assessing mean climate change signals in the global CORDEX-CORE ensemble. Climate Dynamics, 57, 1269–1292. https://doi.org/10.1007/s00382-020-05494-x.

Giorgi F., Jones C. and Asrar G.R. (2009). Addressing climate information needs at the regional level: the CORDEX framework. WMO Bull 58(3):175–183.

Goulden M., Conway D. and Persechino A. (2009). Adaptation to climate change in international river basins in Africa: a review. Hydrol. Sci. J. J. des Sci. Hydrol. 54, 805–828. https://doi.org/10.1623/hysj.54.5.805.

Grodsky S. A, and Carton J. A. (2001). Coupledland/atmosphere interactions in the West African Monsoon , Charney Eyring, V.; Bony, S.; Meehl, G.A.; Senior, C.A.; Stevens, B.; Stou_er, R.J.; Taylor, K.E (**2016**) « Overview of the Coupled Model Intercomparison Project Phase 6 (CMIP6) experimental design and organization.» Geosci. Model Dev. **2016**, 9, 1937–1958.

Groenke B., Madaus L., and Monteleoni C. (2020). ClimAlign: Unsupervised statistical downscaling of climate variables via normalizing flows.In Proceedings of the 10th International Conference on Climate Informatics (pp. 60–66). https://doi.org/10.1145/3429309.3429318

Haag A.V. (2015). Coupling *A* Large-Scale Hydrological Model to *a* High-Resolution Hydrodynamical Model, *A* Study of Floods within the Niger Inner Delta as *a* First Step towards *a* Potential Global Application. Master's Thesis, Department of Physical Geography and Faculty of Geoscience, Utrecht University, Utrecht, The Netherlands.

Hagos S.M. and Cook K.H. (2007). Dynamics of the West African monsoon jump. J. Clim. 20 (21), 5264–5284. https://doi.org/10.1175/2007JCLI1533.1.

Hajat S., Ebi K. L., Kovats R. S., Menne B., Edwards S., Haines A. (2005). The Human Health Consequences of Flooding in Europe: a Review, Springer-Verlag Berlin Heidelberg 2005

Hamadan M. (2002). Synthesis and evaluation of seasonal forecasts in West Africa (DEA). http://horizon.documentation.ird.fr/exl-doc/pleins_textes/divers12-05/010031015.pdf

Hamilton R.A. and Archbold J.W., (1945). Meteorology of Nigeria and adjacent territory. Q. J.R.

Haque M. M., Seidou O., Mohammadian A., Djibo A. G., Liersch S., Fournet S., Karam S., Perera E. D. P. and Kleynhans M. (2019). Improving the Accuracy of Hydrodynamic Simulations in Data Scarce Environments Using Bayesian Model Averaging: A Case Study of the Inner Niger Delta, Mali,West Africa. Water 2019, 11, 1766; doi:10.3390/w11091766

Hastenrath S., (2000). Interannual and longer term variability of upper-air circulation over the tropical Atlantic and West Africa in boreal summer. Int. J. Climatol. 20, 1415–1430.

Hay L.E., Wilby R.L. and Leavesley G.H. (2007). A comparison of delta change and downscaled GCM scenarios for three mountainous basins in the United States. JAWRA. 2007 Apr 20; 36(2):387–97.

Hersbach H., Bell B., Berrisford P., Hirahara S., Horányi A., Muñoz-Sabater J., Nicolas J. *et al*., (2020). The ERA5 global reanalysis. Q. J. R. Meteorol. Soc. 146, 1999–2049. https://doi.org/10.1002/qj.3803.

Holtslag A.A.M., De Bruijn E.I.F. and Pan H.L. (1990). A high resolution air mass transformation model for short-range weather forecasting. Mon Weather Rev 118(8):1561–1575. https ://doi.org/10.1175/1520-0493(1990)118<1561:AHRAM T>2.0.CO;2 http://doi.org/10.1002/hyp.7389

Hulme M., Doherty R., Ngara T., New M., Lister D. (2001). African climate change: 1900–2100. CLIMATE RESEARCH Clim Res. Vol. 17: 145–168, 2001

Hundecha Y., Sunyer M. A., Lawrence D., Madsen H., Willems P., Bürger G., and Vasiliades L. (2016). Inter-comparison of statistical downscaling methods for projection of extreme flow indices across Europe. Journal of Hydrology, 541, 1273-1286.

Hurkmans R., Terink W., Uijlenhoet R., Torfs P., Jacob D., and Troch P. A. (2010). Changes in stream flow dynamics in the Rhine basin under three high-resolution regional climate scenarios. Journal of Climate, 23(3), 679-699.

Hydrological Sciences Journal, 49:1, 21-37, DOI: 10.1623/hysj.49.1.21.53996

Ingram, W. (2016). Extreme Precipitation: Increases All Round. Nature Climate Change, 6, 443-444. https://doi.org/10.1038/nclimate2966

INSTAT, (2011). 4th General Population and Housing Census of Mali (RGPH-2009). Analysis of the Final Results. https://www.odsef.fss.ulaval.ca/sites/odsef.fss.ulaval.ca/files/fonds_gp/cdoc_387_odsef.pdf (25 january 2025)

IPCC, (2001). the scientific basis. In: Intergovernmental Panel on Climate Change, Houghton, J.T., *et al.,* (Eds.), 2001. Contribution of Working Group I to the Third Assessment Report of the Intergovernmental Panel on Climate Change. Cambridge Univ. Press, New York, p. 881.

IPCC, (2007). the scientific basis. In: Intergovernmental Panel on Climate Change, Solomon, S., *et al.,* (Eds.), 2007. Contribution of Working Group I to the Fourth Assessment Report of the Intergovernmental Panel on Climate Change. Cambridge Univ. Press, New York.

IPCC, (2018). Global warming of 1.5◦C. An IPCC Special Report on the Impacts of Global Warming of 1.5◦C above Pre-Industrial Levels and Related Global Greenhouse Gas Emission Pathways, in the Context of Strengthening the Global Response to the Threat of Climate Change, Sustainable Development, and Efforts to Eradicate Poverty V. Masson-Delmotte, P. Zhai, H. O. Portner, ¨ D.

IPCC, (2021). Climate Change 2021: The Physical Science Basis. Contribution of Working Group I to the Sixth Assessment Report of the Intergovernmental Panel on Climate Change (V. Masson-

Delmotte *et al.,* Eds.). Cambridge University Press. Retrieved from https://www.ipcc.ch/report/sixth-assessment-report-working-group-i

IPCC, 2013. Climate change 2013: the physical science basis. In: Stocker, T.F., Qin, D., Plattner, G.K., Tignor, M., Allen, S.K., Boschung, J., Midgley, P.M. (Eds.), Contribution of Working Group I to the Fifth Assessment Report of the Intergovernmental Panel on Climate Change, 2013. Cambridge University Press, Cambridge, UK; New York, NY, USA, p. 1535.

IPCC, 2014. Climate change 2014: synthesis report. In: Team, C.W., Pachauri, R.K., Meyer, L.A. (Eds.), Contribution of Working Groups I. II and III to the Fifth Assessment Report, p. 151. Geneva, Switzerland.

Iradukunda P., Mwanaumo E.M. and Kabika J. (2024). Modelling the future climate impacts on hydraulic infrastructure development in tropical (peri-)urban region: Case of Kigali, Rwanda. Heliyon 2024, 10, e27126. https://doi.org/10.1016/j.heliyon.2024.e27126

Iversen T., Bentsen M., Bethke I., Debernard J.B., Kirkevåg A., Seland O., Drange H., Kristjansson J.E., Medhaug I., Sand M. and Seierstad I.A. (2013). The Norwegian Earth Sys-

Jackson B., S. E. Nicholson., and D. Klotter., (2009). Mesoscale convective systems over western equatorial Africa and their relationship to large-scale circulation. Mon. Wea. Rev., 137, 1272–1294, https://doi.org/10.1175/2008MWR2525.1.

Jang S. and Kavvas M.L. (2015). Downscaling Global Climate Simulations to Regional Scales: Statistical Downscaling versus Dynamical Downscaling. J Hydrol Eng. 2015 Apr 20; 20(1):A4014006.

Janicot S., and Coauthors., 2008. Large-scale overview of the summer monsoon over West Africa during the AMMA field experiment in 2006. Ann. Geophys., 26, 2569–2595, https://doi.org/10.5194/angeo-26-2569-2008.

Janicot S., Moron V. and Fontaine B. (1996). Sahel droughts and Enso dynamics. Geophys. Res. Lett., 23, 515–518.

Jenkins G. S., Adamou G. and Fongang, S. (2002). The challenges of modeling climate variability and change in West Africa. Climatic Change 52, 263–286.

Jobe Z. R., Zolta N Sylvester Z. N., Parker A. O., Howes N., Slowey N., And Pirmez C. (2015). Rapid Adjustment Of Submarine Channel Architecture To Changes In Sediment Supply. Journal Of Sedimentary Research, 2015, V. 85, 729–753

Jones C., Giorgi F. and Asrar G. (2011). The coordinated regional downscaling experiment: CORDEX: an international downscaling link to CMIP5. CLIVAR exchanges, no. 56, International CLIVAR Project Ofce, Southampton, United Kingdom, pp 34–40

Jonkman, S.N., Vrijling, J.K., 2008. Loss of life due to floods. J. Flood Risk Manage. 1 (1), 43–56. doi:10.1111/j.1753-318x.2008.00006.x.

Khan M. S., Coulibaly P., and Dibike Y. (2006). Uncertainty analysis of statistical downscaling methods. Journal of Hydrology, 319(1), 357-382.

Kim J.B., Habimana J.d.D., Kim, S.H. and Bae D.H. (2021). Assessment of Climate Change Impacts on the Hydroclimatic Response in Burundi Based on CMIP6 ESMs. Sustainability 2021, 13, 12037. https://doi.org/10.3390/su132112037

Klutse N.A.B, Sylla M.B., Diallo I., Sarr A., Dosio A., Diedhiou A., Kamga A., Lamptey B., Ali A., Gbobanyini E., Owusu K., Lennard C., Hewitson B., Nikulin G., Panitz HJ. And Büchner M.

(2016). Daily characteristics of West African summer monsoon precipitation in CORDEX simulations. Theor Appl Climatol 123(1–2):369–386. https://doi.org/10.1007/s00704-014-1352-3

Koffi B., Brou A. L., Kouadio K. J. O., Ebodé V. B., N'guessan J. Y., Yangouliba G. I., Konaté Y., Brou D. and Kouassi K. L. (2023). Impact of climate and land use/land cover change on Lobo reservoir inflow, West-Central of Côte d'Ivoire. https://doi.org/10.1016/j.ejrh.2023.101417

Kone F. and Zhong X. (2011). WebGIS to Managing Natural Resource: Case of Flooded Pasture in Lake Débo and Walado Débo. Computer and Information Science, Vol. 4, No. 3; May 2011. doi:10.5539/cis.v4n3p131

Koudahe K., Samson A.O., Adebola A.A. and Djaman K. (2017). Trend analysis in standardised rainfall index and standardised anomaly index in the context of climate change in Southern Togo. Atmospheric Climate Sci 7:401–423. https://doi.org/10.4236/acs.2017.74030

Kuper M., Mullon C., Poncet Y. and Benga E. (2003). Integrated modelling of the ecosystem of the Niger river inland delta in Mali. Ecological Modelling, 164(1), 83–102. http://doi.org/10.1016/S0304-3800(03)00006-1

Kuper M., Mullon C., Poncet Y., Benga E., (2003). Integrated modelling of the ecosystem of the Niger river inland delta in Mali. Ecol. Modell. 164 (1), 83–102.

La Fuente S., Jennings E., Gal G., Kirillin G., Shatwell T., Ladwig R., *et al.,* (2022). Multi-model projections of future evaporation in a sub-tropical lake. Journal of Hydrology, 615, 128729. https://doi.org/10.1016/j.jhydrol.2022.128729

Laing A., and J. M. Fritsch. (1993). Mesoscale convective complexes in Africa. Mon. Wea. Rev., 121, 2254–2263.

Lebel T. and Ali A. (2009). Recent trends in the Central and Western Sahel rainfall regime (1990–2007). *Journal of Hydrology*, *375*(1–2), 52–64. http://doi.org/10.1016/j.jhydrol.2008.11.030

Leroux M. (1997). Climat local, climat global / Local cfimate, global climate. Revue de Géographie de Lyon, 72, 339–345. http://doi.org/10.3406/geoca.1997.4715

Liersch S., Fournet S., Koch H., Djibo A. G., Reinhardt J., Kortlandt J., Weert F. V., Seidou O., Klop E., Baker C., Hattermann F. F. (2019). Water resources planning in the Upper Niger River basin: Are there gaps between water demand and supply? Journal of Hydrology: Regional Studies 21 (2019) 176–194. https://doi.org/10.1016/j.ejrh.2018.12.006

Liersch S., J. Cools., B. Kone., H. Koch., M. Diallo., V. Aich., S. Fournet. and F. Hattermann. (2012). Vulnerability of food production in the Inner Niger Delta to water resources management under climate variability and change. Environmental Science and Policy, 2012.

Limsakul A., Singhruck P., (2016). Long-term trends and variability of total and extreme precipitation in Thailand. Atmos. Res. 169, 301–317. doi:10.1016/j.atmosres.2015.10.015. Mahe, G.I.L., Mariko, A., and Orange, D. (2013).

Lohmann U. and Roeckner E. (1996). Design and performance of a new cloud microphysics scheme developed for the ECHAM4 general circulation model. Clim Dyn 12:557–572

Louis J.F. (1979) A prametric model of vertical eddy fluxes in the atmosphere. Bound Layer Meteorol 17(2):187–202

Lu J., and Delworth T.L. (2005). Oceanic forcing of the late 20th century Sahel drought. Geophys. Res. Lett. 32, 1–5. https://doi.org/10.1029/2005GL023316.

Mahe G., Bamba F., Soumaguel A., Orange D., and Olivry J. C. (2009). Water losses in the

Mahé G., Olivry J.C., Dessouassi R., Orange D., Bamba F., Servat E. (2000). Relations eaux de surface-eaux souterraines d'une rivière tropicale au Mali. C. R. Acad. Sc., Paris, série II a, 330 : 689-692.

Mahé G., Olivry J.C., Dessouassi R., Orange D., Bamba F., Servat E., (2000). Surface water-groundwater relationships of a tropical river in Mali. C. R. Acad. Sc., Paris, série II a, 330 : 689-692.

Mahe G., Orange D., Mariko A., Bricquet J.P. (2011). Estimation of the flooded area of the Inner Delta of the River Niger in Mali by hydrological balance and satellite data. IAHS Publ. 344, 138–143.

Maiga M. I., Sanogo S., and Adefisan E.A. (2025). Trends and Prospects from Climatic Research of Inner-Niger-Delta Wetland: A Bibliometric Analysis. Journal of Geoscience and Environment Protection, 13, 108-125. https://doi.org/10.4236/gep.2025.132008

Maraun D., Widmann M., Gutierrez J.M., Kotlarski S., Chandler R.E. and Hertig E. (2014). A framework to validate downscaling approaches for climate change studies. Earths Future. 2014 Apr 20; 3(1):1–14.

Marie J., Morand P., N'DJIM H., (2007). Avenir du fleuve Niger – The Niger River's Future. , ISSN: 1633-9924/ISBN: 978-2-7099- 1632-5.

Mariko A., (2003). PhD thesis. Characterization and monitoring of flood dynamics and vegetation cover in the Inner Niger Delta (Mali) by remote sensing, vol. 2. University of Montpellier, France.

Marx A., J. Dusek., J. Jankovec., M. Sanda., T. Vogel., R. van Geldern., J. Hartmann. and J. A. C. Barth. (2017). A review of CO2 and associated carbon dynamics in headwater streams: A global perspective, Rev. Geophys., 55, 560–585, doi:10.1002/2016RG000547.

Maure G., Pinto I., Ndebele-Murisa M., Muthige M., Lennard C., Nikulin G. and Meque A. (2018) The southern African climate under 1.5 °C and 2 °C of global warming as simulated by CORDEX regional climate models. Environ Res Lett 13(6):065002. https://doi.org/10.1088/1748-9326/aab190

Mauritsen T., Bader J., Becker T., Behrens J., Bittner M., Brokopf R., Brovkin V. *et al*., 2019. Developments in the MPI-M Earth System Model version 1.2 (MPI-ESM1.2) and its response to increasing CO2. J. Adv. Model Earth Syst. 11, 998–1038.

Meehl G.A., Boer G.J. Covey C., Latif M. and Stouer R.J. (2000). The Coupled Model Intercomparison Project (CMIP). Bull. Am. Meteorol. Soc. **2000**, 81, 313–318.

Meehl G.A., Covey C., Delworth T., Latif M., Mcavaney B., John F.B., Mitchell R.J., Stoer K., Taylor E. (2007). The WCRP CMIP3 multimodel dataset-A new era in climate change research. Bull. Amer. Meteor. Soc. **2007**, 88, 1383–1394.

Meteorol. Soc., 72: 231-265.

Millennium Ecosystem Assessment, (2005). ECOSYSTEMS AND HUMAN WELL-BEING: WETLANDS AND WATER Synthesis. World Resources Institute, Washington, DC.

Mitsch W. J. and Gosselink, J. G., (1993). *Wetlands* (2nd edition),Van Nostrand Reinhold, New York. MLI/89/003. Décembre 1991. https://www.fao.org/4/V8260B/V8260B14.htm (accessed on 9 August 2024).

Mockus V. (1972). Estimation of Direct Runoff from Storm Rainfall. In Part 630 Hydrology; National Engineering Handbook; USDA: Washington, DC, USA, 1972; Volume 4.

Moges A. A. and Kendie H., (2024). Comparison of SWAT and WEPP for modeling annual runoff and sediment yield in Agewmariyam watershed, Northern Ethiopia. International Journal on Food, Agriculture, and Natural Resources. Volume 05, Issue 01, Page 104-113. ISSN: 2722-4066. DOI: https://doi.org/10.46676/ij-fanres.v5i1.280

Morss R., lazo B Brown., H. Brooks., P. ganderton. and B. Mills, (2008). societal and economie research and applications ffor weather forecasts: priorities for the north american THORPEX program. Bull. Amer. Meteor. Soc., 89, 335-346, doi: 10.1175/BAMS-89-3-335.

Müller W.A., Jungclaus J.H., Mauritsen T., Baehr J., Bittner M., Budich R., Bunzel F.,

Muriel Bergé-Nguyen and Jean-François Crétaux (2015). Inundations in the Inner Niger Delta: Monitoring and Analysis Using MODIS and Global Precipitation Datasets. https://www.researchgate.net/publication/273486591

MUSY A. (2004). Hydrology 1. A science of nature. Lausanne: Polytechnic and University Presses of Romandie, 2004, 314p.

Naik M. and Abiodun B.J. (2024). Modelling the potential of land use change to mitigate the impacts of climate change on future drought in the Western Cape, South Africa. Theor. Appl. Climatol. **2024**, 155, 6371–6392. https://doi.org/10.1007/s00704-024-04995-7

Nashwan M.S., Shahid S., Dewan A., Ismail T., Alias N., (2019). Performance of five high resolution satellite-based precipitation products in arid region of Egypt: an evaluation. Atmos. Res., 104809 doi:10.1016/j.atmosres.2019.104809.

Nasseri M., Tavakol-Davani H., and Zahraie B. (2013). Performance assessment of different data mining methods in statistical downscaling of daily precipitation. Journal of hydrology, 492, 1-14.

Ndhlovu G.Z. and Woyessa Y.E. (2021). Evaluation of Streamflow under Climate Change in the Zambezi River Basin of Southern Africa. Water 2021, 13, 3114. https://doi.org/10.3390/w13213114

Neal J., Schumann G., Bates P., (2012). A subgrid channel model for simulating river hydraulics and floodplain inundation over large and data sparse areas. Water Resour. Res. 48 (W11506).

Neitsch S., Arnold J., Kiniry, J.R., Williams, J.R. (2009). Soil and Water Assessment Tool Theoretical Documentation: Version 2009; Texas Water Resources Institute: College Station, TX, USA, 2011.

Nesbitt S. W. and E. J. Zipser. (2003). The diurnal cycle of rainfall and convective intensity according to three years of TRMM measurements. J. Climate, 16, 1456–1475, https://doi.org/10.1175/1520-0442-16.10.1456.

Nicholson S. E. (2018). The ITCZ and the seasonal cycle over equatorial Africa. American Meteorological Society. DOI:10.1175/BAMS-D-16-0287.1

Nicholson S. E. (2009). A revised picture of the structure of the ‘‘monsoon’’ and land ITCZ over West Africa. Clim Dyn (2009) 32:1155–1171, DOI 10.1007/s00382-008-0514-3

Nicholson S.E. and Klotter D. (2020). The tropical easterly jet over Africa, its representation in six reanalysis products, and its association with Sahel rainfall. Int J Climatol 41(1):328–347. https://doi.org/ 10. 1002/ joc. 6623

Nikulin G., Lennard C., Dosio A., Kjellström E., Chen Y., Hänsler A., Kupiainen M., Laprise R., Mariotti L., Maule CF., van Meijgaard E., Panitz HJ., Scinocca J.F., Somot S. (2018). The efects of 1.5 and 2 degrees of global warming on Africa in the CORDEX ensemble. Environ Res Lett 13(6):065003

Nogherotto R., Tompkins A.M., Giuliani G., Coppola E. and Giorgi, F. (2016). Numerical framework and performance of the new multiple-phase cloud microphysics scheme in RegCM4.5: precipitation, cloud microphysics, and cloud radiative effects. Geoscientific Model Development, 9, 2533–2547. https://doi.org/10.5194/gmd-9-2533-2016.

Nordeng TE. (1994). Extended versions of the convective parametrization scheme at ECMWF and their impact on the mean and transient activity of the model in the tropics. Tech. rep., ECMWF Research Department, Europea

Normandin c., Frappart F., Diepkilé A. T., Marieu V., Mougin E., Blarel F., Lubac B., Braquet N., and Ba A. (2018). Evolution of the Performances of Radar Altimetry Missions from ERS-2 to Sentinel-3A over the Inner Niger Delta. Remote Sens. 2018, 10, 833 ; doi :10.3390/rs10060833

O'Neill B.C., Tebaldi C., Vuuren D.V., Erying V., Fridelingstein G., Knutti R., Kriegler E., Lamarque J.F., Lowe J., Meehl J., Moss R., Riahi K., Sanderson B.M., (2017). The roads ahead: Narratives for shared socioeconomic pathways describing world futures in the 21st century. Global Environ. Chang., 42, 169–180. https://doi.org/10.1016/j.gloenvcha.2015.01.004.

Oettli P.., Sultan B., Baron C. and Vrac M. (2011). Are regional climate models relevant for crop yield prediction in West Africa? Environ. Res. Lett. 6 (2011) 014008 (9pp) doi:10.1088/1748-9326/6/1/014008

Ogbonda K. H., Aminigo R. E. and Abu G. O. (2007). InXuence of temperature and pH on biomass production and protein biosynthesis in a putative *Spirulina* sp. Bioresource Technology 98 (2007) 2207–2211

Ogilvie A., Belaud G., Delenne C., Bailly J. S., Bader J. C., *et al*.. (2015). Decadal monitoring of the Niger Inner Delta flood dynamics using MODIS optical data. Journal of Hydrology, 2015, 523, pp.368-383. 10.1016/j.jhydrol.2015.01.036. hal-01196991

Ogilvie A., Belaud G., Delenne C., Bailly J., Bader J., Oleksiak A., Ferry L., Martin D., (2015). Decadal monitoring of the Niger Inner Delta flood dynamics using MODIS optical data. J. Hydrol. Elsevier 523, 368–383. https://doi.org/10.1016/j. Jhydrol.2015.01.036.

Olivry J. C. (1995). Hydrological functioning of the Niger Basin and modeling test of the flooding of the Inner Delta. In: Large Peri-Atlantic River Basins: Congo, Niger, Amazon (ed. by J. Boulègue and J. C. Olivry), 267–280. INSU/ CNRS/ ORSTOM, Paris, France.

Orange D., Gréard M., Cissé N., Ouattara M., (2000). Elements for the creation of an environmental quality observation network in the Niger Basin (in Mali): suspended solids, a quality indicator. Studies and reports Gihrex, ER54, IRD, Bamako, Mali, 43 p.

Ott I., Duethmann D., Liebert J., Berg P., Feldmann H., Ihringer J., and Wagner, S. (2013). High-resolution climate change impact analysis on medium-sized river catchments in Germany: an ensemble assessment. Journal of Hydrometeorology, 14(4), 1175-1193.

Parker D. J., Diop-kane M. and Lafore J. P. (2018). Meteorology of Tropical West Africa. June 2018 edition

Pedinotti. V, Boone. A, Decharme. B, Cr´etaux. J. F, Mognard. N, Panthou. G, Papa. F, and Tanimoun. B. A. (2012). Evaluation of the ISBA-TRIP continental hydrologic system over the Niger basin using in situ and satellite derived datasets. Hydrol. Earth Syst. Sci., 16, 1745–1773, 2012 www.hydrol-earth-syst sci.net/16/1745/2012/doi:10.5194/hess-16-1745-2012

Pfeifer S. (2006). Modeling cold cloud processes with the regional climate model REMO. PhD thesis, University of Hamburg

Picouet C., (1999). Geodynamics of a tropical hydrosystem with little human impact: the upper Niger basin and its inland delta. PhD thesis, Sciences, Univ. Montpellier, 454 p.

Picouet C., Orange D., Mahé G, Olivry J. C. (2002). Role of the Inner Niger River Delta in regulating water and sediment balances.

Pilkington A. and Meredith J. (2009). The evolution of the intellectual structure of operations management—1980–2006: a citation/co-citation analysis. J Oper Manage 2009;27(3):185–202.

Poncet Y. and Orange D. (1999). Water, a driver of shared resources: the example of the inner Niger Delta in Mali. Aménagement et Nature, 132: 97-108.

Prein A. F., Langhans W., Fosser G., Ferrone A., Ban N., Goergen K., *et al.,* (2015). A review on regional convection-permitting climate modeling: Demonstrations, prospects, and challenges. Reviews of Geophysics, 53(2), 323–361. https://doi.org/10.1002/2014RG000475

Pritchard A. (1969). Statistical bibliography or bibliometrics? J Doc 1969;25(4):348–9.

Qian Y., Ghan SJ. and Leung L.R. (2009). Downscaling hydroclimatic changes over the Western US based on CAM subgrid scheme and WRF regional climate simulations-Qian-2010. International Journal of Climatology—Wiley Online Library. International Journal of Climatology. 2009 Apr 20; 30(5):675–93.

Quensière J. I. (1994). Fishing in the Central Niger Delta. Vols I and II. IER, ORSTOM Editions, Karthala, Paris https://horizon.documentation.ird.fr/exl-doc/pleins_textes/divers/40722.pdf

Ramos-Rodrígue A. R., and Ruíz-Navarro, J. (2004). Changes in the intellectual structure of strategic management research: A bibliometric study of the Strategic Management Journal, 1980–2000. *Strategic Management Journal, 25*(10), 981–1004.

Raschendorfer, M. (2001). The new turbulence parameterization of LM. COSMO Newsletter, 1, 89–97.

Rauch M., Bliefernicht J., Maranan M., Fink A. H. and Kunstmann, H. (2024). Interannual rainfall variability in west africa: reconstruction based on atmospheric circulation patterns. Int. J. Climatol. doi: 10.5281/zenodo.14046484

Rauscher S.A., Coppola E., Piani C., Giorgi F. (2010). Resolution effects on regional climate model simulations of seasonal precipitation over Europe. Climat Dyn. 2010 Apr 20; 35(4):685–711.

Rebelo L., Johnston R., Hein T., Weigelhofer G., Dhaeyer T., Kone B., and Cools, J. (2012). Challenges to the integration of wetlands into IWRM: The case of the Inner Niger Delta (Mali) and the Lobau Floodplain (Austria). environmental science and policy 34 (2013) 58–68. http://dx.doi.org/10.1016/j.envsci.2012.11.002

Redelsperger J.L., Thorncroft C.D., Diedhiou A., Lebel T., Parker DJ. and Polcher J. (2006). African Monsoon multidisciplinary analysis. An international research project and field campaign. Bull Am Meteorol Soc 87:1739–1746. doi:10.1175/BAMS-87-12-1739.

Remedio A.R., Teichmann C., Buntemeyer L., Sieck K., Weber T., Rechid D., Hoffmann P., Nam C., Kotova L. And Jacob D. (2019). Evaluation of new CORDEX simulations using an updated Köppen–Trewartha climate classification. Atmosphere, 10(11), 726. https://doi.org/10.3390/atmos10110726.

Rennick M. A., (1981). Some sensitivity experiments with an African wave model. J. Atmos. Sci., volume 38. Rep 10(1):1–18. https://doi.org/10.1038/s41598-020-67146-8

Roeckner E., Arpe K., Bengtsson L., Christoph M., Claussen M., Dümenil L., Esch M., Giorgetta M., Schlese U. and Schulzweida U. (1996). The atmospheric general circulation model ECHAM-4: model description and simulation of presentday climate, Vol. 218. Hamburg: Max-Planck-Institut für Meteorologie, p. 171. MPI report. https://doi.org/10.17617/2.1781494.

Rojas R., Feyen L., Bianchi A., and Dosio A. (2012). Assessment of future flood hazard in Europe using a large ensemble of bias-corrected regional climate simulations. Journal of Geophysical Research: Atmospheres, 117(D17).

Schmidli J, Goodess C. M, Frei C, Haylock M. R, Hundecha Y, Ribalaygua J, *et al.,* (2007). Statistical and dynamical downscaling of precipitation: An evaluation and comparison of scenarios for the European Alps. Journal of Geophysical Research: Atmospheres. 2007 Apr 20; 112(D4).

Schuol J., Abbaspour K.C., Srinivasan R., Yang H., (2008). Estimation of freshwater availability in the West African sub-continent using the SWAT hydrologic model. Journal of Hydrology 352, 30–49.

Seiler R., Schmidt J., Diallo O., and Csaplovics, E. (2009). Flood monitoring in a semi-arid environment using spatially high resolution radar and optical data. Journal of Environmental Management, 90(7), 2121–2129. http://doi.org/10.1016/j.jenvman.2007.07.035

Seland Ø., Bentsen M., Olivié D., Toniazzo T., Gjermundsen A., Graff L.S., Debernard J.B., *et al.*, (2020). Overview of the Norwegian Earth System Model (NorESM2) and key climate response of CMIP6 DECK, historical, and scenario simulations. Geosci. Model Dev. 13, 6165–6200.

Servat E., Paturel J. E., Kouame B., Travaglio M., Ouedraogo M., Boyer J. F., Lubes-Niel H., Fristch J. M., Masson J. M. and Marieu, B. (1998). Identification, characterization and consequences of hydrological variability in West and Central Africa. In: Water Resources Variability in Africa during the XXth Century (ed. by E. Servat, D. Hughes, J. M. Fritsch and M. Hulme) (Proc. Abidjan Conf.), 323–337. IAHS Publ. 252. IAHS Press, Wallingford, UK

Soares P. M. M., Careto J. A. M., Cardoso R. M., Goergen K., and Trigo, R. M. (2019). Land-atmosphere coupling regimes in a future climate in Africa: From model evaluation to projections

Sørland S.L., Brogli R., Pothapakula P.K., Russo E., Van de Walle J., Ahrens B., Anders I., Bucchignani E., Davin E.L., Demory M.-E., Dosio A., Feldmann H., Früh B., Geyer B., Keuler K., Lee D., Li D., van Lipzig N.P.M., Min S.-K., Panitz H.-J., Rockel B., Schär C., Steger C. and Thiery W. (2021). COSMO-CLM regional climate simulations in the Coordinated Regional Climate Downscaling Experiment (CORDEX) framework: a review. Geoscientific Model Development, 14, 5125–5154. https://doi.org/10.5194/gmd-14-5125-2021.

Stanzel P., Kling H. and Bauer H. (2018). Climate change impact on West African rivers under an ensemble of CORDEX climate projections. Climate Services 11 (2018) 36–48. https://doi.org/10.1016/j.cliser.2018.05.003

Stevens B., Giorgetta M., Esch, M., Mauritsen T., Crueger T., Rast S., Salzmann M., Schmidt H., Bader J., Block K., Brokopf R., Fast I., Kinne S., Kornblueh L., Lohmann U., Pincus R., Reichler T. and Roeckner E. (2013). Atmospheric component of the MPI-M earth system model: ECHAM6. Journal of Advances in Modeling Earth Systems, 5, 146–172.

Steward J. I. (1994). Utilizing rainfall probabilities referenced to crop seed germination dates to assess risk and develop response farming strategies for Asmara, Eritrea. Workshop for the famine mitigation activities support activity of USAID, US Foreign Disaster Assistance, Asmara.

Stuut J.B., M. Zabel., V. Ratmeyer., P. Helmke., E. Schefuß., G. Lavik. and R. Schneider. (2005). Provenance of present-day eolian dust collected off NW Africa, J. Geophys. Res., 110, D04202, doi:10.1029/2004JD005161.

Su F., Duan X., Chen D., Hao Z. and Cuo L. (2013). Evaluation of the global climate models in the CMIP5 over the Tibetan Plateau. J. Climate, 26, 3187–3208, doi:10.1175/JCLI-D-12-00321.1.

Sultan B. and Gaetani M. (2016). Agriculture in West Africa in the twenty-first century: climate change and impacts scenarios, and potential for adaptation. Front. Plant Sci. 7, 1262.

Sultan B. and Janicot S. (2003). The West African monsoon dynamics. Part II: The "pre-onset" and the "onset" of the summer monsoon. J. Clim. 16, 3407–3427.

Sultan B., Janicot S. and Diedhiou A. (2003). The West African monsoon dynamics. Part I: Documentation of intraseasonal variability. J. Clim., 16, 3389–3406.

Sultan N., Marsset B., Ker S., Marsset T., Voisset M., Vernant A. M., Bayon G., Cauquil E., Adamy J., Colliat J. L. and Drapeau D. (2010). Hydrate dissolution as a potential mechanism for pockmark formation in the Niger delta. journal of geophysical research, vol. 115, B08101, doi:10.1029/2010JB007453, 2010

Sylla M.B., Diallo I., Pal J.S. (2013). West African monsoon in stateof the-art regional climate models. In: Tarhule A (ed) climate variability-regional and thematic patterns. InTech, London

Tabari H., Marofi S., Hosseinzadeh Talaee P., Mohammadi K., (2011). Trend analysis of reference evapotranspiration in the western half of Iran.Agric. For. Meteorol. 151, 128–136.

Tamoffo A. T., Akintomide A., Akinsanola A. A. and Torsten W. T. (2023). Understanding the diversity of the West African monsoon system change projected by CORDEX-CORE regional climate models. Climate Dynamics (2023) 61:2395–2419. https://doi.org/10.1007/s00382-023-06690-1

Taylor K.E., Stouer R.J., Meehl G.A. (2012). An overview of CMIP5 and the experiment design. Bull. Am. Meteorol. Soc. **2012**, 93, 485–498.

Thompson R. M., Payne E. E. Recker, and R. J. Reed., (1979). Structure and properties of synoptic-scale wave disturbances in the intertropical convergence zone of the eastern Atlantic. J. Atmos. Sci., 36, 53–72.

Tiedtke M (1989). A comprehensive mass flux scheme for cumulus parameterization in large-scale models. Mon Weather Rev 117(8):1779–1800. 10.1175/1520-0493(1989)117<1779:ACMFSF>2.0.CO;2

Trenberth K. and Asrar G. (2014). Challenges and Opportunities in Water Cycle Research: WCRP Contributions, Surv. Geophys., 35, 515– 532.https://link.springer.com/article/10.1007/s10712-012-9214-y , January 20th 2025.

Trzaska S. and Schnarr E. (2014). A Review of Downscaling Methods for Climate Change Projections. USAID (United States Agency for International Development by Tetra Tech ARD); 2014.

UNDP (United Nations Development Programme) (2012). Africa Human Development Report 2012. Towards a Food Secure Future. by the United Nations Development Programme Regional Bureau for Africa (RBA) UN Plaza, New York, NY 10017, USA

Van Vuuren D.P., Lucas P.L., Hilderink H., (2007). Downscaling drivers of global environmental change: enabling use of global SRES scenarios at the national and grid levels. Global Environmental Change 17, 114–130.

Vicente-Serrano S.M., Beguería S., Gimeno L., Eklundh L., Giuliani G., Weston D., El Kenawy A., López-Moreno J.I., Nieto R., Ayenew T., Konte D., Ardö J., Pegram G.G.S., (2012). Challenges for drought mitigation in Africa: the potential use of geospatial data and drought information systems. Appl. Geogr. 34, 471–486. https://doi. org/10.1016/j.apgeog.2012.02.001.

Walker G. and Burningham K., (2011). Flood risk, vulnerability and environmental justice: evidence and evaluation of inequality in a UK context. Crit. Soc. Pol. 31 (2), 216–240.

wetland international, (2024). https://www.wetlands.org/blog/wetlands-for-peace-the-inner-niger-delta/

Wetterhall F. (2005). Statistical Downscaling of Precipitation from Large-Scale Atmospheric Circulation. Ph.D. Thesis, Uppala University,Uppsala, Sweden, 2005. Available online: https://www.researchgate.net/publication/260265285_Statistical_Downscaling_of_Precipitation_from_Large%20scale_Atmospheric_Circulation (accessed on 1 January 2025).

World Bank, (2010). Report on the Status of Disaster Risk Reduction in Sub-Saharan Africa. http://www.gfdrr.org/sites/gfdrr/files/publication/AFR.pdf. Yarnal, B., 1993. Synoptic Climatology in Environmental Analysis. Belhaven Press, London.

WWF, (2008). Inner Niger Delta flooded Savanna. In: Encyclopaedia of Earth, Environmental Information Coalition, National Council for Science and the Environment, Cleveland/Washington, DC.

Xu Z. and Yang Z.L. (2015). A new dynamical downscaling approach with GCM bias corrections and spectral nudging. Journal of Geophysical Research: Atmospheres. 2015 Apr 27; 120(8):3063–84.

Xu Z., Han Y., and Yang Z. (2019). Dynamical downscaling of regional climate: A review of methods and limitations. Science China Earth Sciences, 62(2), 365–375. https://doi.org/10.1007/s11430-018-9261-5

Yen H., Park S., Arnold J.G., Srinivasan R., Chawanda C.J., Wang R., *et al.,* (2019). IPEAT+: a built-in optimization and automatic calibration tool of SWAT+. Water 11 (8), 1681. https://doi.org/10.3390/w11081681.

Yonaba R., Adjadi M. L., Tazen F., Koïta M., Biaou A., Zouré C., Queloz P., Karambiri H., Yacouba H. (2023). Future climate or land use? Attribution of changes in surface runoff in a typical Sahelian landscape. Les Comptes Rendus. Géoscience — Sciences

Yu X. C. (1999). From GCMs to river flow: a review of downscaling methods and hydrologic modelling approaches. Progress in Physical Geography: Earth and Environment. 1999 May 7; 23(2):229–49.

Yue S. and Pilon P. (2004). A comparison of the power of the *t* test,

Zwarts L., P. Van Beukering, B. Kone, E. Wymenga, and D. Taylor. (2006). The Economic and Ecological Effects of Water Management Choices in the Upper Niger River: Development of Decision Support Methods. International Journal of Water Resources Development, 22(1):135–156.

Zwarts L., van Beukering P., Kone B., and Wymenga E. (2005). The Niger, a Lifeline. Effective water management in the Upper Niger Basin. Altenburg and Wymenga Ecologisch Onderzoek BV. ISBN-10: 9080715069 ISBN-13: 978-9080715066.

APPENDICES

1. Trends and Prospects from Climatic Research of Inner-Niger-Delta Wetland

Summary

The fate of wetlands in arid regions has become a matter of concern in the context of global warming. The Inner Niger Delta (IND) has received increasing attention from researchers and others to explore whether this largest wetland in Africa will shrivel due to climate change and increasing water use. An essential study goal is to understand what has been done so far in the Research of Inner-Niger-Delta Wetland in order to address its future challenges. The present study provides a comprehensive analysis of climate related research on the IND wetland through bibliometric means to diagnosis the evolution, lag and hotspot of relevant features in the literature. Key aspects of analysis included (i) trends of IND wetland related research (ii) nature of collaboration networks, (iii) co-occurrence of keywords and (iv) emerging themes related to IND wetland over the last three decades, between the years 1991-2022. The results indicate that the IND wetland gained momentum in 2000, peaking in 2013 and then in 2018. IND wetland research has, on average, reach 2.5 publication in 2000 and exceed 5 papers by 2017. The leading countries that have produced high numbers of published documents are in order, France, Nigeria, USA, Germany and Mali. Therefore, more efficient scientific collaboration among regional African institutions is recommended to face local perspectives. The identified emerging topics are Niger delta, climate change, floods and rivers. The variables considered in analyses are river discharge, evapotranspiration, water level and rain. Variables relevant to global temperature warming are missing which implies that researches on Inner Niger Delta wetland are less focusing on climate change and variability analyses.

1.1 Methodology

The current study used the Scopus databases to retrieve relevant documents on the wetland situated in the Niger river in Mali- namely, the Inner Niger Delta. Scopus is a prominent online academic database that significantly influences scholarly literature because it provides access to a vast array of journals and sources across various fields of knowledge (Baas *et al.,* 2020). A literature review was conducted on the Scopus platform in order to assess the publication pattern relevant to IND wetland. The approach consists of conducting a scientific mapping of research topics related to the IND wetland in order to understand thematic trends, developments, the nature of collaboration networks and general narrative in line with the biggest wetland in Africa. Bibliometric analysis was defined by Pritchard as the application of mathematics and statistical methods to books and other media of communication (Pritchard A. 1969). Two widely used bibliometric methods are citation analysis and content analysis. Citation analysis implies a relationship between citing and cited works in a particular research area and allows one to identify core literatures, journals, countries, etc., (Pilkington *et al.,* 2006). Publications using bibliometric methods have grown over the years. Yet, large bibliographic datasets have made classic review methods cumbersome and impractical (Ramos-Rodrígue and Ruíz-Navarro, 2004). The search term "Inner Niger Delta Wetland" was used, and an analysis was conducted using Scopus Science, which provides details such as the number of publications per year, the countries where the studies were published, and the authors with the highest number of papers on the topic. Initially, 223 articles were identified, and 153 publications were ultimately selected as of May 11, 2023. The dataset for the bibliometric analysis was downloaded from Scopus in the form of a bib (BibTeX Bibliographical Database) file, and the Bibliometrix package in R application was employed to process the data. The extracted information included details such as author names, affiliations, article titles, keywords, abstracts, and citation counts.

1.2 Some results

1.2.1 General characteristics of bibliometric analysis

The general information about the data used for this study is presented in Table 1. Details are based on search results in the scopus database which included 153 publications for the period from 1966 to 2022. These articles were compiled by 533 authors and published in 110 sources with an average number of publication years of 11.4. The publications are mainly research article (122) and conference paper (22) with 47.06% of international co-authorships.

Figure 1 shows the evolution of the number of publications over the study period; the curve shows the cumulative number of publications. It highlighted an increase in the number of publications of about 2.5 per year from 1966 to 2022. The cumulative number of posts showed an upward trend over time. The evolution of the annual average of the number of publications is low from 1966 to 2000, from 2000 to 2022 the curve increases in sawtooth and reaches its Maximin in 2013 and 2018, the value of 2022 is low compared to the previous year’s exception of 2014. IND wetland research has reached 2.5 publications in 2000 and exceeded 5 papers by 2017.

Table 1: the main information about the analyzed articles based our keyword research.

Description	Results
MAIN INFORMATION ABOUT DATA	
Timespan	1966:2022
Sources (Journals, Books, etc)	110
Documents	153
Annual Growth Rate %	2.51
Document Average Age	11.4
Average citations per doc	16.31
References	5865
Keywords Plus (ID)	1402
Author's Keywords (DE)	427
Authors	533
Authors of single-authored docs	16
Single-authored docs	20
Co-Authors per Doc	4.68
International co-authorships %	47.06
Article	122
book chapter	4
conference paper	22
conference review	3
Review	2

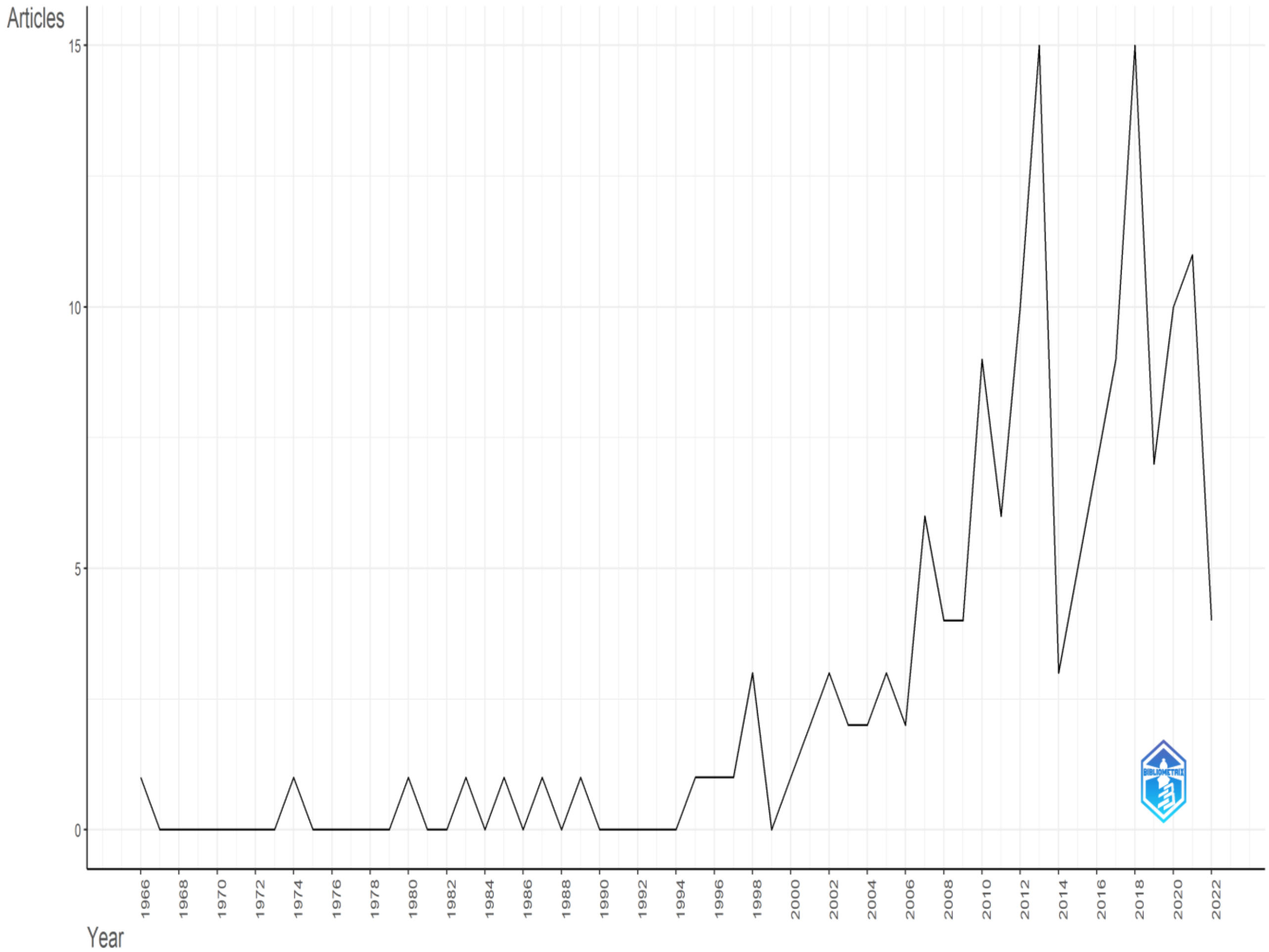

Figure 1: Annual evolution and the cumulative distribution of the number of publications of publication over the study period.

1.2.2 Source patterns

Table 2: the classification of journals based on their impact

	Source	H_Index	TC	NP	PY_Start
1	Journal of African Earth Sciences	4	29	7	2016
2	Environmental Science and Policy	3	84	3	2013
3	Hydrological Sciences Journal	3	45	4	2016
4	Iahs-Aish Proceedings and Reports	3	10	4	2013
5	Iahs-Aish Publication	3	44	5	1998
6	Journal of Ornithology	3	48	3	2011
7	Ostrich	3	26	3	2007
8	Water (Switzerland)	3	45	3	2016
9	Arabian Journal of Geosciences	2	7	2	2015
10	Climatic Change	2	69	2	2012

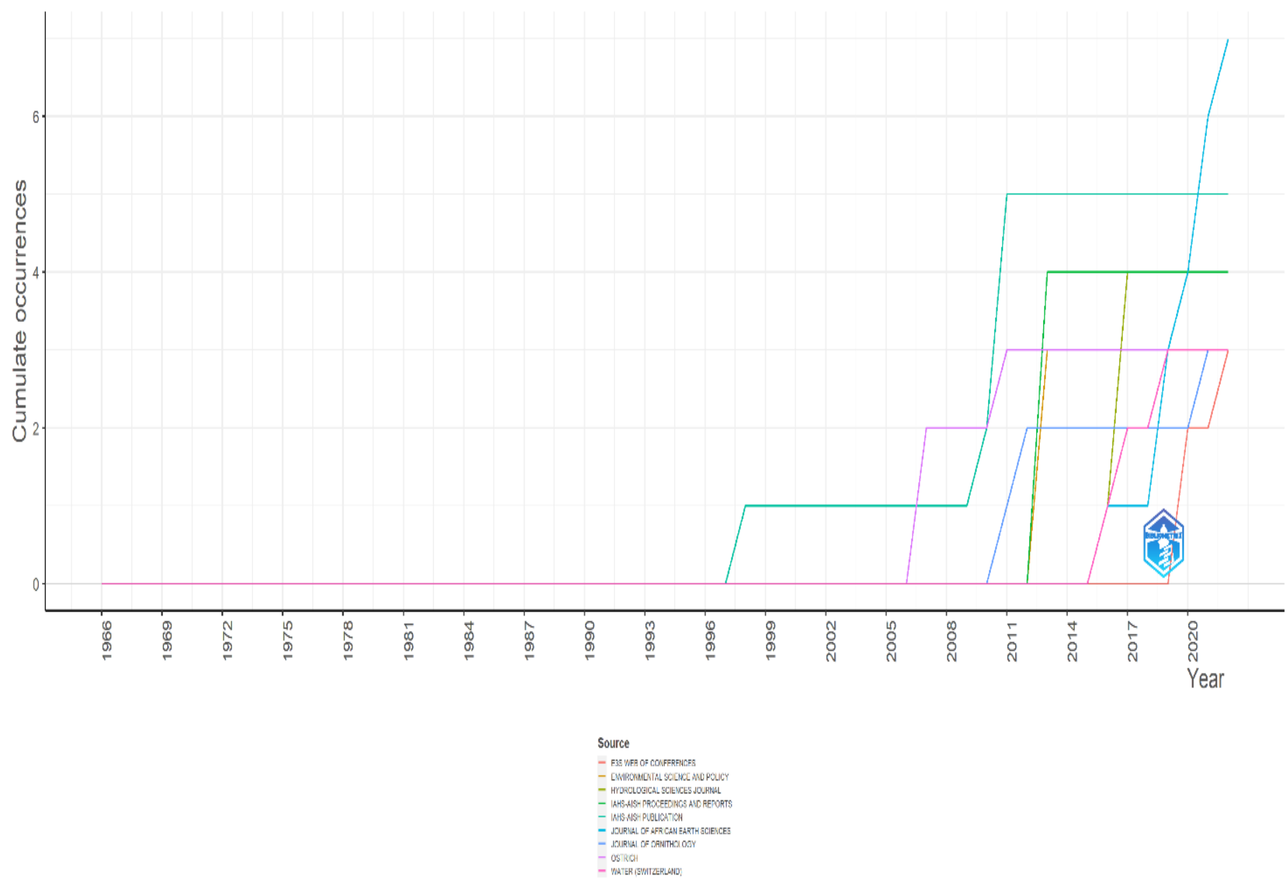

Figure 2: The source production over time

A total of 153 scientific articles were published for the period from 1966 to 2022 in 110 sources. The h-index is a specific index that refers to the number of published articles that have been cited at least h times (Bertoli-Barsotti and Lando 2017). As shown in Table 2, "Journal of African Earth Sciences" and "Environmental Science and Policy" are the two most relevant and top-ranked sources with the highest h-index (7 and 3 papers, respectively) and the total number of citations (29 and 84, respectively). The journal "Hydrological Sciences Journal" ranks third with 4 cited articles and 45 citations.

1.2.3 Main authors

Table 3: the top 10 of the most relevant authors

#	Authors	H_Index	TC	NP	PY_Start
1	Granjon L	5	142	5	2002
2	Liersch S	5	100	6	2012
3	Mahe G	5	81	10	1997
4	Bamba F	4	75	4	1997
5	Flade M	4	56	4	2011
6	Fofana B	4	62	4	2007
7	Fournet S	4	87	5	2012
8	Hattermann Ff	4	109	5	2012
9	Kone B	4	88	6	2007
10	Mariko A	4	54	5	2003

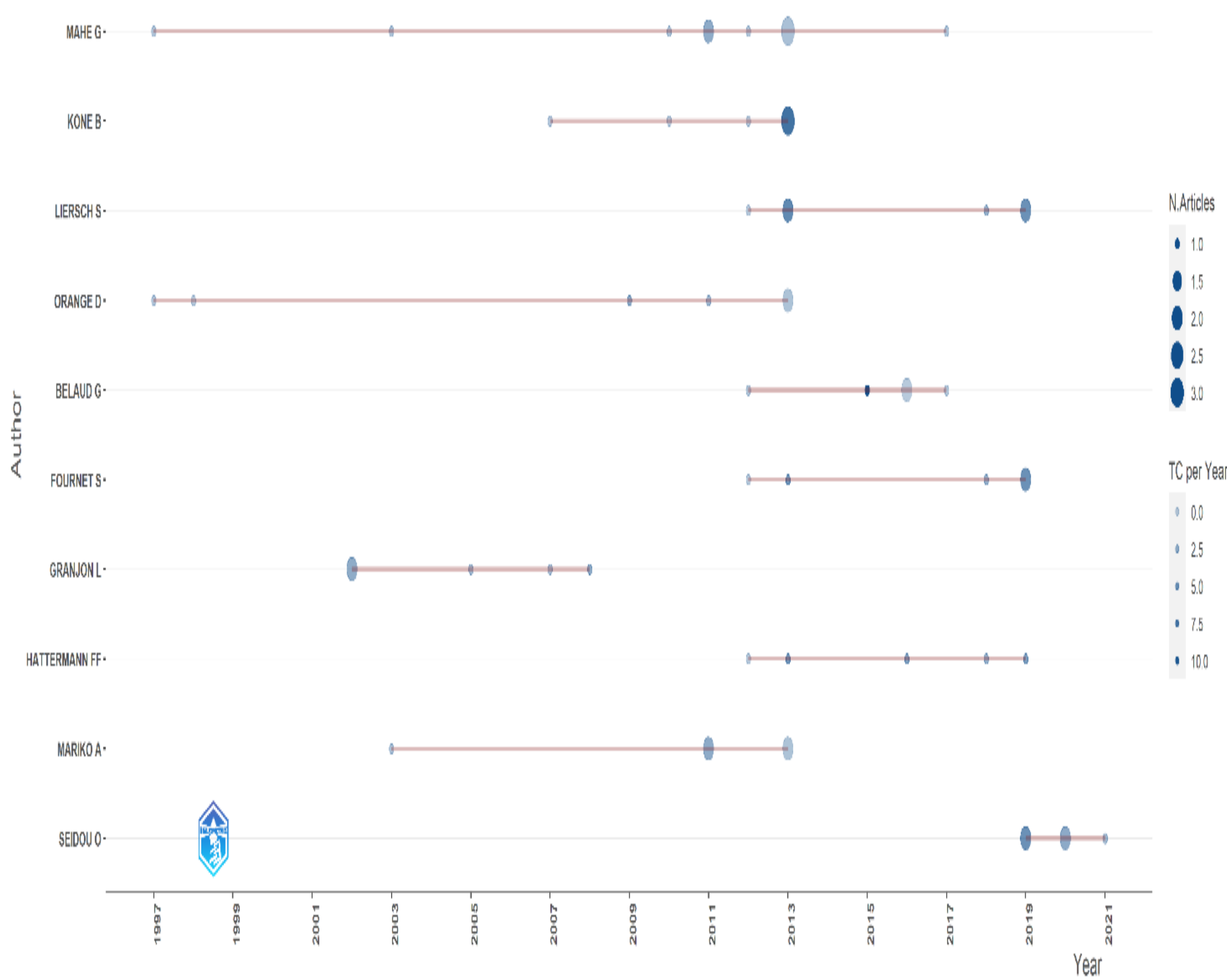

Figure 3: Author's production over time

Authors reports included a filter to identify the main authors and countries on the Inner Niger Delta studies. Table 3 summarizes author productivity characterized by h-index, total number of citations (Tc), number of articles (Np) and year of first publication (Py_Start) during the study period. In terms of h-index, Granjon L, de Liersch S, and Mahe G have the greatest influence, with an index value of 5, followed by Bamba F., Fofana B. and Flade M., who have an index value of 4 each. Regarding the number of citations, the first two places are occupied by Granjon L and Liersch S with 5 and 6 articles respectively. The third place is occupied by Kone B with 6 articles. Figure 3 shows the evolution of authors over time. The volume and color depth of the sphere are related to the annual number of article citations. This shows that Mahe G has the large number of posts over time followed by Kone B and Liersch S with 6 posts each.

1.2.4 Main countries

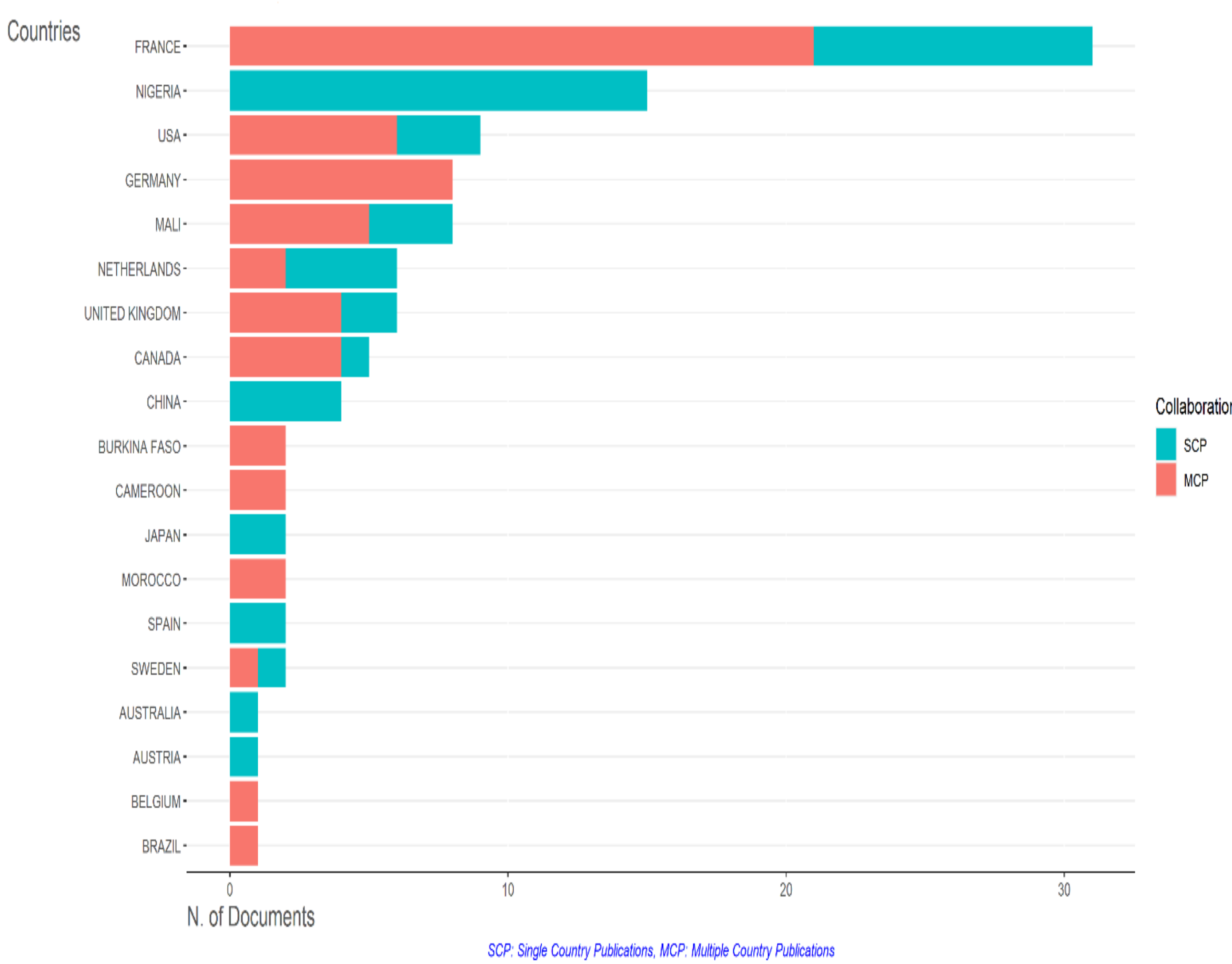

Figure 4: Top 20 countries of study's authors

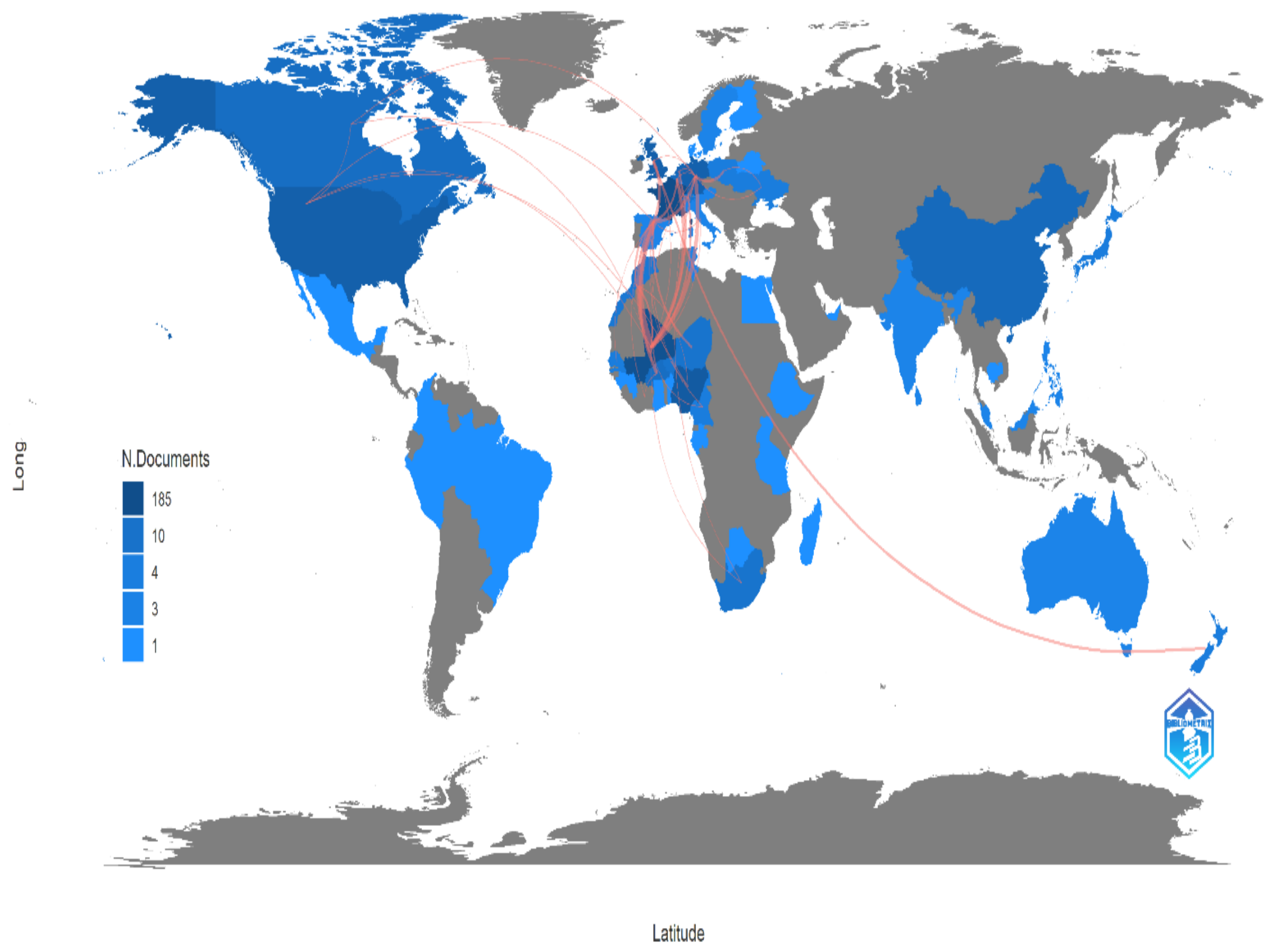

Figure 5: Country collaboration map

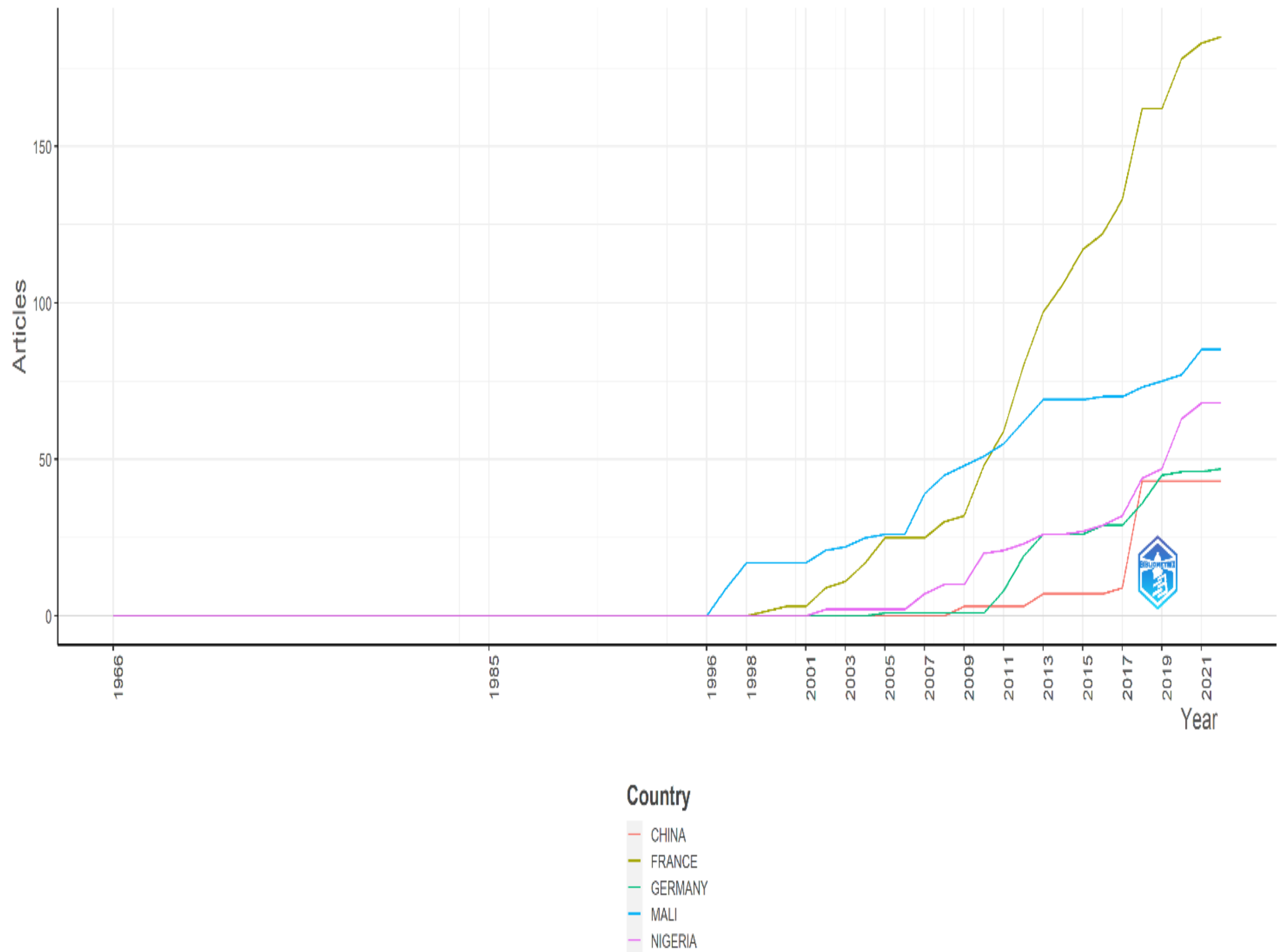

Figure 6: Country production over time

Publishing articles in different countries can usually reflect the influence and importance of a given topic. Fifty-one countries are involved in this study. Figure 4 describes the top 15 countries where authors have collaborated within the same country: single-country publications (SCP) and between countries: multi-country publications (MCP). The total number of items is the sum of SCP and MCP. France occupies the first position with 31 publications, representing approximately 20.26% of the total articles published (national and international), followed by Nigeria with 15 articles, representing 9.80% of the total publications. France is far ahead of other countries in terms of multi-country publications (21 articles), which partly reflects the fact that France is more active in researching the sustainability of the Inner Niger Delta. Regarding the average amount of article citations, France and Germany have the highest cross-country publication rates (0.20 and 0.05, respectively). African countries occupy an important place with the participation of 19 countries over the 51 countries ahead of Europe and Asia. Most of the top 19 countries are developed countries, with the exception of three African countries. The scientific production of the country is shown in Figure 5. The greatest number of articles published in terms of frequency is indicated by the darker blue. This result also shows the interest of researchers for the inner delta of the Niger which contributes to the achievement of sustainable development objectives in the West African sub-region.

1.2.5 Most-cited articles in the world

Table 4: Ten global cited documents dealing with the Inner Niger Delta wetland

#	Paper	Journal	Years	Total Citations
1	DEPTUCK ME	Marine and Petroleum Geology	2003	335
2	OGBONDA KH	Bioresource Technology	2007	163
3	SULTAN N	Journal Of Geophysical Research	2010	116
4	OGILVIE A	Journal of Hydrology	2015	98
5	JOBE ZR	Journal of Sedimentary Research	2015	65
6	REYMENT RA	Palaeogeography, Palaeoclimatology, Palaeoecology	1966	64
7	CUBRY P	Current Biology	2018	56
8	FLEISCHMANN A	Journal of Hydrology	2018	53
9	NORMANDIN C	Remote sensing	2018	51
10	PEDINOTTI V	Hydrology and Earth System Sciences	2012	50

Commonly cited references from a specific research area can reveal the knowledge base of that area (Marx *et al*. 2017). Table 4 shows the 10 global papers cited related to the Inner Niger Delta over the period of 1966 to 2022. Publications by Deptuck *et al*., (2003) Analyzed high resolution 2D and 3D multichannel seismic data, mainly from the upper fan of near seafloor channel-dig systems on the Niger Delta Slope and in the Arabian Sea, reveal a high level of detail and architectural complexity. Detailed study of one particular channel-dig system on the Niger Delta Slope shows a period of incision followed by three distinct phases of channel development during its aggradation history. Channel sinuosity evolves dynamically, with some meander loops undergoing periods of accelerated meander growth while others show little lateral migration. Ogbonda *et al*., (2007) studied the influence of temperature and pH on biomass production and protein biosynthesis in an environment isolated from hydrocarbon pollution in the brackish Niger Delta. The effect of pH was modulated by temperature and vice versa during biomass production. Offers a good source of natural protein that could be readily accepted by rural communities as single cell protein in the form of feed, food and health supplements when properly processed. Sultan *et al*., (2010) used acquired geophysical, geological and geotechnical modeling to monitor the evolution of hydrate dissolution causing sediment collapse and pockmark formation in the Niger Delta. The results showed that gas hydrate dissolution (gas hydrate becomes a mixture of water and dissolved gas) under a local decrease in gas concentration at the base of the Gas Hydrate Occurrence Zone (GHOZ) can explain the excess pore pressure and fluid flow surrounding the central hydrate zone and the collapse of sediments at the edge of the GHOZ. The different stages of deformation (or development) of the detected pockmarks confirm that a local process such as the amount of gas flow across faults rather than a regional one is driving these depressions. Ogilvie *et al*., (2015) exploited 526 MODIS satellite images for 8 days with 500 m resolution to study the spatial and temporal dynamics of the annual flood in the Inner Niger Delta over the period 2000-2011. Results show that previous correlations between discharge levels and inundated areas were refined to account for hysteresis as the flood recedes and the variable magnitude of the flood. Direct precipitation assessed over the flooded areas refined the wetland water balance and infiltration estimates. Knowledge gained about the timing, duration, and extent of flooding across the wetland and in lakes, floodplains, and irrigated plots can assist farmers in agricultural water management. Jobe *et al*., (2015) Investigated changes in sediment supply and sizing over the past 130 years in the complex architectural evolution of the Y-channel system on the western slope of the Niger Delta. The show that the inner dikes accumulated rapidly as flows sought equilibrium. The dataset unequivocally links changes in underwater channel architecture to changes in sediment supply and size. Changes in the upstream-downstream sediment delivery system have profound implications for submarine channel architecture and reservoir connectivity. Cubry *et al.,* (2018) used 246 new whole genome sequences, to find the geographic origin of the domestication of African rice (Oryza glaberrima) which remains elusive, the results showed that the cradle of its domestication was in the Inner Niger Delta. Fleischmann *et al.,* (2018) included a bidirectional coupling scheme in a large-scale hydrological-hydrodynamic model (HHM) and tested different model structures, in order to assess which processes are important to simulate in large semi-arid wetlands and how these processes interact with the water balance components. Model outputs were in good agreement with flow and water levels at upstream and downstream stations in the inner Niger delta, as well as for flooded areas in the delta region. Model estimates of annual water loss in the delta ranged from 20.1 to 30.6 km3/yr, while annual evapotranspiration ranged from 760 mm/yr to 1130 mm/yr. Normandin *et al.,* (2018) evaluated the performance of seven altimetry missions, among the most widely used in terrestrial hydrology, using data from a dense in situ network of 19 measurement stations in the Inner Niger Delta (IND) from 1995 to 2017. The results show a very good overall agreement between altimeter data and in situ water levels with a correlation coefficient (R) greater than 0.8 in 80% of cases and a root mean square error (RMSE) less than 0.4 m in 48% of cases. Better agreement is found for recently launched missions such as SARAL, Jason-3 and Sentinel-3A than for previous missions.

Pedinotti *et al*., (2012) evaluated the capacity of the Niger Basin hydrological system using a coupled global climate model, so that the scheme represents first order processes. The simulations show that the flooding regime leads to a non-negligible increase in evaporation over large flooded areas, which decreases the Niger River discharge by 15% to 50% in localities located after the inland delta depending on the rainfall dataset used as a forcing factor. This improves the simulation of river discharge downstream of the delta, confirming the need to couple the land surface scheme with the flooding model. The deep aquifer reservoir improves the Niger's low flows and the dry season recession law.

1.2.6 Dynamic words over time

Figure 7: Keyword trends

As shown in the previous analysis, Figure 7 reveals that Mali, Niger Delta, climate change, hydrological modeling, floods, rivers and water management are still at the heart of the research documents analyzed. The words "Africa", "Geography", "Niger" and "Nigeria" are also present with prominence in the keyword world map.

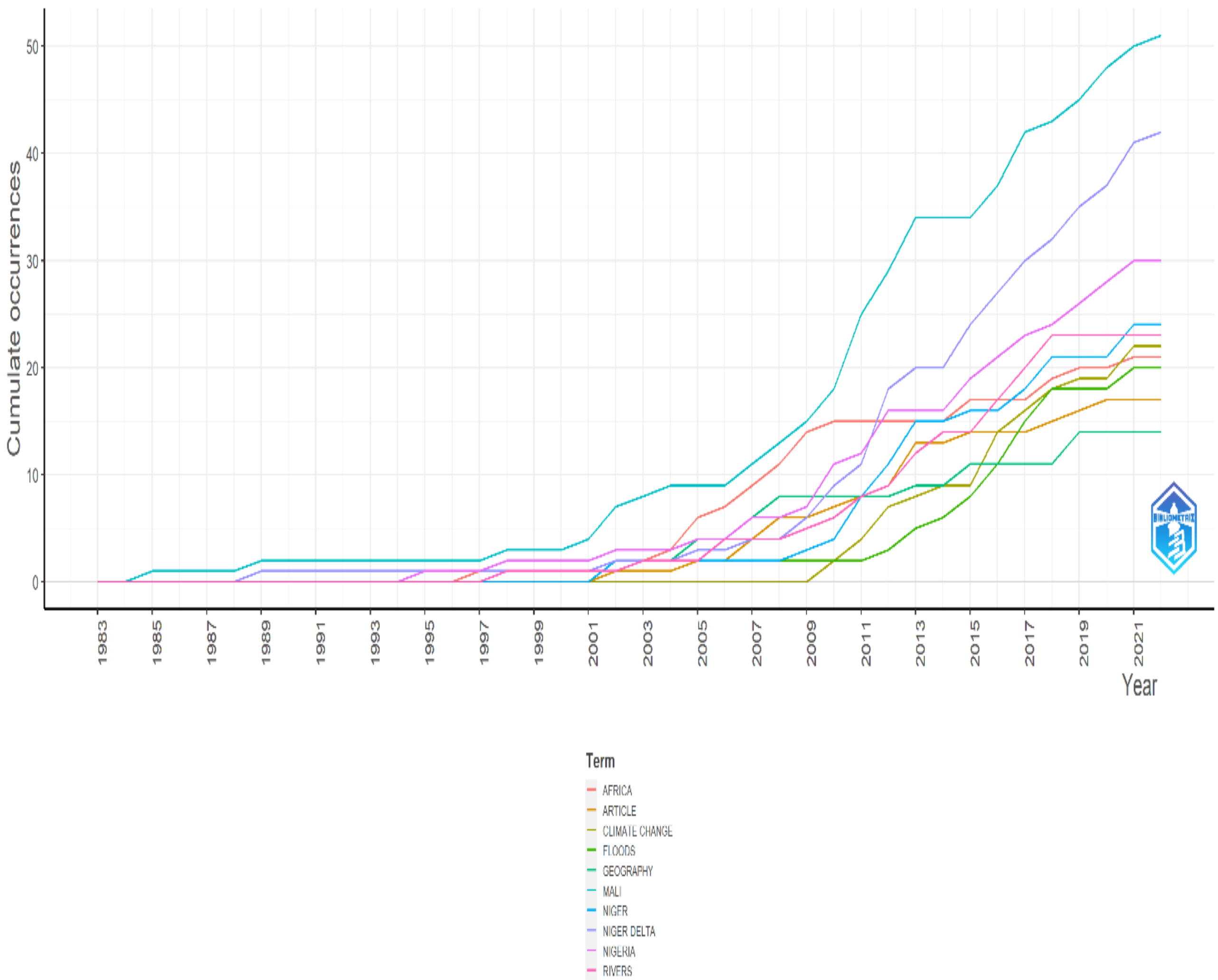

Figure 8: Change and evolution of keyword annual occurrence over time

Words over time for a given topic show the changing rules, evolving relationships, paths and content trends (Figure: 8). Author keywords for studies related to the Inner Niger Delta have increased significantly over the years. Two main periods have been clearly identified. The first period was from 1983 to 2007, with a very low evolution, and the second period was from 2007 to 2022, when the evolution trend was very fast. During these sub-periods, the increase in the occurrence of the words "Mali", "Niger Delta", "climate change", "hydrological modeling", "floods", "rivers" and "water management" was noted. This showed that during this second period, many studies have focused on the impact of climate change, economic impact of the inner Niger delta in the West African region and the hydrological system of the study area.

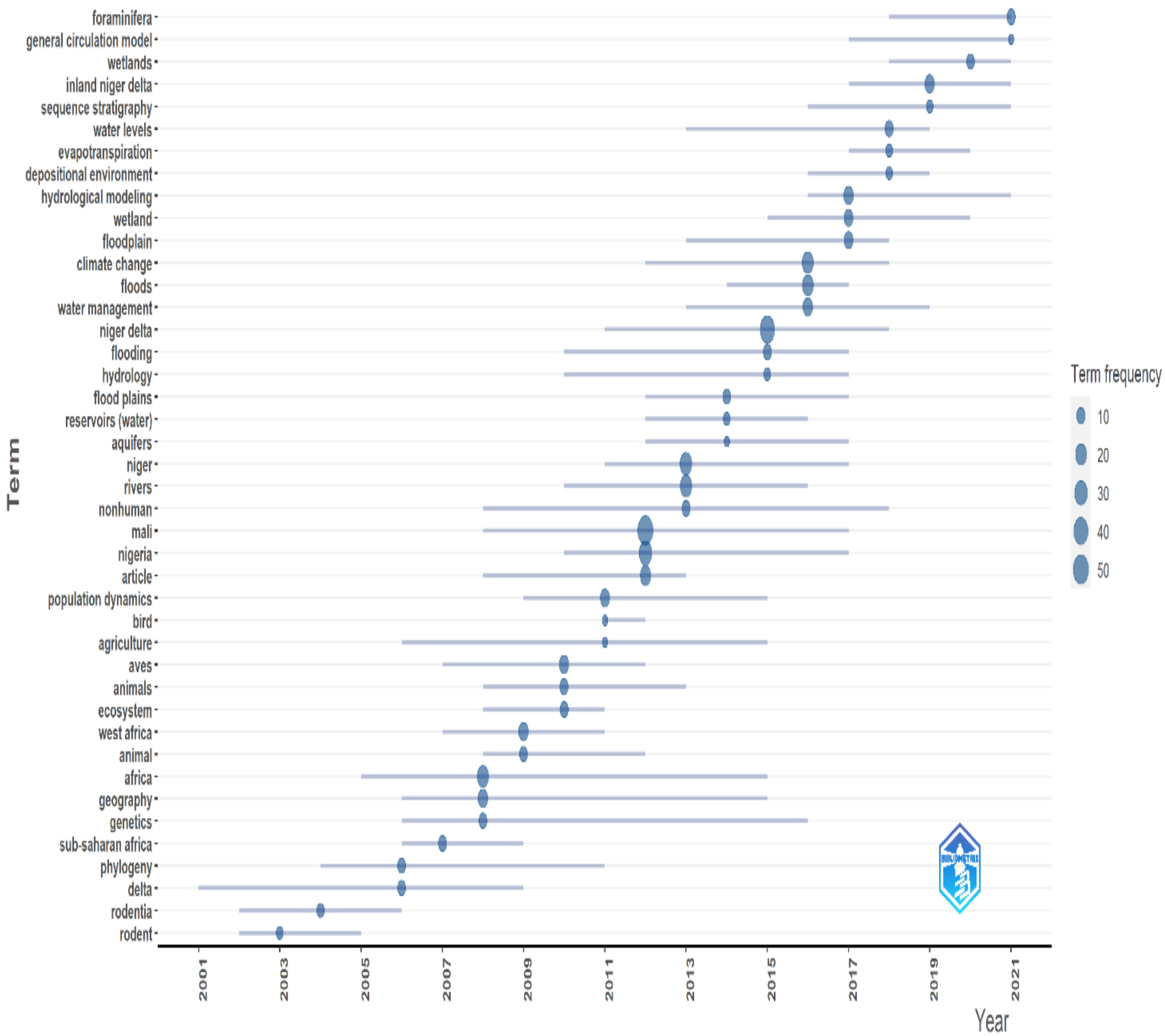

Figure 9: The Trend Topics of Inner Niger Delta over time

Regarding the keywords related to the topics understudy, Figure 2.10 depicts the entry of keywords in the search over a period of study, from 2000 to 2013 the studies focused on agriculture, the evolution of the population, endangered animals. However, during this last decade, more and more researchers started to pay attention to the water management, the floodplain, the climate change, the hydrology modeling, the evapotranspiration, the general circulation model which really contribute to advance research in study area. Therefore, recent dynamics seem to focus on the hydrology and climate change impact of the Inner Niger Delta.

1.3 Discussion

The IND is one of the largest floodplains in the world and is located in the Sahelian Zone in Mali in West Africa. Food production in the IND encompasses mainly three sectors: agriculture, fishery, and livestock. The agricultural system in the IND is therefore very complex and the multiple usage of natural resources is based on community rules and customs that have shaped the way in which societies have administrated this area for a long time (Marie *et al.,* 2007; Moorehead, 1997). Some upstream dams and irrigation structures are already in place, while more are at the planning stage. The infrastructures aim to increase economic development and food security (Md Mominul *et al*., 2019). This study can help researchers better understand how the subject has evolved over time and varied from one place to another place.

The whole of West Africa has been faced with extreme climate variations over the past 5 decades with extended extreme drought conditions during the 70s and 80s (Lebel and Ali, 2009). Inner Niger Delta research has attracted the attention of researchers over the past two decades, with several annual publications, which increased from 1 in 2000 to 11 in 2021 and peaked in 2013 and 2018 with 15 publications. Indeed, since the beginning of the 20th century, there has been a decline in the trend of precipitation in Mali (Funk *et al*., 2012). This increasing number of publications shows a trend of continued growth, demonstrating that more and more researchers have become interested in this area of research. A total of 51 countries had published in this research area. Among these countries, Europe is the most represented by France and Germany, which are led by more published articles. France is of great interest with approximately 20.26% of the total number of articles published. Followed by Africa represents by 19 countries out of the 51 countries; nevertheless, Nigeria and Mali with respectively 9.80% and 5.22% of the articles published. The current research situation exhibits the weak collaboration among regional institution to undertake scientific research with local perspectives. However, research on the Inner Niger Delta is characterized by the limited availability of literature and databases according to the Ministry of the Environment (2002 annual report). In the same perspective, according to (Neal *et al*., 2012; Kuper *et al*., 2003) despite the availability of global numerical models, and the extent of their field of application and in-depth studies carried out in the field, knowledge on the state of the environment are still insufficient. Knowledge of floodplain topography remains insufficient to properly model floodplains. Therefore, with all of the above, more similar studies reinforce the need for continued research and knowledge generation as the Inner Niger Delta contributes significantly to food security and employment in West Africa, particularly in Mali. The research on the Inner Niger Delta is multidisciplinary which combines climate, agriculture, livestock, fisheries, ecosystems, environment, bioresources technology, biochemistry, and plant and soil science. Given the economic importance of the inundation areas, there have been several studies examining the dynamics of the flooded areas. The techniques used include the generation of time series of inundation maps using satellite imagery (Berge-Nguyen and Cretaux, 2015; Ogilvie *et al*., 2015; Zwarts *et al*., 2005; Mariko, 2003), the development of empirical functions that linked the water level at key stations to the inundation extent (Mahe *et al*., 2011; Zwarts *et al*., 2005; Mariko, 2003; 2015), and numerical simulations using numerical models (Haque *et al.,* 2019; Schröder *et al*., 2019; Fleischmann *et al*., 2018; Haag, 2015; Neal *et al*., 2012; Dadson *et al*., 2010).

The evolution of the keywords during the study period revealed that the Inner Niger Delta contributes to the achievement of sustainable development objectives in the West African region. The current focus of studies on the Inner Niger Delta has shown that more researchers are interested in hydrology, agriculture, livestock, fisheries and the impacts of climate change on the flooded area of the delta. Having adequate knowledge of the characteristics of observed and future changes in flood and rainfall extremes is important for developing appropriate adaptation measures to minimize the impacts on society and the environment. This is particularly important because extreme rainfall is expected to intensify with global warming over large parts of the globe as the concentration of atmospheric water vapor which is a source of rainfall increases in proportion to the saturation concentrations at a rate of about 6–7% per degree rise in temperature according to the thermodynamic Clausius–Clapeyron relationship (Ingram, 2016; Allen and Ingram, 2002).